

**K. Jeyapalan, W. Yao, S. Savathchandra, N. Narayan, S. McMahon, J. Kang**

# **Airborne GPS**

**Final Report**

April 1995

Sponsored by the  
Iowa Department of Transportation  
and the Iowa Highway Research Board

Iowa DOT Project HR-359  
ISU-ERI-Ames-95162



**Iowa Department  
of Transportation**

# report

**College of  
Engineering  
Iowa State University**

The opinions, findings, and conclusions expressed in this publication are those of the authors and not necessarily those of the Iowa Department of Transportation.

K. Jeyapalan, W. Yao, S. Savathchandra,  
N. Narayan, S. McMahon, J. Kang

# **Airborne GPS**

Final Report

April 1995

Sponsored by the  
Iowa Department of Transportation  
and the Iowa Highway Research Board

Iowa DOT Project HR-359  
ISU-ERI-Ames-95162



## CONTENTS

Executive Summary . . . . .	1
1. Introduction . . . . .	3
2. Photogrammetry and Kinematic GPS . . . . .	5
2.1. Photogrammetry . . . . .	5
2.2. Kinematic GPS . . . . .	8
2.3. Application of Kinematic GPS in Photogrammetry . . . . .	13
3. Analysis of First Test . . . . .	17
4. Analysis of Second Test . . . . .	29
5. Analysis of Third Test . . . . .	35
6. Analysis of Final Test . . . . .	55
6.1. ISU and Highway 30 Project . . . . .	55
6.2. Ground and Flight Control . . . . .	55
6.3. Flight Mission . . . . .	55
6.4. Processing of GPS Data . . . . .	62
6.5. Photo Coordinate Observation . . . . .	69
6.6. Analysis of the Flight Data . . . . .	69
6.7. Analysis of Refined Test Flight Data . . . . .	78
7. Applications of Airborne GPS . . . . .	83
7.1. Rectifying Aerial Photos . . . . .	83
7.2. Producing Orthophotos . . . . .	85
7.3. Stereo Plotting . . . . .	85
7.4. Base Components . . . . .	87
7.5. $\phi$ and $\omega$ Angles for Leveling . . . . .	87
7.6. Orientation Angle and Translation . . . . .	87
8. Conclusion and Recommendation . . . . .	89
9. Acknowledgments . . . . .	91
10. Bibliography . . . . .	93
Appendix. Processing of GPS Data for 1994 Project . . . . .	99

## GRAPHS

Graph 3.1. Camera-wing Z difference vs. time. . . . .	24
Graph 3.2. St. Louis test 1 (photogrammetry) vs. GPS. . . . .	25
Graph 3.3. Original and filtered height. . . . .	26
Graph 5.1. Flight path of Surdex aircraft. . . . .	40
Graph 5.2. Position solution for tail antenna for flight #1. . . . .	41
Graph 5.3. Comparison of $\omega$ values–high flight. . . . .	43
Graph 5.4. Comparison of $\omega$ values–low flight. . . . .	44
Graph 5.5. Original and filtered C-R. . . . .	45
Graph 5.6. Change in length of wing with time. . . . .	46
Graph 5.7. Spec for high flight–high frequency. . . . .	48
Graph 5.8. Spec for high flight–low frequency. . . . .	49

## FIGURES

Figure 2.1. Coordinate system. . . . .	6
Figure 2.2. Stereo plotter. . . . .	7
Figure 2.3. Global positioning system. . . . .	9
Figure 2.4. Interferometric method. . . . .	10
Figure 2.5. Z-12 technical specifications. . . . .	11
Figure 2.6. Ashtech Z-12 <sup>tm</sup> GPS receiver. . . . .	12
Figure 2.7. Multiantenna locations. . . . .	14
Figure 2.8. Triplet . . . . .	15
Figure 3.1. Aircraft used in tests. . . . .	18
Figure 3.2. Aircraft dimension. . . . .	19
Figure 3.3. Camera and receiver inside aircraft. . . . .	20
Figure 3.4. St. Louis GCP flight plan. . . . .	21
Figure 4.1. Campus flight plan diagram. . . . .	30
Figure 4.2. Low-flight campus flight plan. . . . .	33
Figure 5.1. Aircraft with four antennas. . . . .	36
Figure 5.2. Change in scale of wings . . . . .	47
Figure 6.1. ISU campus control. . . . .	56
Figure 6.2. Highway 30 flight, 1994. . . . .	57
Figure 6.3. Highway 30 control. . . . .	58
Figure 6.4. Airport control. . . . .	59
Figure 6.5. GPS receiver arrangement in the aircraft. . . . .	60
Figure 6.6. GPS data collection on photo mission. . . . .	61
Figure 6.7. Project 1994. . . . .	63
Figure 6.8. Campus flight 1994. . . . .	64
Figure 6.9. Base station GPS data collection . . . . .	65
Figure 6.10. Antenna locations at taxi point. . . . .	66
Figure 6.11. Computation of $\phi_G$ , $\omega_G$ , $k_G$ . . . . .	67
Figure 6.12. Sources of error in $\omega_P$ . . . . .	76
Figure 7.1. Rectification. . . . .	84
Figure 7.2. Orthophoto production . . . . .	86

## TABLES

Table 3.1. Camera antenna position. . . . .	22
Table 3.2. Wing antenna position. . . . .	23
Table 3.3. Comparison of $\omega$ by GPS and photogrammetry. . . . .	28
Table 4.1. Camera location from navigation software. . . . .	31
Table 4.2. Comparison of GPS navigation and photogrammetry. . . . .	32
Table 5.1. Camera antenna position. . . . .	37
Table 5.2. Right wing antenna position. . . . .	38
Table 5.3. Tail antenna position. . . . .	39
Table 5.4. Omega, phi, kappa, and scale by GPS. . . . .	42
Table 5.5. Comparison of $\omega$ values. . . . .	50
Table 5.6. Comparison of exterior orientation elements. . . . .	52
Table 6.1. Results of flight 1 for entire time. . . . .	68
Table 6.2. Data of flight 1 for exposure time. . . . .	70
Table 6.3. Photo-GPS location. . . . .	71
Table 6.4. GPS-Photo orientation. . . . .	73
Table 6.5. Results of combination of high and low flights. . . . .	74
Table 6.6. $\omega_G$ to $\omega_p$ using different weights. . . . .	77
Table 6.7. GPS-Photo locations using refined data. . . . .	79
Table 6.8. $\omega_G$ to $\omega_p$ using refined data. . . . .	81
Table 6.9. First and second difference in $\omega_p - \omega_G$ . . . . .	82
Table A-1. Data of flight 1 for entire time. . . . .	102
Table A-2. Results of flight 1 for entire time. . . . .	103

## EXECUTIVE SUMMARY

The airborne Global Positioning System (GPS) research project began in April 1993; a series of four tests were carried out in St. Louis, Missouri and in Ames, Iowa. All of the tests, except one, were performed in cooperation with Ashtech, a GPS firm located in Sunnyvale, California and Surdex Inc., a photogrammetric firm located in St. Louis, using Cessna aircraft, LMK 2000 cameras, and Ashtech receivers. The photo coordinates were observed using a Wild STK1 stereo comparator and were processed using Sat9, RO, Albany, and Calib softwares. The GPS data were processed using GPPS and PNAV software. The objective of this research project was to use a GPS to determine the best aerial camera location and orientation for mapping.

In the first test, the camera antenna and left wing antenna were mounted on the aircraft, which was flown over the St. Louis site. The test proved that observations can be taken using wing and camera antennas and that wing motion can be modeled to get the  $\omega$  rotation.

In the second test, the navigation antenna was mounted on the aircraft's fuselage. A Trimble C/A code receiver was used with real-time photo mission navigation software. In a flight over the Iowa State University (ISU) campus test site, Aerial Services Inc. took photographs. This test proved that pinpoint navigation is feasible in the x-y direction and has an accuracy of  $\pm 25$  meters. Because the C/A code was used in real time, the accuracy may be about  $\pm 50$  meters in the z direction, which can be avoided by using either a P code GPS receiver or the usual on-board aneroid barometer.

In the third test, four antennas were used: camera, left wing, right wing, and tail. In this test flight over the St. Louis site, two GPS L<sub>1</sub>/L<sub>2</sub> P12 receivers and one 3DF GPS receiver were used. The test proved that the tail antenna is not suitable due to multipath, that the 3DF GPS receiver is not suitable for airborne GPS applications because it is an L<sub>1</sub> GPS receiver, and that at least seven satellites are needed for reliable PNAV solutions.

In the final test, one navigation antenna; four airborne GPS antennas: camera, left wing, right wing, and forward; four Z12 receivers on-board; and two Z12 receivers on the reference stations were used. This test confirmed that (1) photo coordinates have to be observed two or more times to eliminate small errors, (2) ground elevations established by GPS may have  $\pm 10$  centimeters errors because of local geoid undulation, (3) the photographic site has to be within 10 kilometers of the reference base station, (4) the camera antenna coordinates have to be corrected for geoid undulation, and (5) the accuracy of the Z12 is 0.2 millimeters, which neglects the multipath, resulting in the accuracy of  $\pm 0.0001$  radians or better in the  $\omega$  angle.

In summary, the project showed that airborne GPS is feasible for aerial camera location and orientation. In block triangulation, no ground control is required if the site is within 10 kilometers of the reference base station. In a strip, a self calibration is required to transform  $\omega_G$  to  $\omega_p$  and the

calibration site is within 10 kilometers of the photographic site or the height differences between two or more ground control points in the direction perpendicular to the flight are known.

The project was conducted by the Engineering Research Institute of ISU with funding provided by a grant from the Iowa Highway Research Board.

## 1. INTRODUCTION

A Global Positioning System (GPS) can be used in different applications. The objective of this project, Airborne GPS, was to use a GPS to determine the aerial camera location and orientation that best facilitated mapping done from aerial photographs without any ground control.

In the period April 1993 to April 1995, K. Jeyapalan, Wu Yao, S. D. Savathchandra, Nadella V. Narayan, Scott M. McMahon, and Jingfeng Kang organized this research, conducted four test flights, and analyzed the data. The first test flight was performed in June 1993 at St. Louis, with the objective of testing the multiantenna concept using two antenna on the aircraft. The second test in August 1993 was conducted over the Iowa State University (ISU) campus at Ames. This flight evaluated the use of GPS for pinpoint navigation. The third test flight over St. Louis was flown in October 1993, with four antenna on aircraft; its objective was to evaluate the 3DF GPS receiver and the antenna locations.

On the basis of these three test results, a final test flight over the Mustang Project area in Ames and the ISU campus was conducted in June 1994. Analysis of these data showed that airborne GPS can be used (1) in pinpoint navigation with an accuracy of 25 meters or better, (2) to determine the location of the camera nodal point with an accuracy of 10 centimeters or better, and (3) to determine the orientation angles of the camera with an accuracy of 0.0001 radians or better.

In addition, the exterior orientation elements determined by airborne GPS can be used to rectify aerial photos, to produce orthophotos, and in direct stereo plotting. Further research is recommended in these areas to maximize the use of airborne GPS.

Previous reports [34, 35] have discussed in detail the theory of GPS and photogrammetry. Also the previous reports gave details of the software—Sat9, RO, Albany, Geolab, GPPS, and Calib—used in this project except for PNAV. Ashtech Inc. developed the PNAV software, which is briefly described in the appendix.

The work performed for this research project and its conclusions and recommendations are in the following chapters:

2. Photogrammetry and kinematic GPS
3. Analysis of first test
4. Analysis of second test
5. Analysis of third test
6. Analysis of final test
7. Applications of airborne GPS
8. Conclusions and recommendations

## 2. PHOTOGRAMMETRY AND KINEMATIC GPS

References [34,35] give detailed information about photogrammetry and GPS. The objective of this chapter is to describe briefly photogrammetry and kinematic GPS as they relate to airborne GPS.

### 2.1. Photogrammetry

In photogrammetry the photo coordinates  $(x, y)$  are related to the ground coordinates  $(X_G, Y_G, Z_G)$  (see Fig. 2.1) by the following equation:

$$x - x_o = f \left( \frac{a11(X_G - X_o) + a12(Y_G - Y_o) + a13(Z_G - Z_o)}{a31(X_G - X_o) + a32(Y_G - Y_o) + a33(Z_G - Z_o)} \right) + \text{radial distortion} + \text{decentering distortion} + \text{refraction}$$

$$y - y_o = f \left( \frac{a21(X_G - X_o) + a22(Y_G - Y_o) + a23(Z_G - Z_o)}{a31(X_G - X_o) + a32(Y_G - Y_o) + a33(Z_G - Z_o)} \right) + \text{radial distortion} + \text{decentering distortion} + \text{refraction}$$

where  $x_o, y_o, f$  are interior orientation elements,  $(X_o, Y_o, Z_o)$  are the nodal point coordinates in the ground coordinates system (see Fig. 2.1).

and

$$A = R_K R_\phi R_\omega = \begin{pmatrix} a11 & a12 & a13 \\ a21 & a22 & a23 \\ a31 & a32 & a33 \end{pmatrix}$$

Where  $R_K, R_\phi, R_\omega$  are the rotation matrix required to make the photo coordinates axes  $(x, y, z)$  parallel to the ground coordinate axes by rotating first about  $x$  axis by  $\omega$ , then about  $y$  axis by  $\phi$ , and finally about  $z$  axis by  $K$ . The  $K, \phi$ , and  $\omega$  are known as the orientation angles. The  $X_o, Y_o, Z_o, K, \phi$ , and  $\omega$  are known as the exterior orientation elements.

The objective of photogrammetry is to determine  $(X_G, Y_G, Z_G)$  of a point from the photo coordinates of two or more photographs. This is done by three methods: analog, analytical, and self calibration.

In the analog method, the interior orientation and radial and decentering distortions are assumed to be small. The projectors are used to project the images and produce the stereo models (see Fig. 2.2). When producing the stereo model, five of the twelve exterior orientation elements

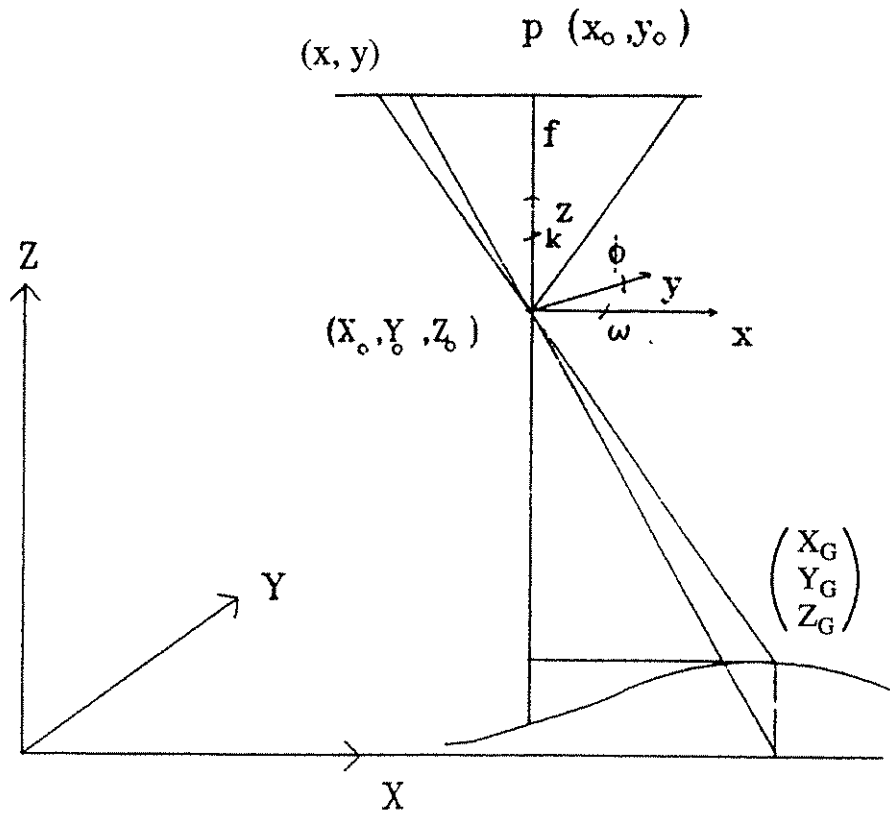


Figure 2.1. Coordinate system.

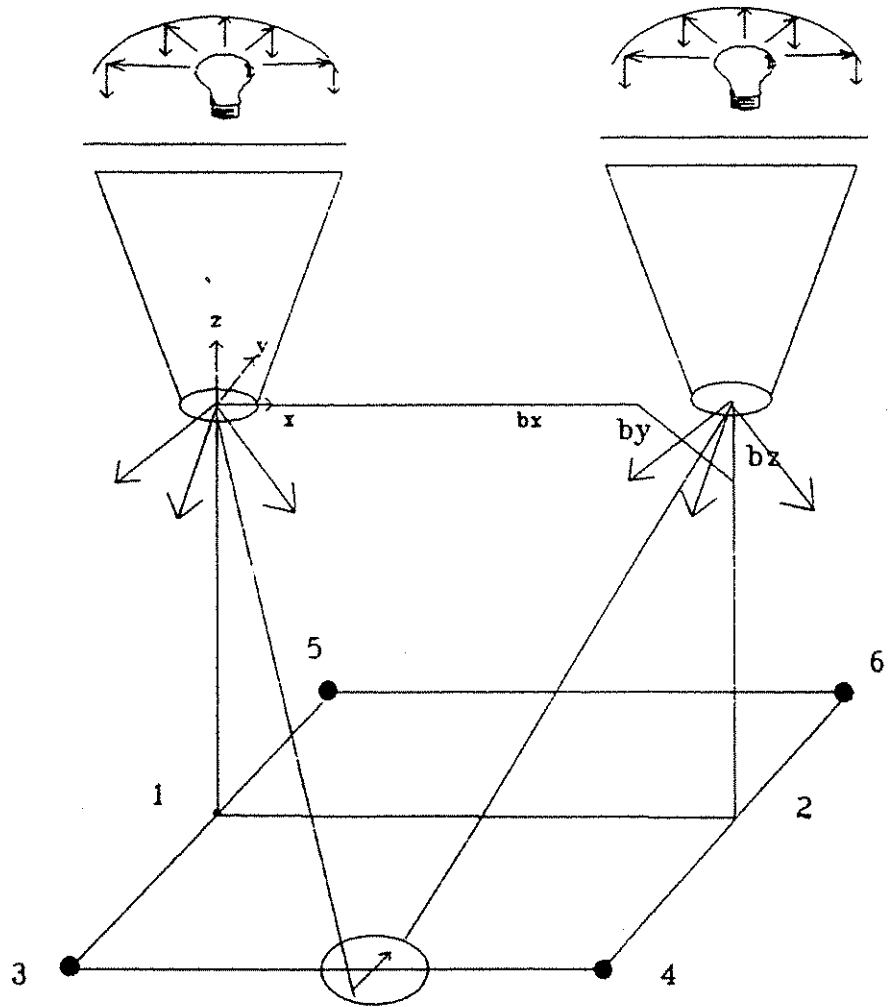


Figure 2.2. Stereo plotter.

are determined by relative orientation. The stereo model is scaled and leveled using external ground control points, determining the other seven exterior orientation elements. Special instruments such as a Zeiss Z8 are designed to produce the stereo model and then plot the map.

In the analytical method, the photo coordinates are corrected for interior orientation and for radial and decentering distortions given by the calibration of the camera. The photo coordinates of two or more photos, together with three or more known ground controls, are simultaneously adjusted to give the ground coordinates. Software such as Albany is capable of such adjustment. Some stereo plotters, which are connected to computers for doing these computations in real time and which assist in driving the plotters, are known as analytical plotters.

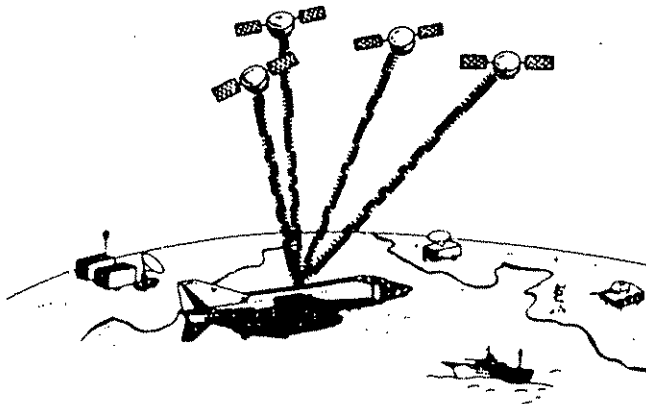
In self calibration, the interior orientation elements, the radial and decentering lens distortion elements, and the exterior orientation elements are simultaneously determined with unknown ground control points using the photo coordinates of two or more photos and a number of ground control points. The method used is normally the least-squares constraint method in which any of the parameters are constrained to its known accuracy. The program such as Calib is capable of this adjustment.

## 2.2. Kinematic GPS

The GPS consists of 24 satellites orbiting about 20,000 kilometers above the earth (see Fig. 2.3). The satellites transmit information in two carrier frequencies  $L_1$  and  $L_2$  modulated by two codes P and C/A code.

Differential GPS tracks the same satellites from two stations. Using the carrier phase frequency, the base line vector can be computed accurately (see Fig. 2.4). The accuracy depends on the accuracy of the phase measurement, error due to the multipath, and the ionospheric error depending on the distance between the two stations. The use of P and C/A code may eliminate the multipath, and use of  $L_1$  and  $L_2$  may eliminate the ionospheric error. The Z12 Ashtech receiver measures the phase to an accuracy of 0.2 millimeters and has the capability of tracking  $L_1$  and  $L_2$  frequencies (see Fig. 2.5).

In kinematic GPS one of the receivers is fixed at the base station and the other is free to move. The phase angle from each satellite is measured continuously. However, only portions of the phase angle less than  $2\pi$  are measured at one time; hence the receiver has to keep track of the total phase angle and the integer number of  $2\pi$ . When a receiver moves, it may lose track of a satellite and lose the integer number of  $2\pi$ . Knowing the position of the base receiver and the position of the rover, using the other satellites, the lost integer count can be calculated. The PNAV software is capable of resolving the integer ambiguity on the fly, provided there are more than seven satellites at a time (see Fig. 2.6)



**CHARACTERISTICS**

- SIGNALS: L<sub>1</sub> - 1575 MHz (P & C/A CODE)  
L<sub>2</sub> - 1227 MHz (P or C/A CODE)
- EXPECTED ACCURACY (90%)

	P SIGNAL	C/A SIGNAL
POSITION	30 FT	< 300 FT
VELOCITY	0.1 FT/SEC	< 1 FT/SEC
TIME	10 NS	< 100 NS

**GPS PROGRAM SCHEDULE**

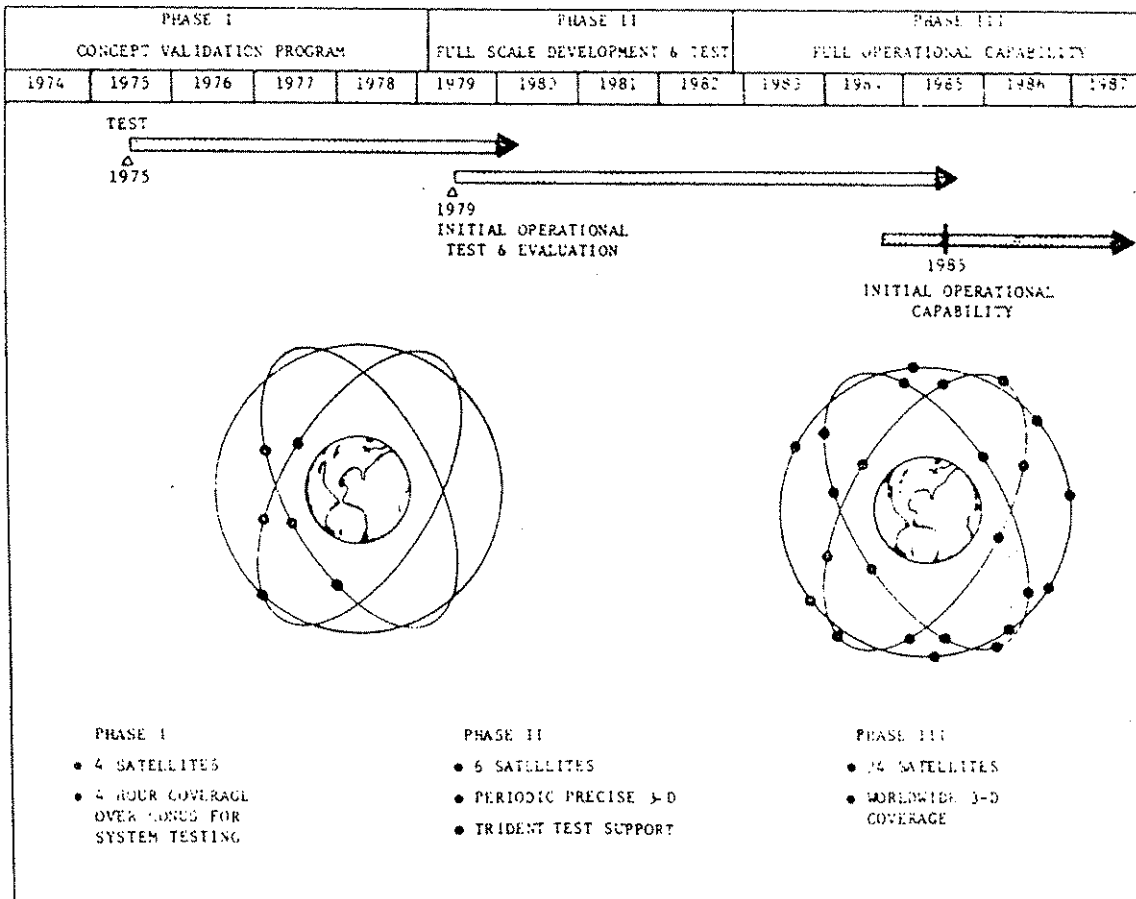


Figure 2.3. Global positioning system.

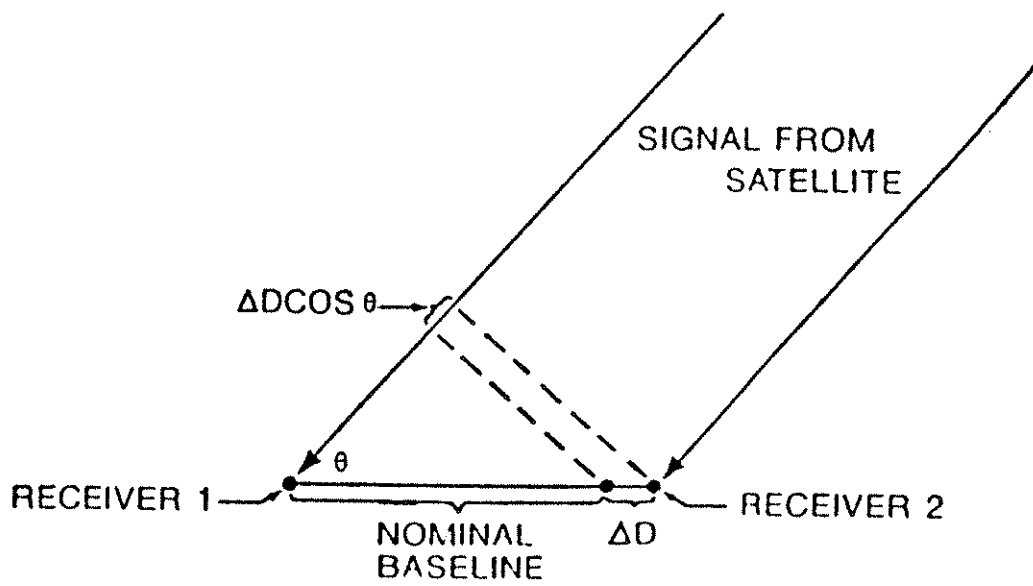


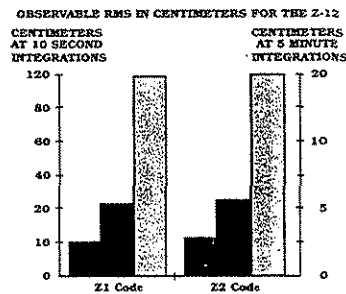
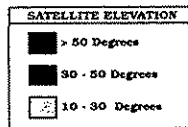
Figure 2.4. Interferometric method.

## Z-12 Technical Specifications

### Measurement Precision

<b>C/A (&gt;25°)</b>		
Carrier phase	(25 Hz)	0.15 cm
	(1 sec)	0.02 cm
Pseudo-range	(10 sec)	20.00 cm
	(5 sec)	3.60 cm
<b>P-Code A/S Off (&gt;25°)</b>		
L1 Carrier phase	(10 sec)	0.10 cm
	(5 min)	0.02 cm
L1 Pseudo-range	(10 sec)	5.00 cm
	(5 min)	0.90 cm
L2 Carrier phase	(10 sec)	0.10 cm
	(5 min)	0.02 cm
L2 Pseudo-range	(10 sec)	7.00 cm
	(5 min)	1.30 cm
Real-Time Differential Position		<1 m
	(PDOP<4)	
Statis. Rapid Static or Pseudo-Kinematic Survey		5 mm + 1 ppm

### P-Code A/S On (Z-Tracking)



### Systematic Errors (Between Satellites)

Pseudo-Range (all bands)	< 1.00 cm
Carrier Phase (all bands)	< 0.01 cm

Ashtech P-Code GPS receivers have been FGCC tested and are capable of performing first order survey (report available upon request).

Z-12, Z-Tracking, PNAV and PRISM II are trademarks of Ashtech Inc.

Specifications are subject to change without notice



### Environmental

Waterproof to	5 psi
<b>Temperature Ranges</b>	
Receiver/data Logger	
Operating	-20° to +55°C
Storage	-30° to +75°C
Antenna	
Operating	-40° to +65°C
Storage	-55° to +75°C
<b>Humidity</b>	100%
<b>Weight</b>	
Receiver	8.8 lbs
Antenna	3.75 lbs
<b>Speed (Max)</b>	Does not exceed 1,000 nautical miles-per-hour
<b>Altitude (Max)</b>	Does not exceed 60,000 Ft.

*Higher altitude and velocities up to 25,000 nautical miles-per-hour options are available in the U.S. and under validated export license for other countries.*

### Standard Features

- 12 Channel "All-In-View" operation
- Automatic Switching to Z-Tracking when A/S is activated.
- Full wavelength carrier on L1 and L2
- 21 Watt power consumption (typical)\*
- 10 - 32 VDC input
- 2 Power inputs
- Audible alarm for low power
- Internal RAM data recorder
- 8-Line by 40-character display
- 4 RS-232 ports (115,200 baud max)
- Static, rapid static, kinematic, pseudo-kinematic surveys
- Waypoint navigation
- Real-time data outputs
- 1 PPS timing signal
- Cold start - 2 Minutes to first data
- Warm start - <30 Seconds to first data
- 1 Year warranty

### Standard Accessories

- Precision geodetic antenna
- 10-meter antenna cable
- External power cable
- RS-232 data cable (Z-format)
- Battery and charger
- Rotatable Tribrach adapter
- High-impact shipping case
- Receiver operating manual (Shipping weight of standard Z-12 package is 48 pounds)

### Optional Features

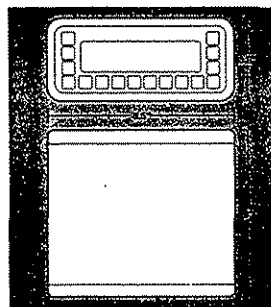
- External frequency standard input 1 to 20 MHz in 10KHz steps
- Real-time differential GPS RTCM format
- Expanded internal memory

### Optional Accessories

- Survey Tribrach
- Kinematic bipod and pole
- 10, 30 and 60-meter antenna cable Expandable to 150 meters w/line amps
- External battery
- Battery charger 110/120 VAC
- PRISM IITM Software Package
- PNAV Software Package

\*Display off/with LNA

### Dimensions



1170 Kifer Road • Sunnyvale, CA 94086 • (408) 524-1400 • Fax (408) 524-1500  
 Park Place Moscow • 113 Leninski Prospekt • Moscow • Russia • (7502) 256-5400 • Fax (7502) 256-5360  
 Blenheim Office Park • Lower Road • Long Hanborough • Oxfordshire OX8 8LN • England • 44 993 883 533 • Fax 44 993 883 977



294

Figure 2.5. Z-12 technical specifications.

# Ashtech Z-12™ GPS Receiver



## Full GPS Capability with Anti-Spoofing Turned On

Ashtech's "Dual-Line Digital" Z-12 GPS Receiver sets the standard in GPS receiver performance and technology for precise surveying and navigation applications. This revolutionary new GPS receiver permits uninterrupted use even when Anti-Spoofing (AS) is turned on. When Anti-spoofing is turned on, the Z-12 receiver automatically activates its Z-Tracking™ mode which mitigates the effects of AS. When AS is off, the Z-12 automatically reverts to P-Code mode.

The Z-12 is a new receiver. It is the result of major improvements in all areas of receiver design: RF, digital processing hardware, and substantial algorithmic improvement. As a result, not only does the receiver deliver unmatched performance in "Z" mode, but the performance in "P" mode is world-class (substantially improved over the performance of the pioneering Ashtech P-12).

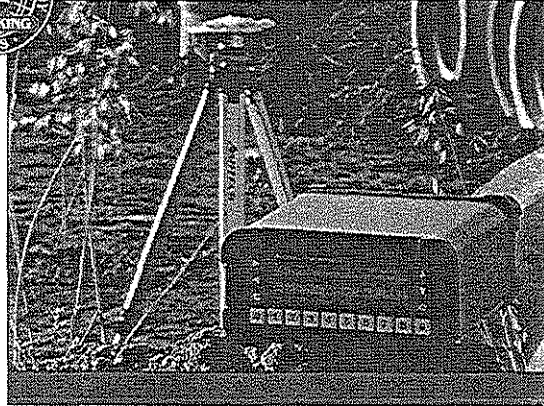
The technological advance represented by this receiver is even more dramatic under Anti-Spoofing (A/S) conditions where the patented Z mode observables enjoy an over 13 dB SNR advantage over their "P-codeless" (cross-correlation) competitors while maintaining the P-mode's freedom from receiver caused systematic errors. Indeed, the receiver measures the same things in both modes: C/A carrier phase and pseudo-range, P1 carrier phase and pseudo-range, P2 carrier phase and pseudo-range, all with full (not 1/2) carrier wavelengths. There are no "glitches" associated with a mode change, no changes in the already negligible systematic errors. For the overwhelming majority of users, the performance of the receiver when A/S is enabled is indistinguishable from the "A/S off" performance.

The Ashtech receiver's patented Z technique is the only available technology that offers an over 13 dB improvement in SNR over cross-correlating receivers along with full wavelength carrier phases on both P-code bands when A/S is enabled.

### Mile-a-Minute Surveying

Dual-frequency reception eliminates ionospheric refraction effects, which means medium-to-longer baselines can be measured more accurately. High-quality measurements on both the L1 and L2 bands in the Z-Tracking mode or the P-Code mode also enable significantly shorter station occupation time — this translates into increased productivity for high-precision survey crews. Centimeter-level surveying of baselines of one mile using one minute station occupation times has been successfully demonstrated in Z-Tracking Mode!

GPS surveying. The PNAV module is based on an advanced Kalman filter design which allows for nearly instantaneous centimeter-level surveying and navigation for station separations under 10 kilometers.



### Seconds vs. Minutes

A 13 dB SNR advantage means a factor of 20 less in integration time for the same observable RMS. Based on actual measurements on real satellites, we need to integrate for 10 seconds to the cross correlation competition's 5 minutes. There are two great advantages to having shorter correlation times for the same SNR:

- The ability to track rapidly varying ionosphere with full observable accuracy. This cannot be accomplished with cross correlating receivers.
- Acquisition transients settle in seconds while the competition has to wait minutes before their A/S observables reach equivalent accuracy.

The ability to derive any useful information at low elevations is critically tied to SNR. When faced with low SNR, the user has a terrible choice: either integrate for such a long time that there is essentially no data at low elevations, or accept huge errors. For all non-classified "A/S on" solutions, the SNR falls off with elevation angle as the square of normal code SNR. That is, if the P mode SNR drops (with elevation angle) by a factor of 4, all civilian A/S techniques yield a drop in the SNR of a factor of 16.

### Better Jam Immunity

Because of Ashtech's Dual-Line Digital processing capability, jam immunity is substantially improved over other single bit receivers. The receiver does not lose lock near transmitters or high voltage power lines. The result is higher productivity, robust performance and virtually no restrictions due to an encrypted satellite signal.

### PNAV "On-the-Fly" Ambiguity Resolution

Ashtech's newest application software package is called PNAV (for Precision Navigation). This software, combined with dual-frequency data from Z-12 receivers provides a powerful new capability in GPS. PNAV is a precision trajectory package providing post-processed positions and can provide centimeter level accuracy on-the-fly. This capability is especially valuable for creation of robust photogrammetric flight trajectories.

A PNAV survey version which produces vectors for network adjustments is a standard feature of the PRISM II™ software package.



Figure 2.6. Ashtech Z-12™ GPS receiver.

### 2.3. Application of Kinematic GPS in Photogrammetry

If a GPS antenna is fixed above the camera nodal point in an aircraft (camera antenna), then its position, (see Fig. 2.7.) determined in real time by the kinematic mode, can be used to take aerial photos at predetermined locations. Thus kinematic GPS is used in pinpoint navigation for photogrammetric mapping.

Using differential kinematic GPS, the camera's location ( $X_0, Y_0, Z_0$ ) can be determined precisely. Thus, in a stereo pair, of the 12 exterior orientation elements, six can be determined by kinematic GPS methods. Five of the exterior elements can be determined by relative orientation and the twelfth element,  $\omega$ , has to be determined by external ground control.

In a triplet with two photos in the y direction and two photos in the x direction (see Fig. 2.8.), kinematic GPS can be used to determine nine exterior orientation elements and the relative orientation to determine the other nine exterior orientation elements.

In an aircraft, if four antennas are mounted as shown in Fig. 2.7 such that the left wing antenna and the right wing antenna are along the y axis of the aircraft and the camera antenna C and the forward antenna F are along the x axis, then kinematic GPS can be used to determine the locations of these antennas at the time of the exposure. From the location of the antennas, the rotation angles of the aircraft with respect to the ground system ( $X_G, Y_G, Z_G$ ) can be obtained from:

$$\sin \omega_G = (Z_r - Z_l) / LR$$

$$\sin \phi_G = (Z_f - Z_c) / FC$$

$$\sin K_G = (Y_f - Y_c) / FC$$

If R is the rotation matrix which makes the camera axis ( $x_c, y_c, z_c$ ) parallel to the aircraft axis ( $x_A, y_A, z_A$ ), then the rotation angles of the camera is given by:

$$A = R A' R^T$$

where

$$A' = R K_G * R \phi_G * R \omega_G \text{ and } A = R K_c * R \phi_c * R \omega_c$$

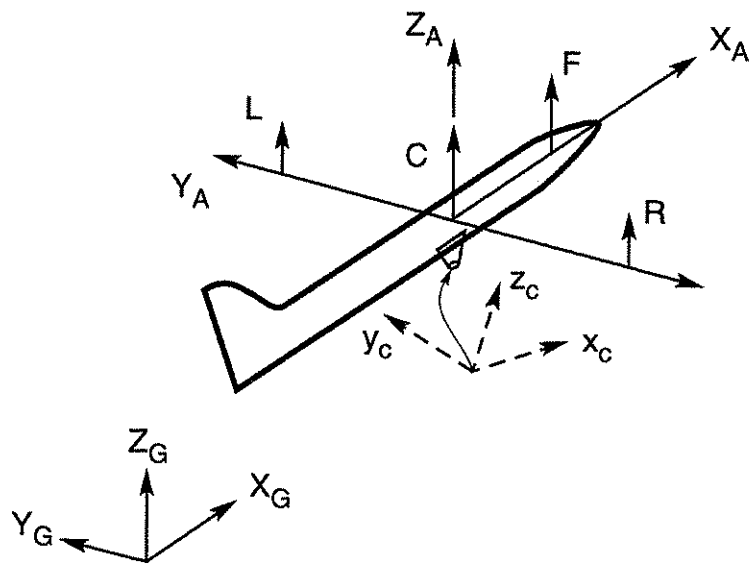


Figure 2.7. Multiantenna locations.

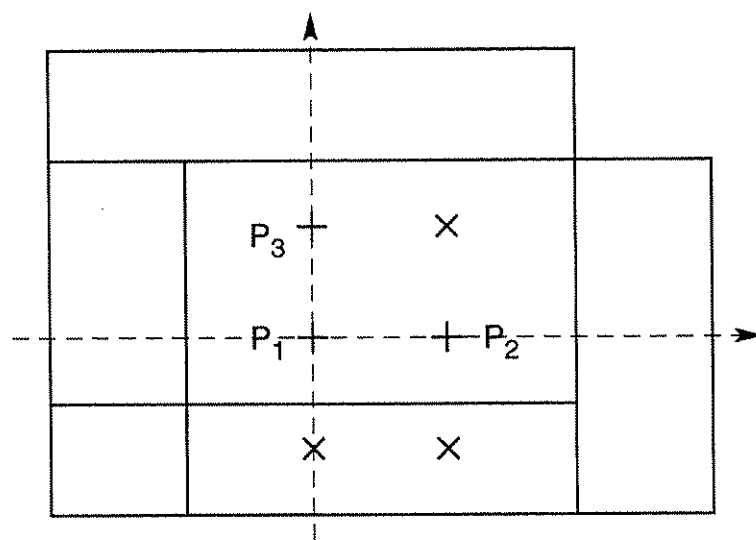


Figure 2.8. Triplet

Thus in an aerial photo all of the exterior orientation can be determined by kinematic GPS provided the parameters of the matrix  $R$  are determined by calibration. No ground control is required for rectification, stereo plotting, and orthophoto production.

### 3. ANALYSIS OF FIRST TEST

Figure 3.1 shows the Cessna 335 aircraft used in this project. An L<sub>1</sub>/L<sub>2</sub> GPS antenna was mounted about 1.164 meters above the nodal point of the camera. The camera was located on the center fuselage floor with its lens 0.775 meters above the taxiway. The second antenna (L<sub>1</sub>) was mounted on the left wingtip aft of the wingtip fuel tank. The wingtip L<sub>1</sub> antenna was approximately 1.62 meters above the taxiway and 5.12 meters from the camera antenna (see Fig. 3.2).

A P-12 GPS receiver was set over the base station, surdex, and two P-12 GPS receivers were placed inside the aircraft, connected to the camera and wing antennas (see Fig. 3.3). The GPS receivers recorded the position at every one-second interval. Photographs were taken over the test range in St. Louis at flying heights of 1,500 feet and 3,000 feet (See flight plan, Fig. 3.4). The GPS was used to tie the control points in the test range to the National Geodetic Network, enabling the control point coordinates to be transformed to the NAD83 system.

The GPS data were processed using the PNAV software. This software has the unique capability of precisely computing relative locations between two GPS stations when one or both receivers are moving. Tables 3.1 and 3.2 show the camera and wing antenna locations at the exposure times of the camera. Graph 3.1 shows the Z difference between the camera and wing antennas, indicating that the Z difference in the low flight was not reliable because the wing antenna is an L<sub>1</sub> antenna and was sometime tracking  $\leq$  four satellites (see Table 3.2). An L<sub>1</sub>/L<sub>2</sub> antenna enables the P code to be accessed and seven or more satellites enable the resolution of the ambiguity during the flight.

High and low flight photographs were observed using the wild stereocomparator. The data were initially processed by Albany software and then by Calib. Calib is a special software which can simultaneously calibrate the camera as well as constrain both exterior orientation elements and ground control.

Graph 3.2 shows the omega,  $w$ , angle from photogrammetry and GPS. The difference between them may be due to such factors as (1) deflection of the wing due to lift of the aircraft, (2) initial angular difference between the film plane of the camera and the plane of the aircraft wing, and (3) initial angular difference between the x axis of the camera and the main axis of the aircraft.

The difference arising out of the first factor may be difficult to model, but this may be overcome by using a filtering technique. Graph 3.3 shows the original and filtered height differences between the camera and wing antennas for the high-altitude flight. It appears that filtering eliminates the effect of the deflection to a first order. The second and third causes could be modeled by the equation



Figure 3.1. Aircraft used in tests.

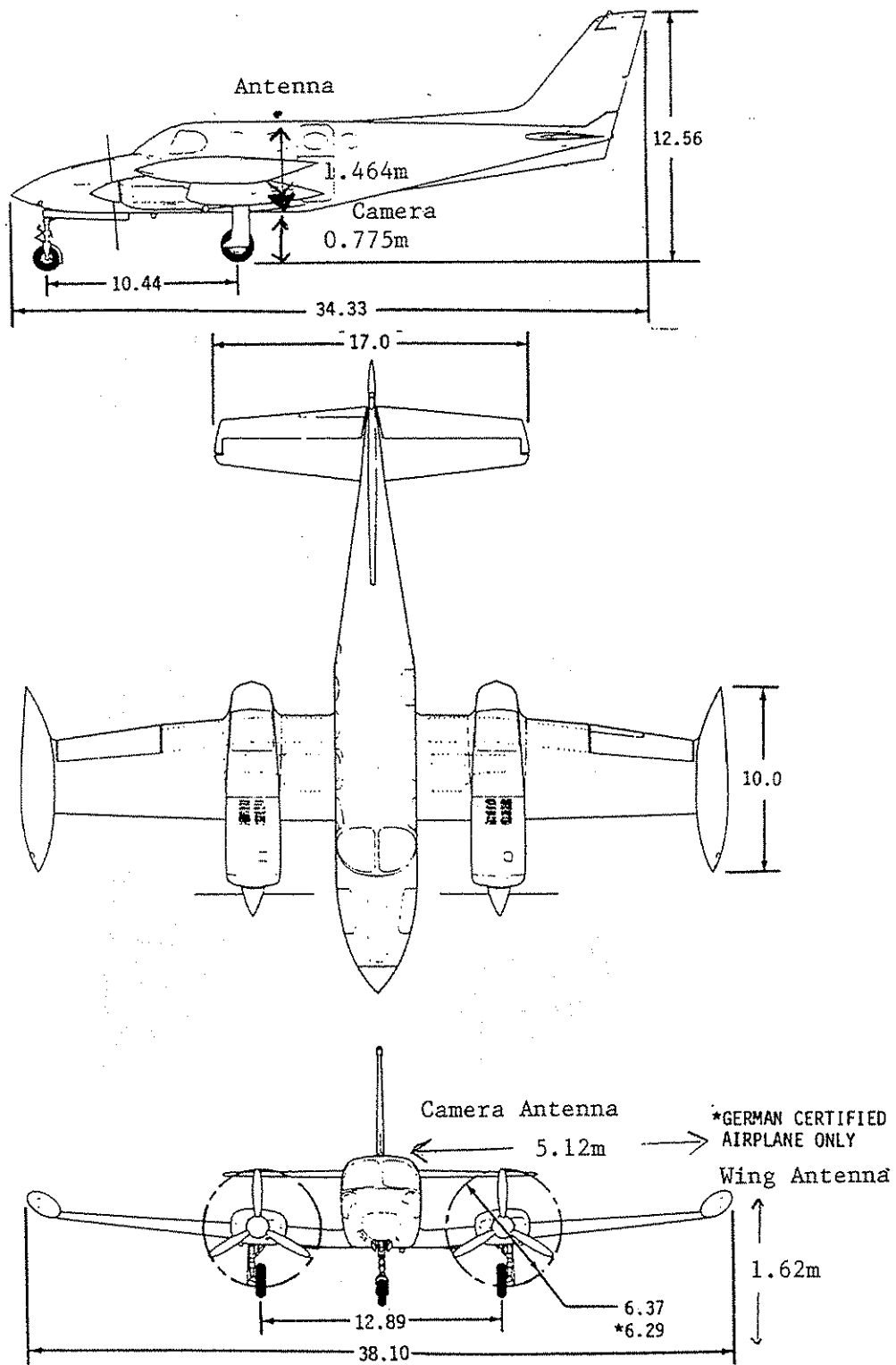
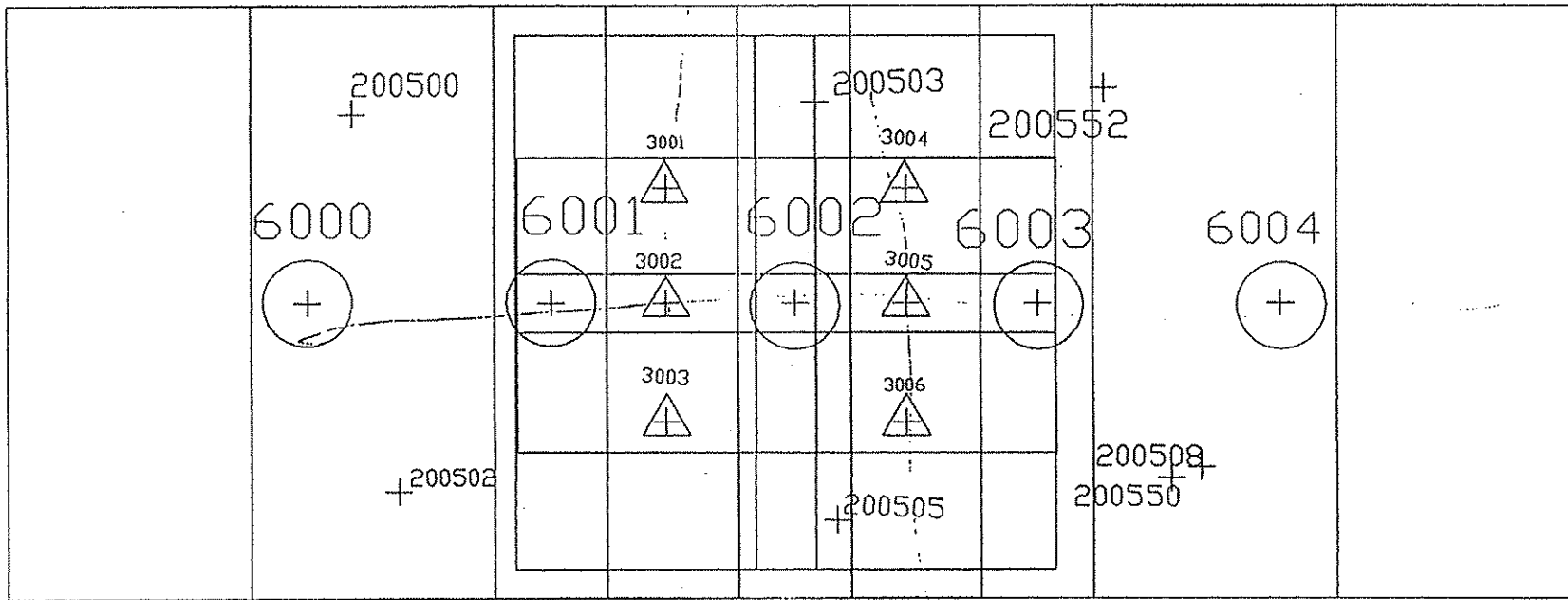


Figure 3.2. Aircraft dimension.



Figure 3.3. Camera and receiver inside aircraft.

3001 66685.6853	3004 68497.4139	6001 65811.6967	6000 63969.052
25938.7365	25938.7365	25034.2290	25034.229
3002 66685.4023	3005 68497.1309	6002 67654.3419	6004 71321.264
25033.1552	25033.1552	25034.229	25034.229
3003 66685.6853	3006 68497.4139	6003 69487.8032	
24127.5739	24127.5739	25034.2290	



Blue photo (circles)

scale = 1:5994.7

Flying Height = 912 Meters  
= 3000 ft

Green Photos (Triangles)

Scale = 1:3000

Flying Height = 456 meters  
= 1500 ft

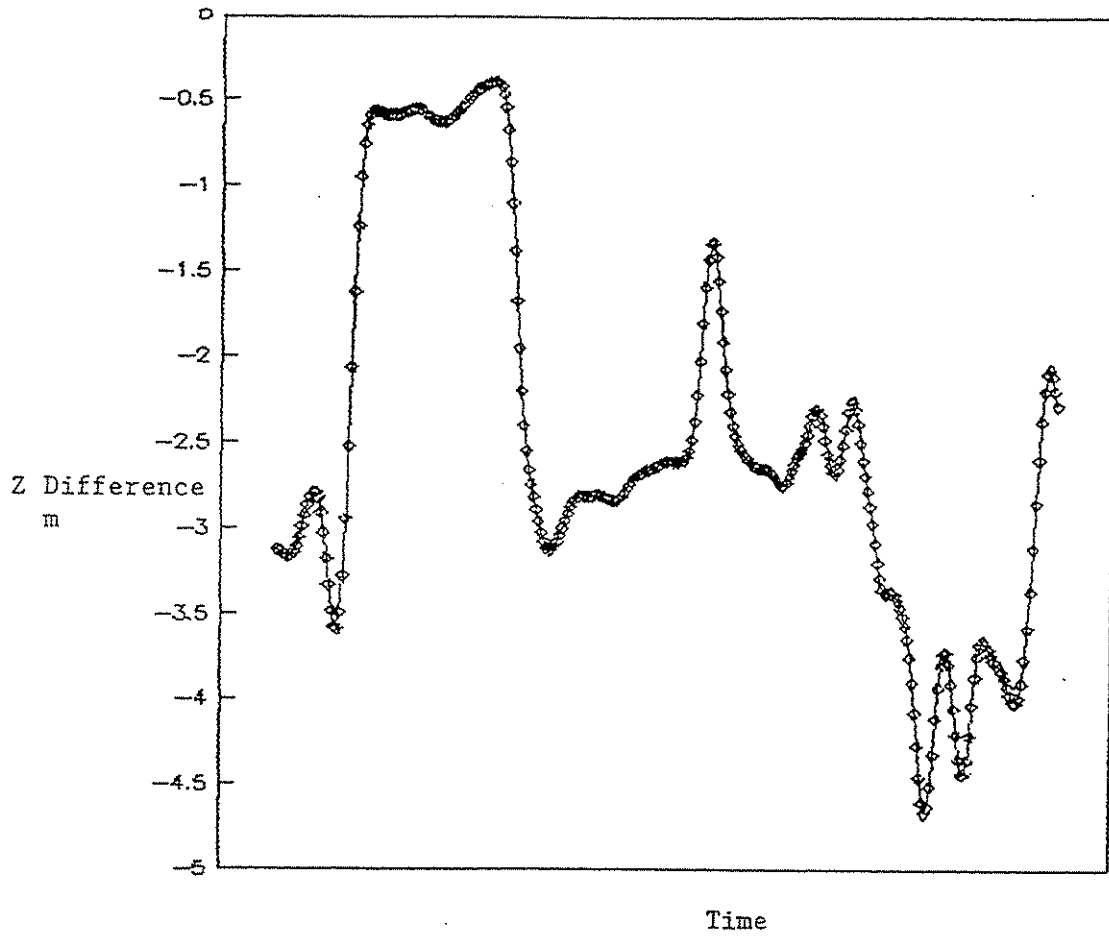
Figure 3.4. St. Louis GCP flight plan.

Table 3.1. Camera antenna position.

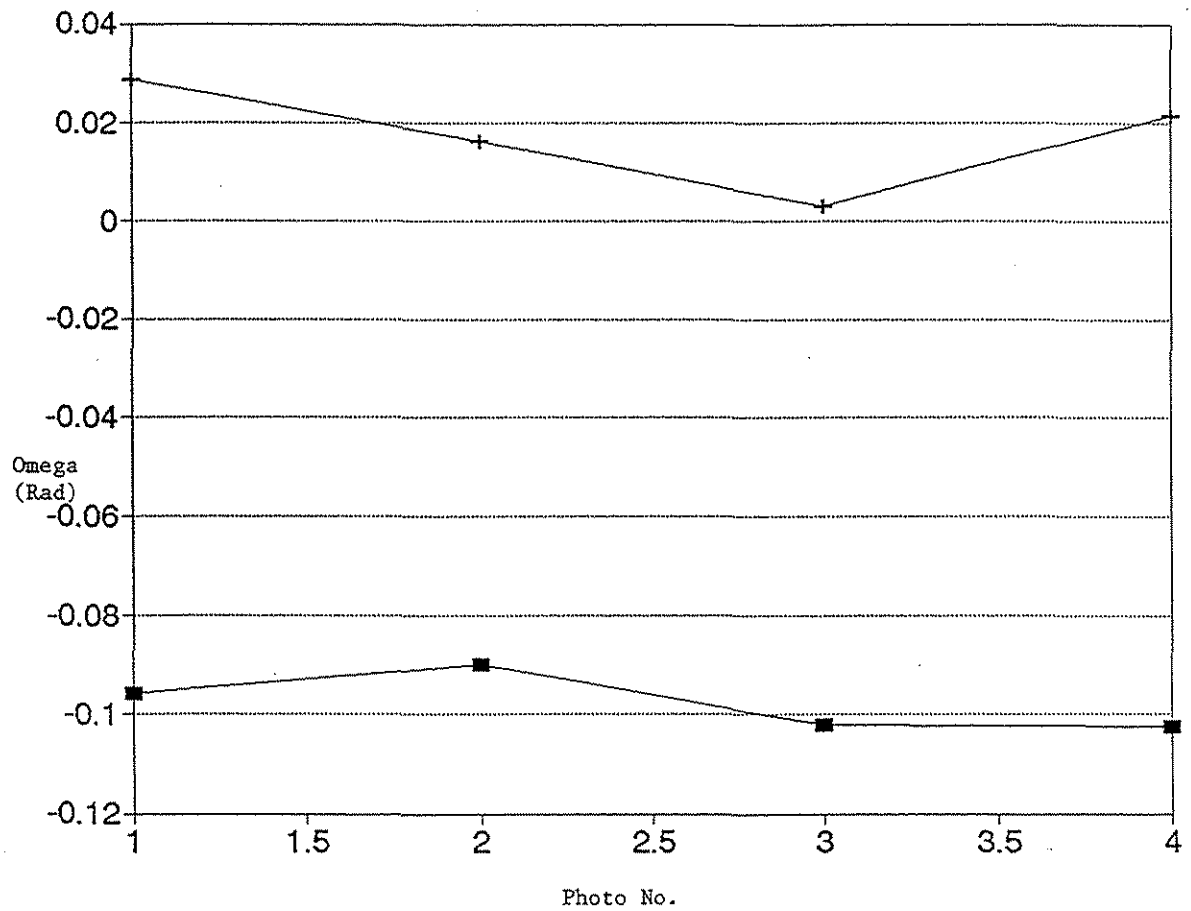
Ashtech, Inc. GPPS-2		Program:		PPDIFF-PNAV		Version: 1.0.00			
Fri Jun 25 15:23:08 1993		Differentially Corrected: Y							
SITE	MM/DD/YY	HH:MM:SS	SVs	PDOP	LATITUDE	LONGITUDE	HI	RMS	FLA
CAM	06/18/93	18:16:23.585673	5	2.7	N 38.60814481	W 90.53163375	1068.8826	2.049	I
CAM	06/18/93	18:16:29.828086	5	2.7	N 38.60840557	W 90.52561823	1068.0290	1.826	I
CAM	06/18/93	18:16:36.017254	6	1.7	N 38.60851563	W 90.51963235	1069.0855	1.635	I
CAM	06/18/93	18:16:42.185334	6	1.7	N 38.60841572	W 90.51366884	1068.0791	1.509	I
CAM	06/18/93	18:16:48.337325	6	1.7	N 38.60812420	W 90.50773600	1069.7288	1.310	I
CAM	06/18/93	18:19:45.655955	6	1.7	N 38.60427379	W 90.53802597	1072.8417	0.068	I
CAM	06/18/93	18:19:51.969862	6	1.7	N 38.60419676	W 90.53187493	1070.5799	0.065	I
CAM	06/18/93	18:19:58.331937	6	1.7	N 38.60414787	W 90.52563637	1063.9343	0.066	I
CAM	06/18/93	18:20:04.669017	6	1.7	N 38.60418914	W 90.51944614	1068.6901	0.066	O
CAM	06/18/93	18:20:10.985137	6	1.7	N 38.60423492	W 90.51330227	1071.9530	0.066	O
CAM	06/18/93	18:20:17.316511	6	1.7	N 38.60418153	W 90.50713015	1070.2359	0.068	O
CAM	06/18/93	18:27:28.610186	6	2.2	N 38.60962613	W 90.53931169	614.2640	0.079	I
CAM	06/18/93	18:27:32.032063	6	2.2	N 38.60729378	W 90.53932446	607.9829	0.080	I
CAM	06/18/93	18:27:35.487433	6	2.2	N 38.60492525	W 90.53932403	605.9202	0.081	I
CAM	06/18/93	18:27:38.936745	6	2.2	N 38.60256145	W 90.53929651	603.2630	0.081	I
CAM	06/18/93	18:27:42.375848	6	2.2	N 38.60021814	W 90.53924389	604.8433	0.082	I
CAM	06/18/93	18:27:45.815082	6	2.2	N 38.59788925	W 90.53916872	609.2007	0.083	I
CAM	06/18/93	18:27:49.275442	6	2.2	N 38.59554716	W 90.53908677	614.3134	0.083	I
CAM	06/18/93	18:30:31.346137	5	2.3	N 38.61053401	W 90.53297650	612.2416	0.087	O
CAM	06/18/93	18:30:34.777854	5	2.3	N 38.60824978	W 90.53302490	614.5882	0.089	O
CAM	06/18/93	18:30:38.224967	5	2.3	N 38.60594255	W 90.53308690	611.5037	0.089	O
CAM	06/18/93	18:30:41.670012	5	2.3	N 38.60362118	W 90.53311293	608.0161	0.089	O
CAM	06/18/93	18:30:45.123006	5	2.3	N 38.60128680	W 90.53310013	609.9188	0.091	O
CAM	06/18/93	18:30:48.589834	5	2.3	N 38.59893760	W 90.53307505	608.5319	0.091	O
CAM	06/18/93	18:30:52.051058	5	2.3	N 38.59658578	W 90.53303432	609.0656	0.092	O
CAM	06/18/93	18:30:55.489186	5	2.3	N 38.59424555	W 90.53297811	610.0461	0.093	O
CAM	06/18/93	18:35:46.817115	6	1.9	N 38.61054596	W 90.52604396	601.0599	0.081	O
CAM	06/18/93	18:35:50.267464	6	1.9	N 38.60821712	W 90.52594924	604.3646	0.081	O
CAM	06/18/93	18:35:53.708846	6	1.9	N 38.60591423	W 90.52585784	610.4836	0.083	O
CAM	06/18/93	18:35:57.143818	6	1.9	N 38.60362267	W 90.52577089	611.4512	0.083	O
CAM	06/18/93	18:36:00.598300	6	1.9	N 38.60131925	W 90.52568096	610.4351	0.083	O
CAM	06/18/93	18:36:04.050185	6	1.9	N 38.59901886	W 90.52560532	611.1561	0.085	O
CAM	06/18/93	18:36:07.483497	6	1.9	N 38.59673202	W 90.52557260	609.4164	0.085	O
CAM	06/18/93	18:38:53.378486	6	1.8	N 38.61023132	W 90.51881048	609.3129	0.083	O
CAM	06/18/93	18:38:56.831284	6	1.8	N 38.60800856	W 90.51884371	609.5327	0.083	O
CAM	06/18/93	18:39:00.280785	6	1.8	N 38.60579105	W 90.51886314	613.9741	0.083	O
CAM	06/18/93	18:39:03.740073	6	1.8	N 38.60356080	W 90.51886686	616.0788	0.105	O
CAM	06/18/93	18:39:07.180434	6	1.8	N 38.60132478	W 90.51887654	611.1786	0.084	O
CAM	06/18/93	18:39:10.628531	6	1.8	N 38.59907090	W 90.51889881	608.7399	0.084	O
CAM	06/18/93	18:39:14.072252	6	1.8	N 38.59682322	W 90.51894415	606.1720	0.086	O
CAM	06/18/93	18:40:25.916159	6	1.8	N 38.57657710	W 90.55070294	611.3344	0.084	O
CAM	06/18/93	18:40:27.720425	6	1.8	N 38.57764181	W 90.55163432	613.7670	0.084	O
CAM	06/18/93	18:40:29.526078	6	1.8	N 38.57870792	W 90.55256271	616.3448	0.084	O
CAM	06/18/93	18:40:31.434557	6	1.8	N 38.57983469	W 90.55354992	620.2828	0.105	O
CAM	06/18/93	18:40:33.142323	6	1.8	N 38.58084711	W 90.55443476	620.7559	0.081	O
CAM	06/18/93	18:40:34.651138	6	1.8	N 38.58174759	W 90.55521711	617.4002	0.081	O
CAM	06/18/93	18:40:36.159498	6	1.8	N 38.58265405	W 90.55599910	613.9677	0.081	O
CAM	06/18/93	18:40:37.761249	6	1.8	N 38.58362149	W 90.55683210	612.8118	0.081	O
CAM	06/18/93	18:40:39.467067	6	1.8	N 38.58465678	W 90.55771930	613.6106	0.081	O
CAM	06/18/93	18:40:41.072015	6	1.8	N 38.58563332	W 90.55855483	613.5827	0.081	O
CAM	06/18/93	18:45:49.213964	5	1.9	N 38.66405978	W 90.62126894	179.7438	0.044	O

Table 3.2. Wing antenna position.

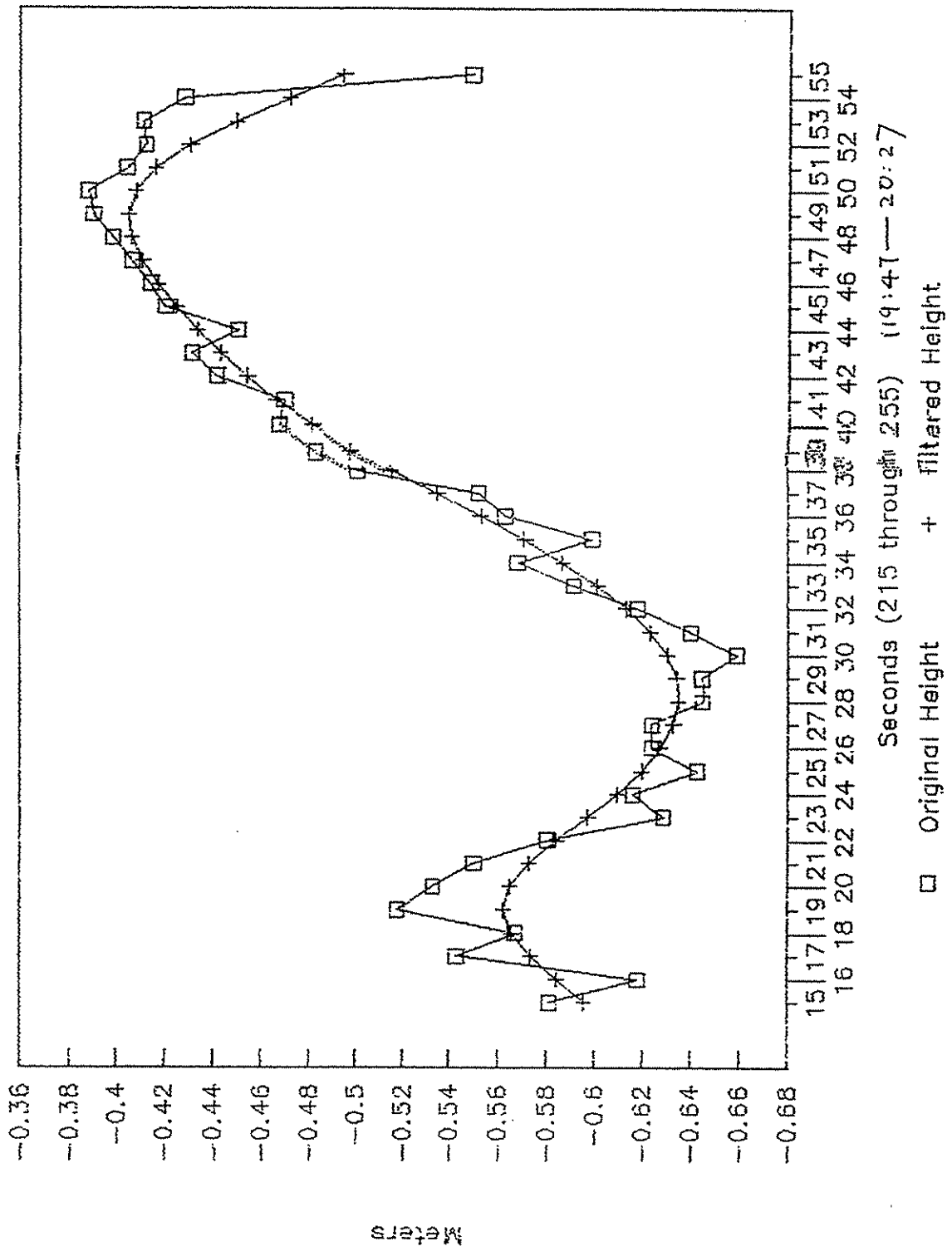
Ashtech, Inc. GPPS-2		Program:		PPDIFF-PNAV		Version: 1.0.00	
Wed Jun 30 10:33:13 1993				Differentially Corrected: Y			
SITE	MM/DD/YY	HH:MM:SS	SVs	PDOP	LATITUDE	LONGITUDE	HI
_WIN	06/18/93	18:16:23.585673	4	3.7	N 38.60819815	W 90.53162880	1069.5884
_WIN	06/18/93	18:16:29.828086	4	3.7	N 38.60845906	W 90.52560963	1069.1986
_WIN	06/18/93	18:16:36.017254	5	1.8	N 38.60856843	W 90.51962076	1070.5178
_WIN	06/18/93	18:16:42.185334	5	1.8	N 38.60846829	W 90.51365598	1069.5413
_WIN	06/18/93	18:16:48.337325	5	1.8	N 38.60817890	W 90.50772654	1070.2871
_WIN	06/18/93	18:19:45.655955	6	2.4	N 38.60432737	W 90.53802231	1072.2670
_WIN	06/18/93	18:19:51.969862	7	1.5	N 38.60425058	W 90.53187378	1070.0468
_WIN	06/18/93	18:19:58.331937	7	1.5	N 38.60420161	W 90.52563515	1063.3098
_WIN	06/18/93	18:20:04.669017	7	1.5	N 38.60424303	W 90.51944541	1068.0905
_WIN	06/18/93	18:20:10.985117	7	1.5	N 38.60428885	W 90.51330098	1071.4706
_WIN	06/18/93	18:20:17.316511	7	1.5	N 38.60423532	W 90.50712638	1069.8176
_WIN	06/18/93	18:27:28.610186	5	2.4	N 38.60962970	W 90.53928599	613.0895
_WIN	06/18/93	18:27:32.032063	5	2.4	N 38.60729634	W 90.53928820	607.3155
_WIN	06/18/93	18:27:35.487433	5	2.4	N 38.60492668	W 90.53926395	605.4586
_WIN	06/18/93	18:27:38.936745	5	2.4	N 38.60256367	W 90.53925329	602.6547
_WIN	06/18/93	18:27:42.375848	5	2.4	N 38.60022195	W 90.53921353	603.8206
_WIN	06/18/93	18:27:45.815082	5	2.4	N 38.59789286	W 90.53913753	608.1482
_WIN	06/18/93	18:27:49.275442	5	2.4	N 38.59555054	W 90.53905437	613.1926
_WIN	06/18/93	18:30:31.346137	4	20.8	N 38.61142047	W 90.53322753	634.8411
_WIN	06/18/93	18:30:34.777854	5	2.3	N 38.60825889	W 90.53297292	610.8343
_WIN	06/18/93	18:30:38.224967	5	2.3	N 38.60594821	W 90.53303491	609.5768
_WIN	06/18/93	18:30:41.670012	5	2.3	N 38.60362754	W 90.53305199	606.3610
_WIN	06/18/93	18:30:45.123006	5	2.3	N 38.60128920	W 90.53303954	608.9579
_WIN	06/18/93	18:30:48.589834	5	2.3	N 38.59894026	W 90.53301455	607.4602
_WIN	06/18/93	18:30:52.051058	5	2.3	N 38.59658793	W 90.53297397	608.0400
_WIN	06/18/93	18:30:55.489186	5	2.3	N 38.59424812	W 90.53291786	609.0595
_WIN	06/18/93	18:35:46.817115	0	17.4	N 38.61136476	W 90.52605769	638.4910
_WIN	06/18/93	18:35:50.267464	4	35.0	N 38.60910617	W 90.52599801	644.4634
_WIN	06/18/93	18:35:53.708846	4	35.3	N 38.60690914	W 90.52592090	656.4001
_WIN	06/18/93	18:35:57.143818	4	35.6	N 38.60472721	W 90.52584555	660.5251
_WIN	06/18/93	18:36:00.598300	5	2.1	N 38.60254253	W 90.52575816	660.2306
_WIN	06/18/93	18:36:04.050185	5	2.1	N 38.60039630	W 90.52567464	651.9298
_WIN	06/18/93	18:36:07.483497	5	2.1	N 38.59826567	W 90.52562565	638.0428
_WIN	06/18/93	18:38:53.378486	6	1.8	N 38.61022467	W 90.51873878	609.3553
_WIN	06/18/93	18:38:56.831284	6	1.8	N 38.60800168	W 90.51877199	609.6206
_WIN	06/18/93	18:39:00.280785	6	1.8	N 38.60578509	W 90.51879142	614.0297
_WIN	06/18/93	18:39:03.740073	6	1.8	N 38.60355435	W 90.51879511	616.1731
_WIN	06/18/93	18:39:07.180434	6	1.8	N 38.60131907	W 90.51880473	611.2980
_WIN	06/18/93	18:39:10.628531	6	1.8	N 38.59906437	W 90.51882701	606.8798
_WIN	06/18/93	18:39:14.072252	6	1.8	N 38.59681721	W 90.51887242	606.2544



Graph 3.1. Camera-wing Z difference vs. time.



Graph 3.2. St. Louis test 1 (photogrammetry) vs. GPS.



Graph 3.3. Original and filtered height.

$$w_p = w_o + w_G(A \text{ task} + B \text{ sink})$$

where

$w_p$  = camera's omega rotation from photogrammetry

$w_G$  = aircraft's omega rotation from GPS

$k$  = aircraft's kappa rotation from GPS

$A, B, w_o$  = constants

Table 3.3 gives the results of the computation for  $A, B,$  and  $w_o$  for the high flight, showing that the model using the filtered values agrees with the photogrammetric value within 0.0003 radians.

As a first-order correction, this model is satisfactory, considering the fact that error exists as a result of using  $L_1$  wing antenna and the error also exists in  $w$  determined by photogrammetry. These results show that determining  $w$  by GPS is feasible.

Table 3.3. Comparison of  $\omega$  by GPS and photogrammetry.

Photo #	$\Omega_p$ (rad)	Kappa (rad)	$\Omega_g$ (Filtered) (rad)	$\Omega_g$ (Original) (rad)	
6	-0.028599	-0.110516	-0.085093	0.05494	
7	-0.016348	-0.069752	-0.094603	0.07373	
8	-0.031913	-0.068699	-0.105448	0.05692	
9	-0.021480	-0.062829	-0.101363	0.07315	
<b>Comparison of Solution</b>					
Source for Omega	Solution with 6, 7 & 8 Photos			Check with Photo 9	
	$\Omega_0$	A	B	$\Phi_c$	$\Phi_c$ (calculated)
Filtered	0.126903	0.972761	-7.803094	-0.021480	-0.021166
				Error: 1.1%	
Original	-0.084026	0.758840	-2.308862	-0.021480	-0.018022
				Error: 16.1%	

#### 4. ANALYSIS OF SECOND TEST

The objective of this test was to evaluate the use of GPS in obtaining pinpoint aerial photographs. In this test, the aircraft is equipped with an L<sub>1</sub> antenna over the cockpit of the aircraft and C/A code GPS receiver with navigation software. The navigation software triggers the camera when the predetermined location agrees with the limit set for the aircraft's position as determined by the C/A code GPS receiver.

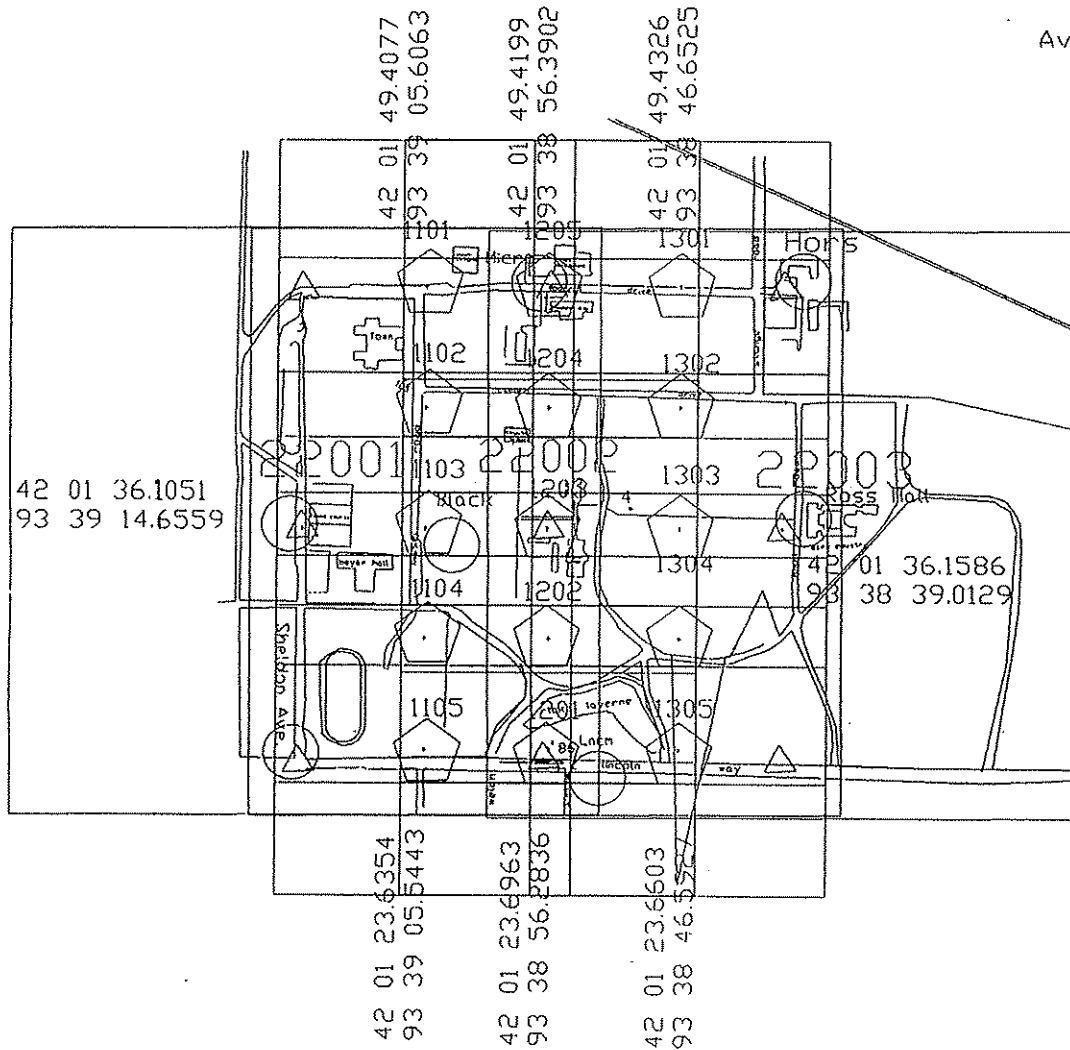
Figure 4.1 shows the proposed flight plan over ISU campus and the predetermined exposure station coordinates. Two flights, one at 1,500-foot flying height (1 inch = 250 feet scale photographs) and the other at 2,250-foot flying height, were proposed.

Typical specifications for aerial photography are that the exposure station is within 1/2 inch on the photograph of the proposed station and the actual flying height is within 5% of the proposed flying height. Thus, a tolerance of  $\pm 50$  meters was set on the GPS navigation system. Due to the uncertainty of the height determination by the C/A code receiver, only latitude and longitude by GPS navigation was entered into the computer on board and the height was determined by the on-board aneroid barometer. Table 4.1 shows the coordinates of the exposure station used by the on-board navigation system.

A block of photographs were observed using the Wild Stereo Comparator, and the block adjustment was performed by the Albany software. Table 4.2 shows the difference between the exposure coordinates that were proposed and then obtained by photogrammetry (Albany software).

Figure 4.2 shows the proposed flight lines, the flight lines from the layout diagram prepared using the exposed photographs, and those using the exposure coordinates determined by Albany.

The flight lines in Figure 4.2 and the standard error of the difference in coordinates of  $\pm 27$  meters indicate that pinpoint navigation is satisfactory. Even though the proposed coordinates (Fig. 4.1) and the navigation coordinates (Table 4.1) are almost identical, they are different from the Albany with a maximum difference of 42 meters and a standard error of  $\pm 27$  meters. This shows that the navigation software's performance is satisfactory but the position determined by C/A code GPS receiver is off by  $\pm 27$  meters. The standard error of  $\pm 27$  meters is within the specification allowed (1/2 inch x 250 feet = 125 feet  $\approx$  40 meters). This error is expected of the C/A code GPS receiver. The accuracy can be improved either by using differential real-time C/A code receiver or a P/code receiver.



Average Terrain Elev. = 295 meters above MSL

△ Triangle  
 Flying height = 2200 Ft above ground  
 Overlap 60 %

Lat. & Longi. of exp. Stations

22001 42 01 36.1051 93 39 14.6559  
 22002 42 01 36.1484 93 38 56.4972  
 22003 42 01 36.1586 93 38 39.0129

⬠ Flying Height = 350 Meters  
 (1150 ft.)

Scale = 1:2300

Overlap 60%  
 sidelap 50 to 60%

Real Coverage larger than map

Lat. & long. of Exp. Stations

1101 42 01 49.4077 93 39 05.6063  
 1102 42 01 42.7797 93 39 05.5904  
 1103 42 01 36.1245 93 39 05.5744  
 1104 42 01 29.9179 93 39 05.5594  
 1105 42 01 23.6354 93 39 05.5443  
  
 1201 42 01 23.6963 93 38 56.2836  
 1202 42 01 29.9302 93 38 56.2983  
 1203 42 01 36.1366 93 38 56.4849  
 1204 42 01 42.7919 93 38 56.4310  
 1205 42 01 49.4199 93 38 56.3902  
  
 1301 42 01 49.4326 93 38 46.6525  
 1302 42 01 42.8046 93 38 46.6371  
 1303 42 01 36.1494 93 38 46.6217  
 1304 42 01 29.9428 93 38 46.6073  
 1305 42 01 23.6603 93 38 46.5927

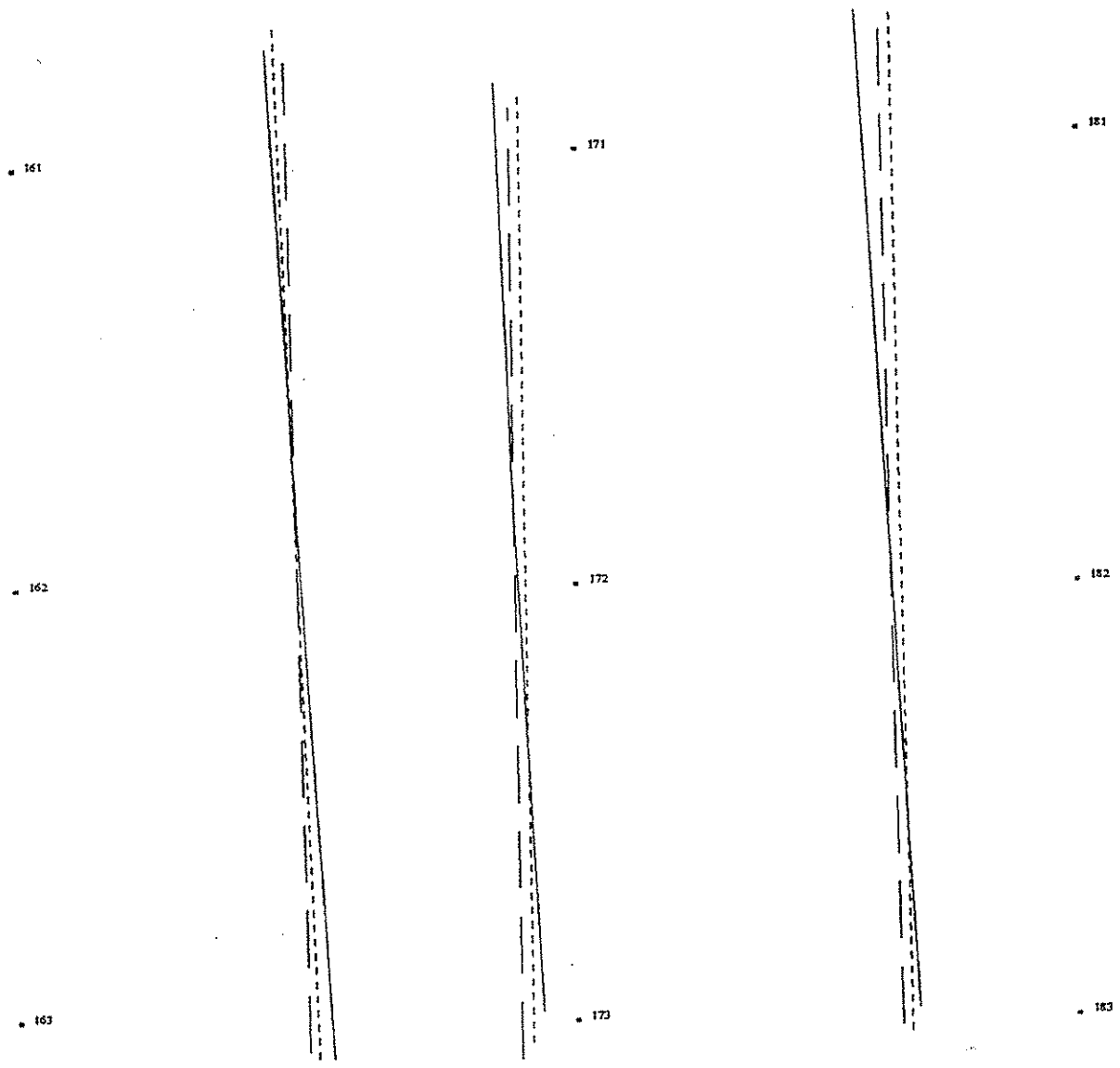
Figure 4.1. Campus flight plan diagram.

Table 4.1. Camera location from navigation software.

00002	930823	184947	ISU	CAMPUS	01	---	N42.090874	W093.516394	04776T	266
00003	930823	185626	ISU	CAMPUS	01	001	N42.030125	W093.651481	02140T	181
00004	930823	185628	ISU	CAMPUS	01	002	N42.028285	W093.651539	02140T	181
00005	930823	185631	ISU	CAMPUS	01	003	N42.026436	W093.651622	02244T	182
00006	930823	185634	ISU	CAMPUS	01	004	N42.024411	W093.651697	02244T	182
00007	930823	185636	ISU	CAMPUS	01	005	N42.022767	W093.651726	02244T	181
00008	930823	185931	ISU	CAMPUS	02	001	N42.023495	W093.648868	02282T	360
00009	930823	185933	ISU	CAMPUS	02	002	N42.025370	W093.648854	02282T	360
00010	930823	185936	ISU	CAMPUS	02	003	N42.027245	W093.648850	02282T	360
00011	930823	185938	ISU	CAMPUS	02	004	N42.029121	W093.648887	02282T	359
00012	930823	185941	ISU	CAMPUS	02	005	N42.030993	W093.648970	02282T	358
00013	930823	190247	ISU	CAMPUS	03	001	N42.030144	W093.646515	02282T	182
00014	930823	190250	ISU	CAMPUS	03	002	N42.028216	W093.646553	02282T	181
00015	930823	190253	ISU	CAMPUS	03	003	N42.026466	W093.646537	02282T	180
00016	930823	190255	ISU	CAMPUS	03	004	N42.024551	W093.646484	02176T	179
00017	930823	190258	ISU	CAMPUS	03	005	N42.022814	W093.646441	02176T	179
00018	930823	190730	ISU	CAMPUS	04	001	N42.026562	W093.653621	03237T	090
00019	930823	190734	ISU	CAMPUS	04	002	N42.026575	W093.648833	03237T	090
00020	930823	190738	ISU	CAMPUS	04	003	N42.026619	W093.644065	03344T	089
00021	930823	190743	ISU	CAMPUS	04	004	N42.026645	W093.639295	03344T	090

Table 4.2. Comparison of GPS navigation and photogrammetry.

<b>Low Flight</b>	<b>Diff. in Easting</b>	<b>Diff. in Northing</b>	<b>Diff. in Elev.</b>
	<b>mts</b>	<b>mts</b>	<b>mts</b>
<b>01</b>	6.638	3.582	-19.400
<b>02</b>	12.840	1.471	-16.908
<b>03</b>	12.416	-1.556	-14.499
<b>04</b>	24.375	36.684	-10.142
<b>05</b>	27.474	42.451	-5.888
<b>Mean</b>	16.747	16.52	-13.364
<b>Stand. Error: 23.5 m</b>			
<b>High Flight</b>			
<b>06</b>	7.239	9.335	-27.730
<b>07</b>	32.522	7.705	-23.320
<b>08</b>	41.224	0.971	-22.300
<b>Mean</b>	26.998	6.00	-24.4
<b>Stand. Error: 27.6 m</b>			



LEGEND

- PROPOSED FLIGHT PLAN
- FLIGHT PLAN FROM LAYOUT
- . - . - FLIGHT PLAN FROM ALBANY

Figure 4.2. Low-flight campus flight plan.

## 5. ANALYSIS OF THIRD TEST

The objective of this test is to evaluate the feasibility of using four antennas on the aircraft, the accuracy of the 3DF receivers, and the reliability of the  $L_1/L_2$  antenna on the wing. This test was done over the test range in St. Louis in October 1993.

After careful study of the Cessna 335 aircraft, it was decided to have one antenna on the left wing, one on the right wing and one on the tail in addition to one above the camera. Figure 5.1 shows the aircraft and the location of the antennas. The camera and right wing were installed with  $L_1/L_2$  antennas and connected to the P12 receivers. The left wing and tail had  $L_1$  antennas; these two were connected to the 3DF receivers. Using a signal splitter, the camera antenna was also connected to the 3DF receivers.

Using the same flight plan as in test one (see Fig. 3.3) aerial photographs were taken over the St. Louis test range at 1,500-foot and 3,000-foot flying heights. Photographs were observed using the Wild stereo comparator, and the block adjustment were done by both Albany and Calib softwares. GPS data were processed by PNAV and 3DF software.

Tables 5.1, 5.2, and 5.3 give the position of the camera, the right wing, and the tail at the camera exposure time as determined by PNAV and 3DF software. These tables indicate that both camera and right wing antennas track seven to eight satellites continuously, while the tail antenna drops to four satellites. These tables also indicate that positions are determined to  $\pm 0.1$  millimeter accuracy. Graphs 5.1 and 5.2 show the flight path of the camera and the tail antennas. From the graphs and the tables, it is seen that the positions of the tail antenna are not reliable. This may be due either to the  $L_1$  antenna or its location on the tail of the aircraft. Because the 3DF software relies on the tail antenna, we were not able to get reliable values on the left wing. Table 5.4 shows the rotation angles computed from the camera, the tail, and right wing antenna locations. Angles kappa and phi depends on the location of the tail antenna and therefore may not be reliable.

Graphs 5.3 and 5.4 show the comparison of omega ( $\omega$ ) rotation angle by Albany (photogrammetry), by Yao (rotation by GPS), and by Ken (rotation by GPS from the initial position) for high and low flights, respectively. As in the first test flight, the graphs indicate a direct relationship between  $\omega$  rotation obtained by GPS and by photogrammetry.

In order to correctly model the relationship between  $\omega$  rotation by GPS and photogrammetry, various analyses were done. Graph 5.5 shows the true difference in height between the right wing and camera and the filtered height difference, indicating that there is flexing of the wing due to air lift, etc., which is independent of the rotation. Graph 5.6 shows the change in length between the camera antenna and the right wing antenna for the high flight. From Figure 5.2, it appears that the change in length is strictly due to flexing of the wing. In order to

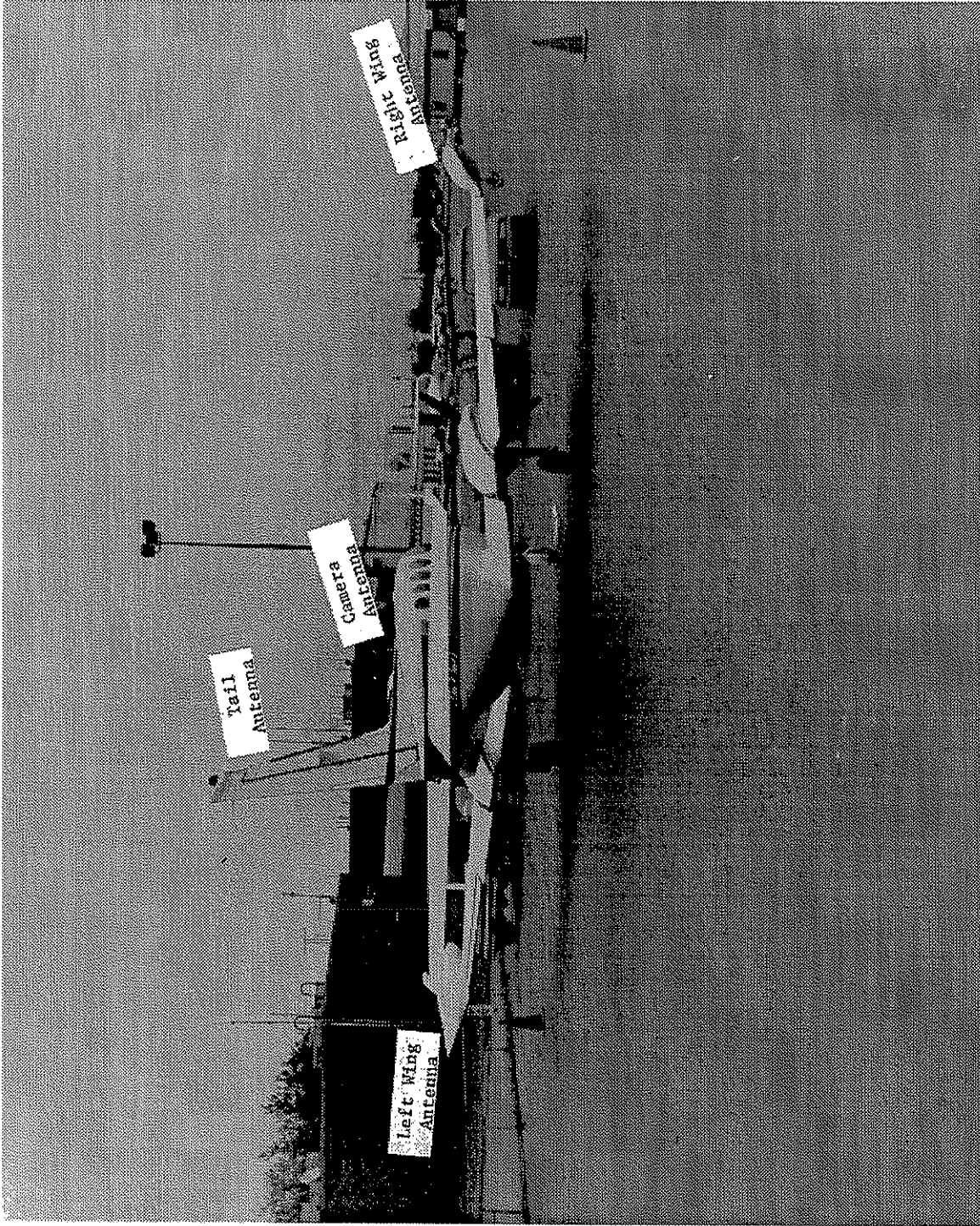


Figure 5.1. Aircraft with four antennas.

Table 5.1. Camera antenna position.

Ashtech, Inc. GPPS-2      Program: PPDIFF-PNAV    Version: 1.0.00  
 Sun Jan 16 22:54:52 1994    Differentially Corrected: Y

SITE	MM/DD/YY	HH:MM:SS	Svs	PDOP	LATITUDE	LONGITUDE	HI	RMS	FLAG
?CAM	10/30/93	14:50:17.320722	5	1.9	N 38.66307853	W 90.64520684	143.7205	0.154	1
?CAM	10/30/93	14:55:49.666998	5	2.0	N 38.66260023	W 90.63527466	142.3183	0.155	1
?CAM	10/30/93	14:56:05.304581	5	2.0	N 38.66260018	W 90.63527463	142.3178	0.155	1
?CAM	10/30/93	15:03:39.986363	7	1.3	N 38.60407215	W 90.54144354	957.6226	0.155	1
?CAM	10/30/93	15:03:45.212922	7	1.3	N 38.60404261	W 90.53616305	962.3996	0.157	1
?CAM	10/30/93	15:03:50.476001	7	1.3	N 38.60401539	W 90.53085989	960.9707	0.158	1
?CAM	10/30/93	15:03:55.714706	7	1.3	N 38.60398297	W 90.52557454	960.3949	0.158	1
?CAM	10/30/93	15:04:00.946909	7	1.3	N 38.60390759	W 90.52029405	964.4583	0.159	1
?CAM	10/30/93	15:04:06.193357	7	1.3	N 38.60378094	W 90.51499654	967.4111	0.160	1
?CAM	10/30/93	15:04:11.487352	7	1.3	N 38.60364861	W 90.50964996	965.0516	0.175	1
?CAM	10/30/93	15:13:12.118887	8	1.2	N 38.59498291	W 90.51962517	657.0267	0.071	1
?CAM	10/30/93	15:13:16.102004	8	1.2	N 38.59735429	W 90.51951564	660.6232	0.071	1
?CAM	10/30/93	15:13:20.574425	8	1.2	N 38.60002335	W 90.51943985	663.6988	0.070	1
?CAM	10/30/93	15:13:25.036935	8	1.2	N 38.60272699	W 90.51948142	662.7284	0.076	1
?CAM	10/30/93	15:13:29.468310	8	1.2	N 38.60545617	W 90.51957245	663.9462	0.070	1
?CAM	10/30/93	15:13:33.929109	8	1.2	N 38.60823181	W 90.51962691	668.7381	0.070	1
?CAM	10/30/93	15:13:38.408214	8	1.2	N 38.61104584	W 90.51960587	665.5211	0.070	1
?CAM	10/30/93	15:15:49.963353	7	1.3	N 38.61090076	W 90.53020496	662.6389	0.070	1
?CAM	10/30/93	15:15:53.159791	7	1.3	N 38.60848756	W 90.53023149	667.4687	0.070	1
?CAM	10/30/93	15:15:56.580263	7	1.3	N 38.60590356	W 90.53029259	665.5371	0.070	1
?CAM	10/30/93	15:16:00.039792	7	1.3	N 38.60328000	W 90.53038132	666.2825	0.071	1
?CAM	10/30/93	15:16:03.551927	8	1.2	N 38.60060243	W 90.53047462	667.5936	0.069	1
?CAM	10/30/93	15:16:07.013033	8	1.2	N 38.59795525	W 90.53053791	670.9608	0.068	1
?CAM	10/30/93	15:16:10.470674	8	1.2	N 38.59530605	W 90.53057048	674.5688	0.069	1
?CAM	10/30/93	15:19:22.125536	7	1.6	N 38.59651863	W 90.52506928	651.3185	0.082	1
?CAM	10/30/93	15:19:26.594989	7	1.6	N 38.59922830	W 90.52488740	656.0809	0.082	1
?CAM	10/30/93	15:19:31.052658	7	1.6	N 38.60195879	W 90.52472534	655.8816	0.081	1
?CAM	10/30/93	15:19:35.503228	7	1.6	N 38.60470340	W 90.52463179	655.7915	0.081	1
?CAM	10/30/93	15:19:39.761709	7	1.6	N 38.60732770	W 90.52460261	653.9743	0.081	1
?CAM	10/30/93	15:19:43.924864	7	1.6	N 38.60989157	W 90.52462232	654.4512	0.080	1
?CAM	10/30/93	15:20:02.309311	7	1.6	N 38.62111373	W 90.52470759	652.0795	0.078	1
?CAM	10/30/93	15:20:05.058039	7	1.6	N 38.62281098	W 90.52473964	650.5285	0.078	1
?CAM	10/30/93	15:20:08.261850	7	1.6	N 38.62479519	W 90.52478695	647.9284	0.078	1
?CAM	10/30/93	15:20:11.005684	7	1.6	N 38.62650210	W 90.52483807	643.9597	0.078	1
?CAM	10/30/93	15:20:16.008092	7	1.6	N 38.62962522	W 90.52493763	641.9240	0.078	1
?CAM	10/30/93	15:20:19.663155	7	1.6	N 38.63189334	W 90.52500538	643.3966	0.091	1
?CAM	10/30/93	15:20:22.400918	7	1.6	N 38.63357601	W 90.52506064	642.3124	0.077	1
?CAM	10/30/93	15:20:26.038116	7	1.6	N 38.63578306	W 90.52516915	643.0581	0.077	1
?CAM	10/30/93	15:20:29.240071	7	1.6	N 38.63769403	W 90.52532560	639.6420	0.076	1
?CAM	10/30/93	15:20:31.981183	7	1.6	N 38.63931093	W 90.52551634	634.2945	0.076	1
?CAM	10/30/93	15:21:08.106349	7	1.6	N 38.65792614	W 90.53817315	533.2000	0.074	1

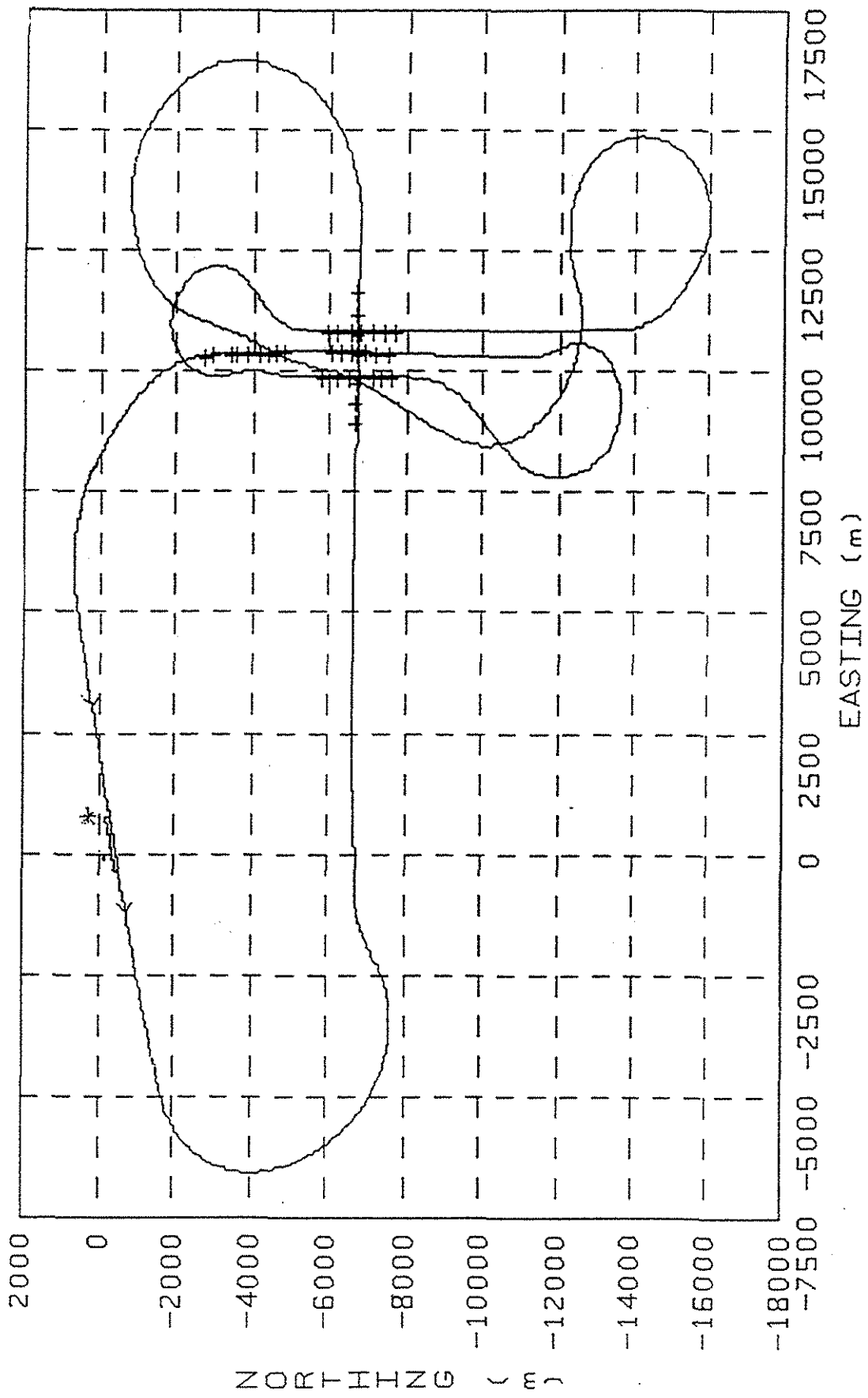
Table 5.2. Right wing antenna position.

Ashtech, Inc. GPPS-2 Program: PPDIFF-PNAV Version: 1.0.00  
 Sun Jan 16 22:51:37 1994 Differentially Corrected: Y

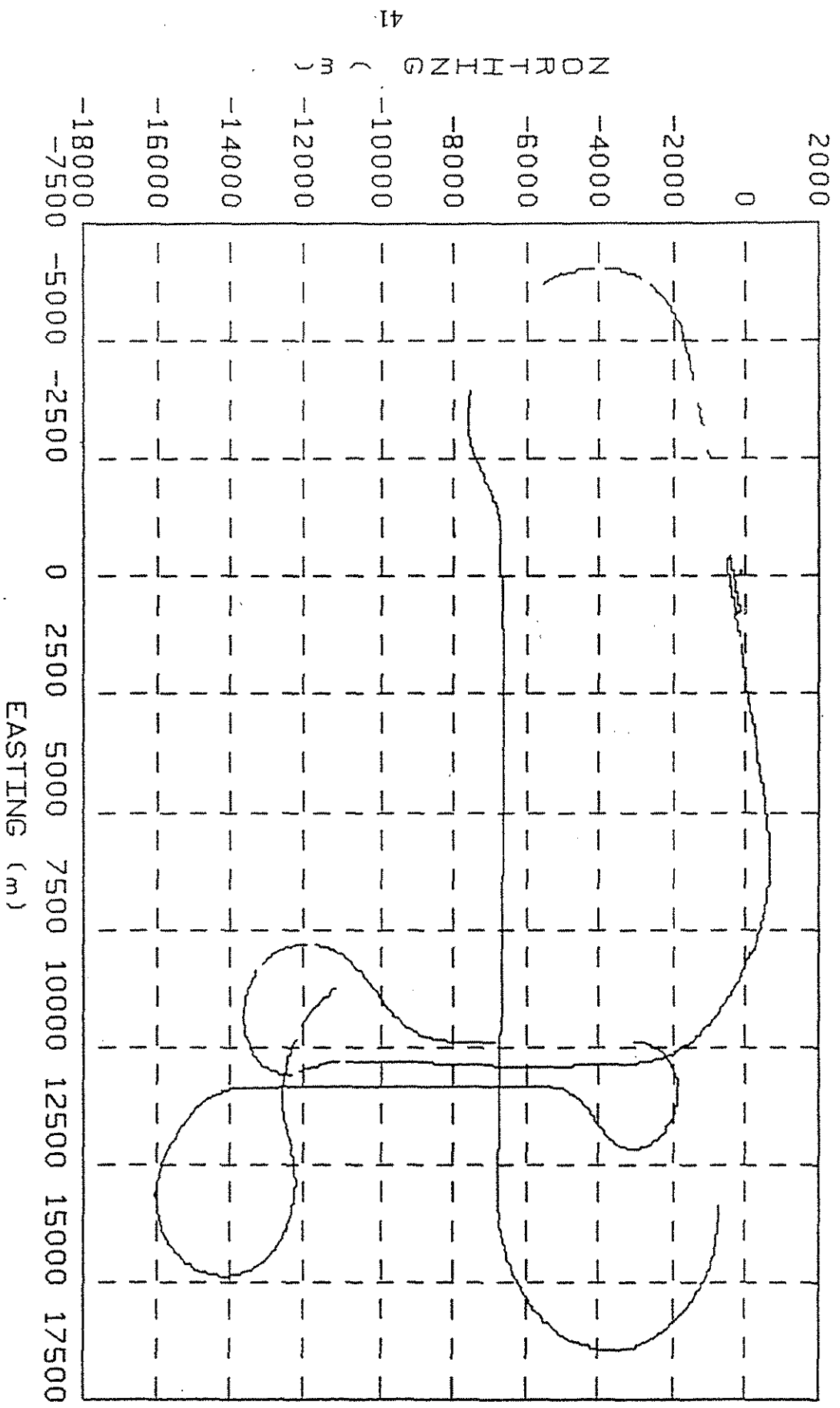
SITE	MM/DD/YY	HH:MM:SS	SVs	PDOP	LATITUDE	LONGITUDE	HI	RMS	FLAG
?CAM	10/30/93	14:50:17.320722	5	1.5	N 38.66303354	W 90.64519402	143.2702	0.761	1
?CAM	10/30/93	14:55:49.666998	5	1.5	N 38.66259613	W 90.63534171	141.9019	0.114	1
?CAM	10/30/93	14:56:05.304581	5	1.5	N 38.66259556	W 90.63534132	141.8528	0.116	1
?CAM	10/30/93	15:03:39.986363	7	1.3	N 38.60402378	W 90.54143370	956.5455	0.126	1 →
?CAM	10/30/93	15:03:45.212922	7	1.3	N 38.60399412	W 90.53615359	961.4036	0.126	1
?CAM	10/30/93	15:03:50.476001	7	1.3	N 38.60396680	W 90.53085106	959.9973	0.127	1
?CAM	10/30/93	15:03:55.714706	7	1.3	N 38.60393423	W 90.52556770	959.3865	0.127	1
?CAM	10/30/93	15:04:00.946909	7	1.3	N 38.60385892	W 90.52028613	963.4223	0.128	1
?CAM	10/30/93	15:04:06.193357	7	1.3	N 38.60373231	W 90.51498788	966.3777	0.128	1
?CAM	10/30/93	15:04:11.487352	7	1.3	N 38.60360132	W 90.50964004	964.0752	0.129	1
?CAM	10/30/93	15:13:12.118887	8	1.2	N 38.59498180	W 90.51956368	657.3025	0.108	1
?CAM	10/30/93	15:13:16.102004	8	1.2	N 38.59735518	W 90.51945409	661.0048	0.108	1
?CAM	10/30/93	15:13:20.574425	8	1.2	N 38.60002675	W 90.51937849	664.1321	0.108	1
?CAM	10/30/93	15:13:25.036935	8	1.2	N 38.60272975	W 90.51941991	663.1829	0.134	1
?CAM	10/30/93	15:13:29.468310	8	1.2	N 38.60545867	W 90.51951109	664.2047	0.108	1
?CAM	10/30/93	15:13:33.929109	8	1.2	N 38.60823156	W 90.51956515	669.0066	0.108	1
?CAM	10/30/93	15:13:38.408214	8	1.2	N 38.61104514	W 90.51954394	665.8106	0.109	1
?CAM	10/30/93	15:15:49.963353	8	1.2	N 38.61090142	W 90.53026876	662.4555	0.169	1
?CAM	10/30/93	15:15:53.159791	8	1.2	N 38.60848782	W 90.53029524	667.2541	0.169	1
?CAM	10/30/93	15:15:56.580263	8	1.2	N 38.60590505	W 90.53035635	665.4179	0.166	1
?CAM	10/30/93	15:16:00.039792	8	1.2	N 38.60328089	W 90.53044516	666.1730	0.166	1
?CAM	10/30/93	15:16:03.551927	8	1.2	N 38.60060212	W 90.53053854	667.5078	0.166	1
?CAM	10/30/93	15:16:07.013033	8	1.2	N 38.59795398	W 90.53060198	670.9756	0.166	1
?CAM	10/30/93	15:16:10.470674	8	1.2	N 38.59530526	W 90.53063438	674.4392	0.167	1
?CAM	10/30/93	15:19:22.125536	7	1.6	N 38.59651770	W 90.52500416	651.2097	0.174	1
?CAM	10/30/93	15:19:26.594989	7	1.6	N 38.59922751	W 90.52482232	655.9499	0.174	1
?CAM	10/30/93	15:19:31.052658	7	1.6	N 38.60196005	W 90.52466025	655.8642	0.174	1
?CAM	10/30/93	15:19:35.503228	7	1.6	N 38.60470494	W 90.52456670	655.7934	0.174	1
?CAM	10/30/93	15:19:39.761709	7	1.6	N 38.60733028	W 90.52453759	654.0230	0.173	1
?CAM	10/30/93	15:19:43.924864	7	1.6	N 38.60989320	W 90.52455735	654.3655	0.173	1
?CAM	10/30/93	15:20:02.309311	7	1.6	N 38.62111606	W 90.52464262	652.0422	0.173	1
?CAM	10/30/93	15:20:05.058039	7	1.6	N 38.62281314	W 90.52467469	650.4391	0.173	1
?CAM	10/30/93	15:20:08.261850	7	1.6	N 38.62479704	W 90.52472191	647.9022	0.173	1
?CAM	10/30/93	15:20:11.005684	7	1.6	N 38.62650488	W 90.52477336	643.7568	0.173	1
?CAM	10/30/93	15:20:16.008092	7	1.6	N 38.62962755	W 90.52487276	641.7796	0.173	1
?CAM	10/30/93	15:20:19.663155	7	1.6	N 38.63189494	W 90.52494022	643.4270	0.173	1
?CAM	10/30/93	15:20:22.400918	7	1.6	N 38.63357899	W 90.52499567	642.3846	0.173	1
?CAM	10/30/93	15:20:26.038116	7	1.6	N 38.63578597	W 90.52510396	643.3714	0.173	1
?CAM	10/30/93	15:20:29.240071	7	1.6	N 38.63769856	W 90.52526071	639.8971	0.173	1
?CAM	10/30/93	15:20:31.981183	7	1.6	N 38.63931656	W 90.52545167	634.7225	0.173	1
?CAM	10/30/93	15:21:08.106349	7	1.6	N 38.65796101	W 90.53812837	533.3244	0.172	1

Table 5.3. Tail antenna position.

Ashtech, Inc. GPPS-2		Program:		PPDIFF-PNAV		Version: 1.0.00	
Wed Feb 09 13:36:53 1994		Differentially		Corrected: Y			
SITE	MM/DD/YY	HH:MM:SS	SVs	PDOP	LATITUDE	LONGITUDE	HI
?CAM	10/30/93	14:50:17.320722	6	1.5	N 38.66306793	W 90.64525918	145.5637
?CAM	10/30/93	14:55:49.666998	5	2.1	N 38.66264597	W 90.63526991	144.0823
?CAM	10/30/93	14:56:05.304581	5	2.1	N 38.66264588	W 90.63526979	144.0913
?CAM	10/30/93	15:03:39.986363	5	2.4	N 38.60407224	W 90.54149706	956.6942
?CAM	10/30/93	15:03:45.212922	5	2.4	N 38.60404302	W 90.53621641	961.5671
?CAM	10/30/93	15:03:50.476001	5	2.4	N 38.60401622	W 90.53091329	960.1770
?CAM	10/30/93	15:03:55.714706	5	2.4	N 38.60398511	W 90.52562833	959.5804
?CAM	10/30/93	15:04:00.946909	5	2.4	N 38.60390879	W 90.52034780	963.6732
?CAM	10/30/93	15:04:06.193357	5	2.4	N 38.60378146	W 90.51505022	966.6614
?CAM	10/30/93	15:04:11.487352	5	2.4	N 38.60364939	W 90.50970366	964.3119
?CAM	10/30/93	15:13:12.118887	5	2.7	N 38.59492882	W 90.51962861	659.8728
?CAM	10/30/93	15:13:16.102004	5	2.7	N 38.59730030	W 90.51951694	663.5087
?CAM	10/30/93	15:13:20.574425	5	2.7	N 38.59996995	W 90.51943823	666.7211
?CAM	10/30/93	15:13:25.036935	5	2.7	N 38.60267350	W 90.51948071	665.7725
?CAM	10/30/93	15:13:29.468310	5	2.7	N 38.60540259	W 90.51957164	666.9113
?CAM	10/30/93	15:13:33.929109	5	2.7	N 38.60817814	W 90.51962947	671.7459
?CAM	10/30/93	15:13:38.408214	5	2.7	N 38.61099212	W 90.51960922	668.5159
?CAM	10/30/93	15:15:49.963353	4	3.2	N 38.61090378	W 90.53041827	667.4687
?CAM	10/30/93	15:15:53.159791	4	3.2	N 38.60850584	W 90.53040440	667.4221
?CAM	10/30/93	15:15:56.580263	4	3.2	N 38.60593984	W 90.53038955	667.3723
?CAM	10/30/93	15:16:00.039792	4	3.5	N 38.60334407	W 90.53037566	667.3558
?CAM	10/30/93	15:16:03.551927	4	3.5	N 38.60066628	W 90.53047026	668.5748
?CAM	10/30/93	15:16:07.013033	4	3.5	N 38.59801908	W 90.53053447	671.9565
?CAM	10/30/93	15:16:10.470674	4	3.5	N 38.59537007	W 90.53056678	675.5016
?CAM	10/30/93	15:19:22.125536	6	1.7	N 38.59646598	W 90.52506780	653.9370
?CAM	10/30/93	15:19:26.594989	6	1.7	N 38.59917573	W 90.52488567	658.7526
?CAM	10/30/93	15:19:31.052658	6	1.7	N 38.60190623	W 90.52472146	658.5154
?CAM	10/30/93	15:19:35.503228	6	1.7	N 38.60465082	W 90.52462763	658.4139
?CAM	10/30/93	15:19:39.761709	6	1.7	N 38.60727520	W 90.52459728	656.6147
?CAM	10/30/93	15:19:43.924864	6	1.7	N 38.60983888	W 90.52461793	657.0066
?CAM	10/30/93	15:20:02.309311	6	1.7	N 38.62106129	W 90.52470231	654.7988
?CAM	10/30/93	15:20:05.058039	6	1.7	N 38.62275859	W 90.52473445	653.2670
?CAM	10/30/93	15:20:08.261850	6	1.7	N 38.62474295	W 90.52478219	650.7481
?CAM	10/30/93	15:20:11.005684	6	1.7	N 38.62644997	W 90.52483182	646.7613
?CAM	10/30/93	15:20:16.008092	6	1.7	N 38.62957284	W 90.52493227	644.6209
?CAM	10/30/93	15:20:19.663155	6	1.7	N 38.63184083	W 90.52500111	646.0876
?CAM	10/30/93	15:20:22.400918	6	1.7	N 38.63352360	W 90.52505489	644.9893
?CAM	10/30/93	15:20:26.038116	6	1.7	N 38.63573064	W 90.52516409	645.6935
?CAM	10/30/93	15:20:29.240071	6	1.7	N 38.63764184	W 90.52531848	642.3139
?CAM	10/30/93	15:20:31.981183	6	1.7	N 38.63925902	W 90.52550826	637.0666
?CAM	10/30/93	15:21:08.106349	5	3.0	N 38.65788779	W 90.53812888	535.9311



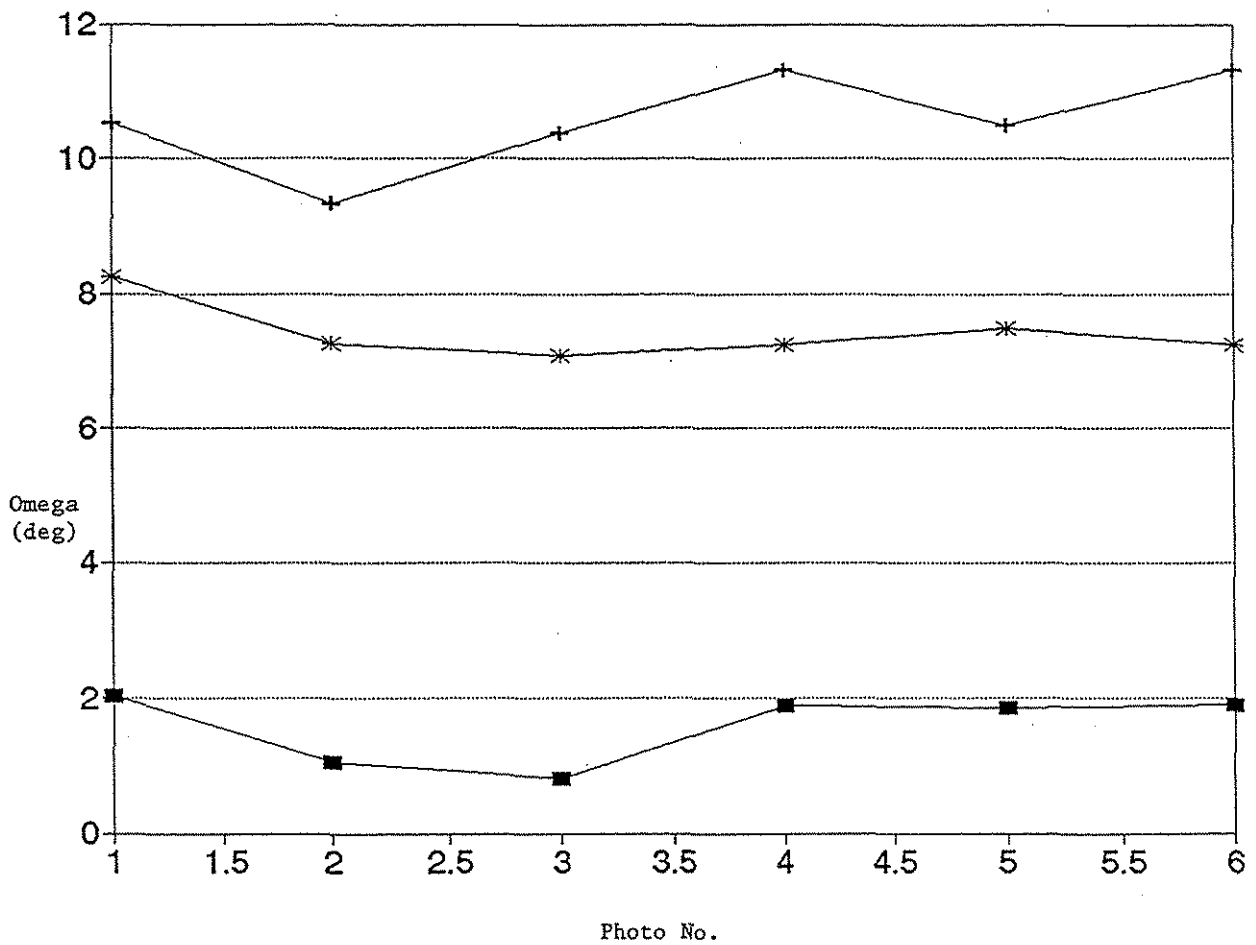
Graph 5.1. Flight path of Surdex aircraft.



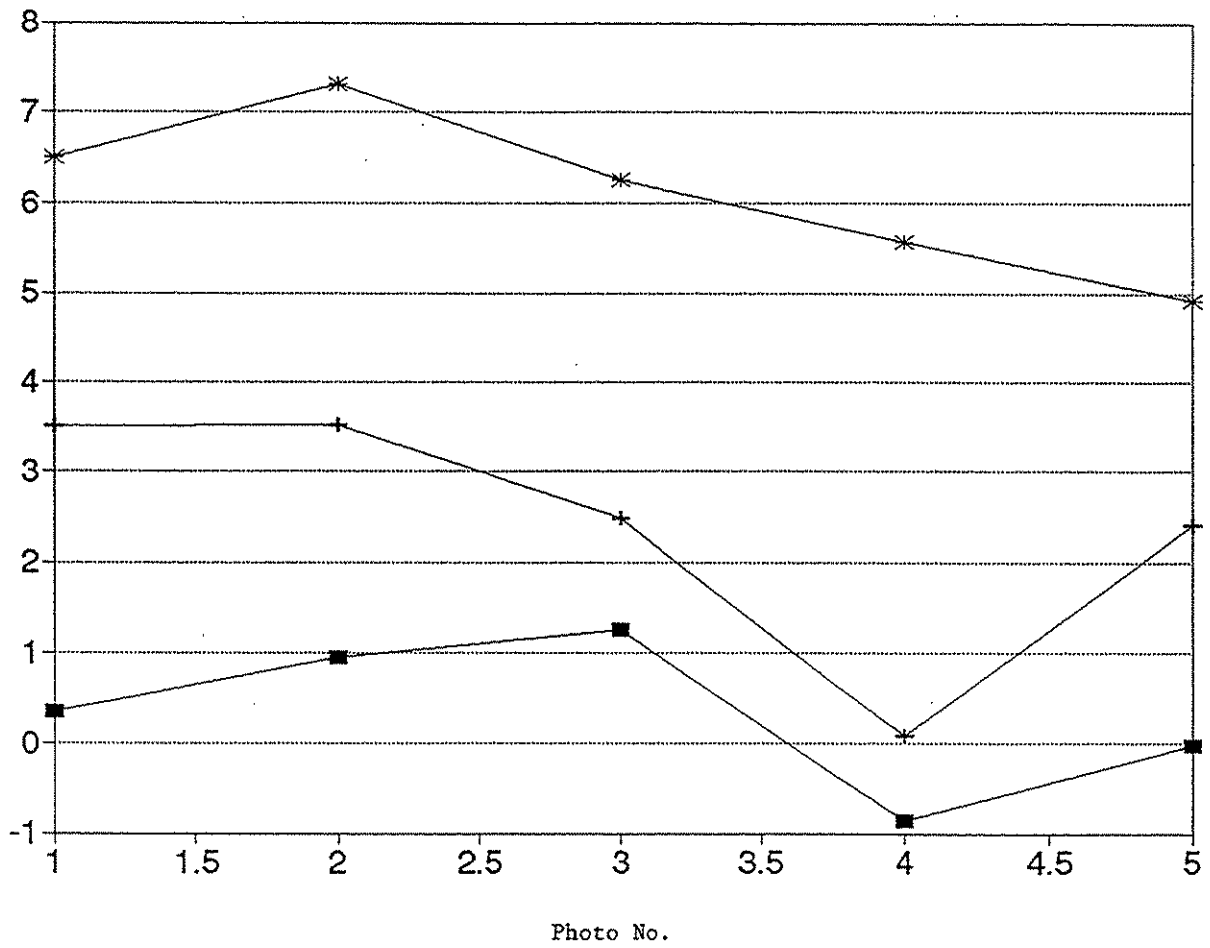
Graph 5.2. Position solution for tail antenna for flight #1.

Table 5.4. Omega, phi, kappa, and scale by GPS.

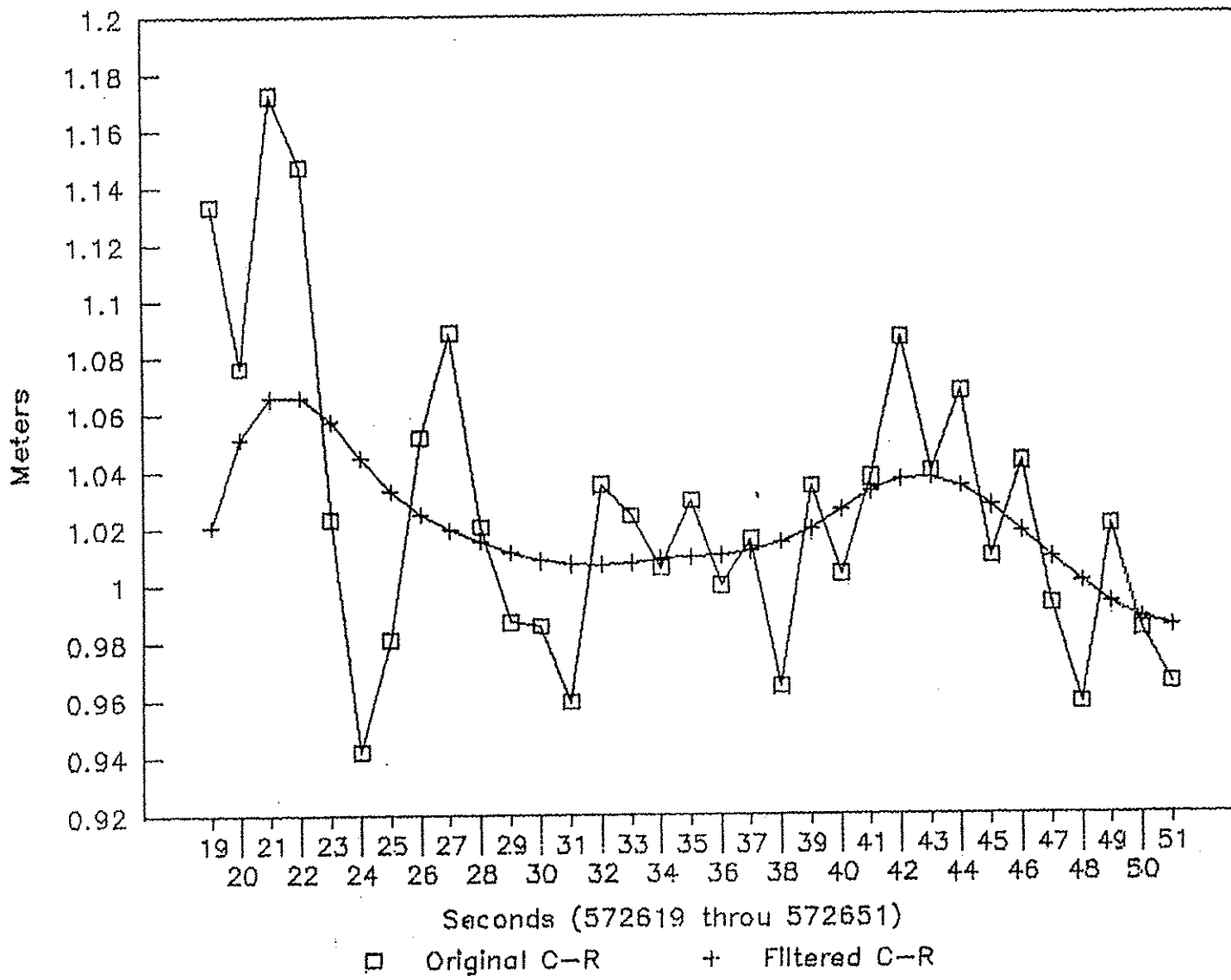
TIME	OMEGA	PHI	KAPPA	S1	S2
571817,	0.0000,	0.0000,	0.0000,	1.0000000,	1.0000000
572149,	-1.5536,	-8.9956,	-81.9887,	1.1422063,	1.0668778
572165,	-1.2610,	-9.5129,	-82.5591,	1.1378442,	1.0668900
572619,	-5.9266,	-1.8219,	-3.3565,	1.0788084,	0.9398876
572625,	-5.1003,	-1.6634,	-3.7456,	1.0775504,	0.9337329
572630,	-4.8630,	-1.6826,	-4.3349,	1.0771735,	0.9334898
572635,	-5.1555,	-2.0088,	-6.0951,	1.0773861,	0.9416347
572640,	-5.4486,	-1.9515,	-5.1212,	1.0794909,	0.9389036
572646,	-5.4332,	-1.8538,	-4.4695,	1.0798780,	0.9365345
572651,	-5.1499,	-1.5881,	-3.1145,	1.0526623,	0.9366953
573192,	-7.4365,	3.3194,	76.2695,	1.0432454,	1.3165053
573196,	-8.7079,	2.7387,	78.6675,	1.0455357,	1.3165023
573200,	-9.3467,	2.4313,	81.6515,	1.0453055,	1.3172101
573205,	-9.5968,	2.2947,	80.8809,	1.0476011,	1.3206856
573209,	-7.1893,	3.5608,	80.5594,	1.0419099,	1.3154584
573213,	-7.3184,	3.4032,	77.2833,	1.0474603,	1.3215734
573218,	-7.5807,	3.2624,	76.7754,	1.0504315,	1.3219815
573349,	-2.4018,	-6.9419,	-76.7326,	1.0816078,	3.7974188
573353,	-2.2128,	-7.2537,	-77.2035,	1.0806124,	3.0052922
573356,	-2.7692,	-6.3369,	-75.7378,	1.0810953,	1.8802952
573360,	-2.9592,	-6.2107,	-76.4399,	1.0816926,	1.4267937
573363,	-3.3806,	-5.8882,	-77.8056,	1.0831685,	1.4182472
573367,	-4.3789,	-4.7623,	-78.8448,	1.0856515,	1.4176348
573370,	-3.4383,	-5.8513,	-78.0535,	1.6664333,	1.5139540
573562,	-2.7856,	5.5473,	76.2424,	1.1035492,	1.2679110
573566,	-2.5011,	5.6939,	76.3724,	1.1026456,	1.2704023
573571,	-3.8056,	5.2237,	78.7878,	1.1029317,	1.2687820
573575,	-4.0222,	5.1359,	79.1332,	1.1030982,	1.2686105
573579,	-4.5448,	4.9395,	80.3442,	1.1029025,	1.2695194
573583,	-2.9862,	5.6652,	79.1369,	1.1013876,	1.2655108
573602,	-3.5491,	5.4360,	79.9809,	1.1016814,	1.2748276
573605,	-2.9277,	5.7395,	79.7234,	1.1014440,	1.2753520
573608,	-3.6883,	5.3283,	79.4591,	1.1023875,	1.2788047
573611,	-1.5700,	6.4914,	80.2650,	1.0984944,	1.2772206
573616,	-2.2845,	6.0816,	79.8362,	1.1002996,	1.2719702
573619,	-4.3498,	4.9739,	79.2215,	1.1041000,	1.2727227
573622,	-4.8214,	4.8210,	80.8192,	1.1026665,	1.2712036
573626,	-7.6286,	3.3367,	80.8501,	1.1077502,	1.2674063
573629,	-6.9550,	3.7520,	82.6766,	1.1046408,	1.2688577
573631,	-8.9896,	2.6449,	83.9357,	1.1054186,	1.2730350
573668,	-0.1679,	5.0996,	57.5901,	1.0694125,	1.2585295



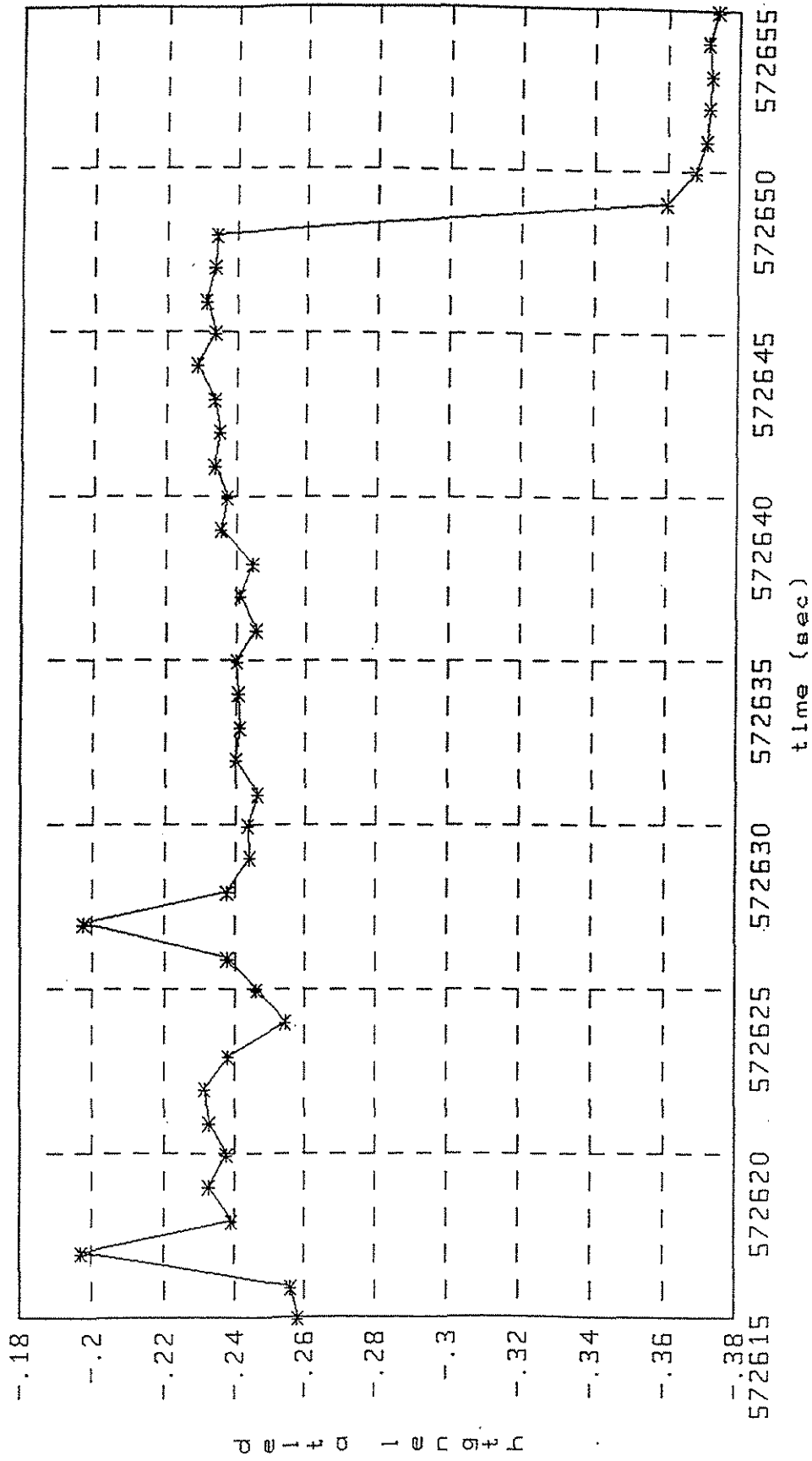
Graph 5.3. Comparison of  $\omega$  values—high flight



Graph 5.4. Comparison of  $\omega$  values—low flight.



Graph 5.5. Original and filtered C-R.



Graph 5.6. Change in length of wing with time.

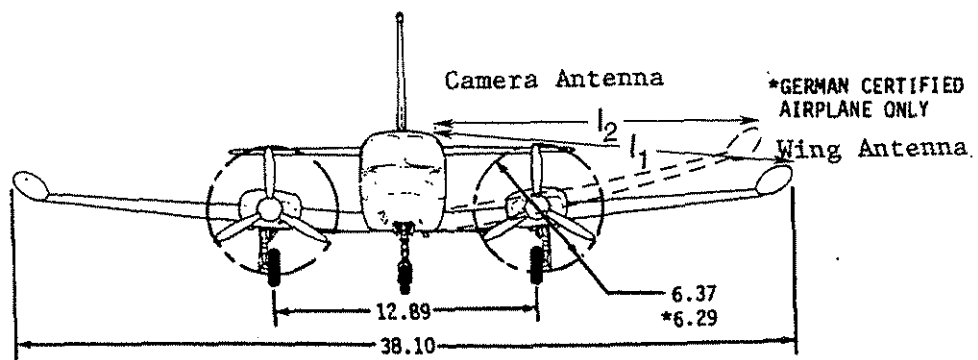
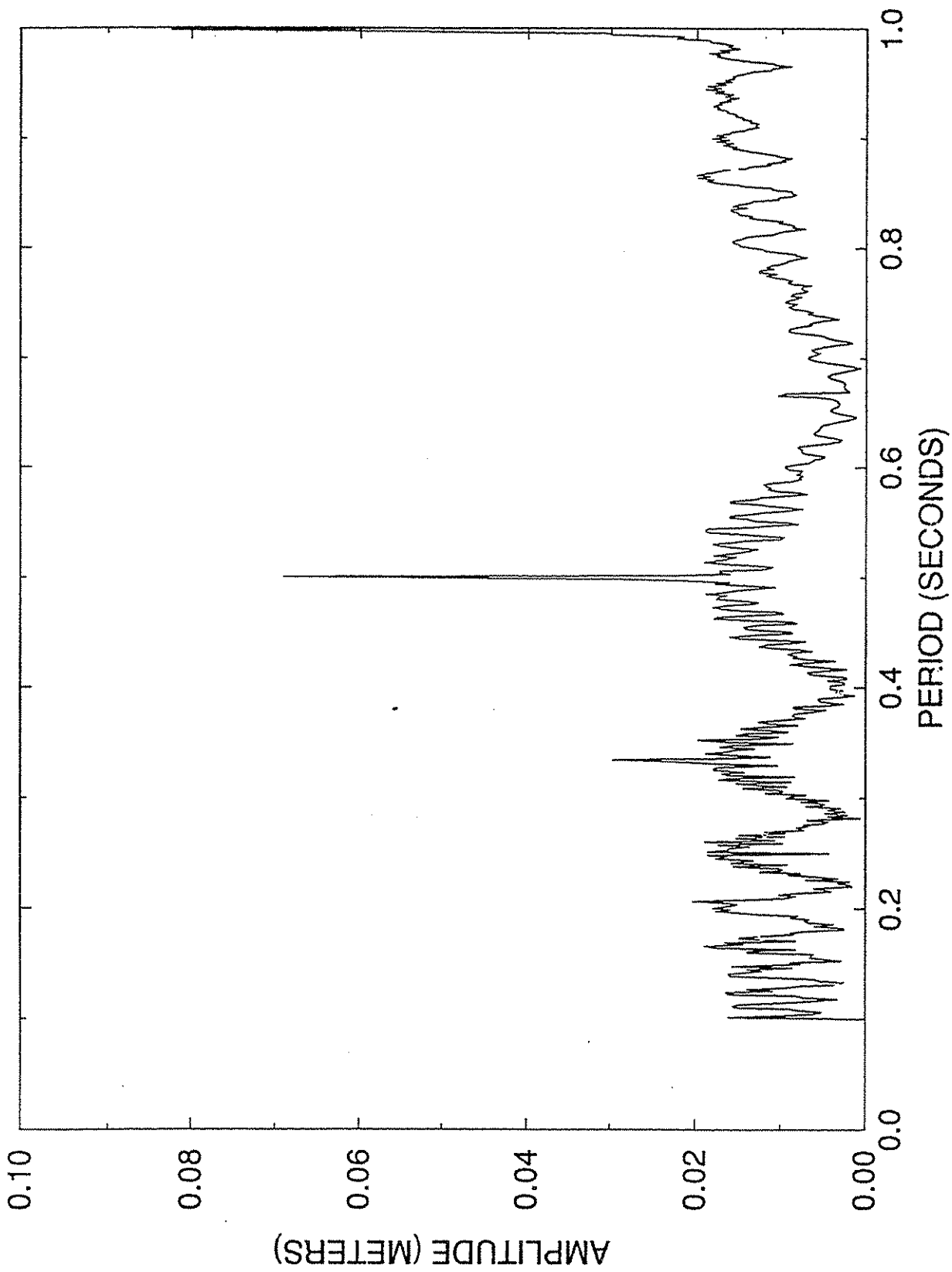
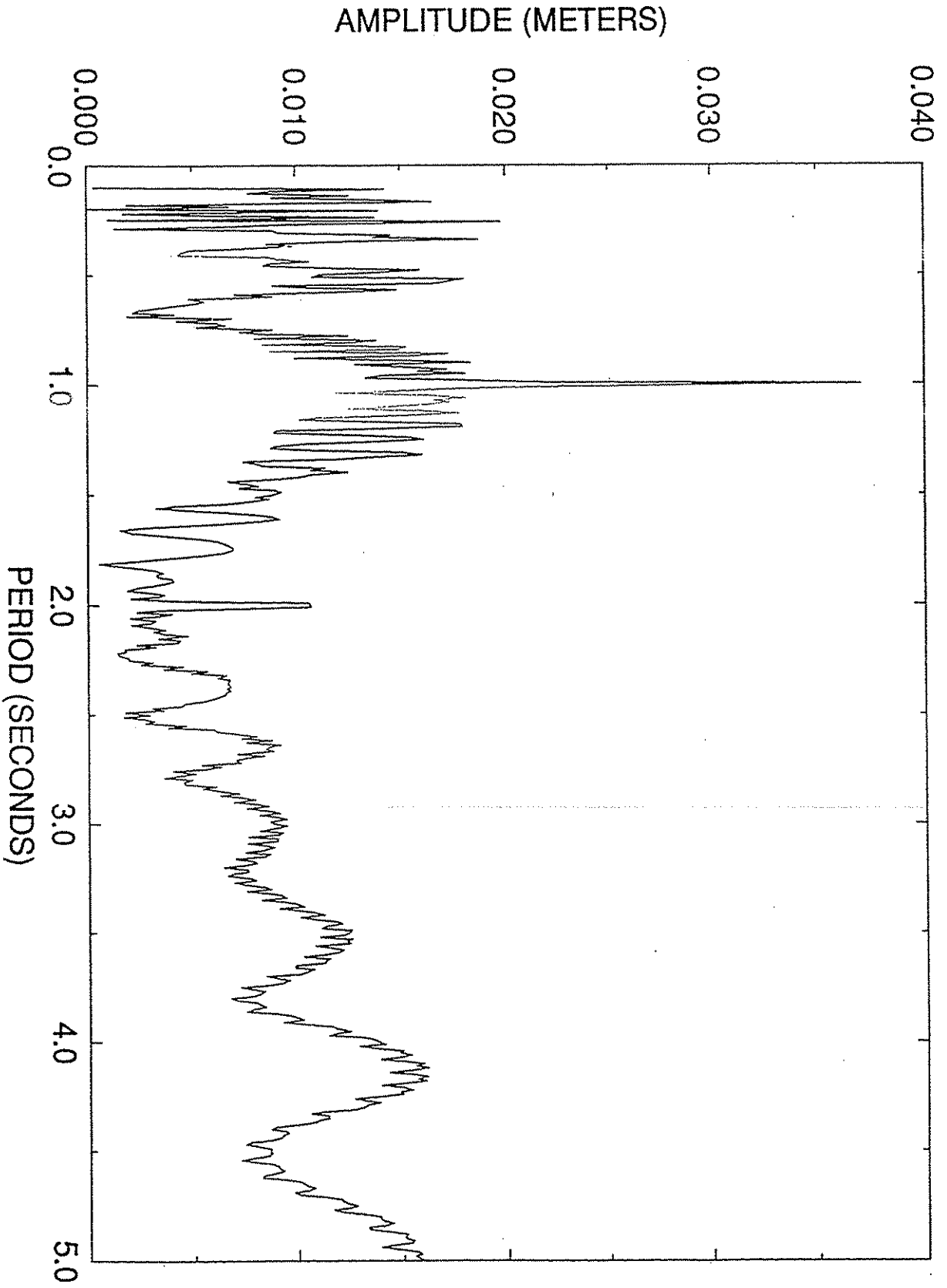


Figure 5.2. Change in scale of wings



Graph 5.7. Spec for high flight-high frequency.



Graph 5.8. Spec for high flight—low frequency.

Table 5.5. Comparison of  $\omega$  values.

Photo #	OMEGAc (Yao) *	OMEGAp (Calib)	OMEGAc (Ken)	
	(In degrees)			
			No Deflection	Deflection
41	2.898	1.824	3.085	8.735
42	2.057	0.948	1.110	7.203
43	1.830	0.722	1.562	7.250
44	2.185	1.691	1.768	7.693
45	2.459	1.671	1.736	7.415
46	2.423	1.530	2.147	7.812
49	-12.374	0.303	-12.814	-7.095
50	-12.931	0.868	-13.747	-8.070
51	-13.146	1.144	-13.516	-7.834
52	-11.069	-0.778	-11.778	-6.007
53	-11.161	-0.020	-11.283	-5.514
56	-6.087	0.871	-2.784	2.900
57	-7.079	0.244	-4.026	1.659
58	-7.173	-0.002	-4.003	1.679
59	-7.421	-0.270	-4.441	1.236
60	-8.460	-1.295	-5.324	0.342
63	-6.971	-0.191	-3.968	1.592
64	-8.135	0.909	-4.744	0.819
65	-8.326	1.304	-4.703	0.859
66	-8.792	1.378	-5.335	0.225
67	-7.436	0.114	-4.435	1.132

\*Using GPS time 571382 as initial time.

determine the amplitude and frequency of the flexing of the wing, a spectral analysis was done using the change in length. Graphs 5.7 and 5.8 show the spectral analysis of the high flight. The spectral analysis indicates that it is possible for the wing to vibrate with an amplitude of 10 centimeters and a frequency of 1 Hertz (1 cycle per sec). The amplitude and frequency may vary depending on the speed, flying height, air pressure, wind speed, amount of fuel in the tank, etc. However, it is felt that change in length (Fig. 5.2) will correspond to the extent of deflection and will have an effect on the calculation of the rotation. Thus, the first-order model developed in the first test is modified as

$$w_p = w_o + w_G(A \cos k_G + B \sin k_G) + C Dl + Dt$$

where C and D are constants, Dl is the change in length from the initial set up, and t is the time in seconds from the initial set up.

Table 5.5 shows the omega angle by GPS (both Ken and Yao) and the omega angle by photogrammetric block adjustment using Calib software for both high and low flights. These values are then used to determine the parameters A, B, C, D, and  $w_o$  by least squares, giving  $w_o = 0.170668$ ,  $A = 0.057366$ ,  $B = 1.305072$ ,  $C = 0.155838$  and  $D = -0.000074$  using Yao's photogrammetric values for both the high and low flights. Using these values, a second-order correction model was developed for the lower flight. Using statistical significance the model was found to be

$$w_p - w_c = A_0 + A_1 X + A_2 Y + A_3 t + A_4 S + A_5 X^2 + A_6 Y^2 + A_7 S^2 + A_8 xt + A_9 xs + A_{10} Ys + A_{11} st + A_{12} t^3$$

where

$w_c$  = omega computed from the first-order model

$A_0, \dots, A_{12}$  = constants

X, Y = coordinates of the camera location

t = time from the initial set up

S =  $l_2/l_1$ , the scale (see Fig. 5.2)

A least-squares fit of this model for the lower flights gave a standard error of 0.00018 radians, indicating a satisfactory solution. This model shows that the first-order model needs to be further corrected for variation in orientation, time, and scale.

Table 5.6 shows the results of a single strip adjustment for the high flight by Calib for two methods. In the first method (which is the present photogrammetric method) only ground controls are constrained; in the second, our proposed method, the nodal point coordinates obtained by GPS and  $w_c$  obtained using the first-order model are constrained.

Table 5.6. Comparison of exterior orientation elements.

Method	$X_0$	$Y_0$	$Z_0$	Kappa	Phi	Omega	$\sigma_0$
1 (With Ground Control)							
	246392.4	307479.9	953.9	0.12388	-0.054975	0.031843	0.15
Stand. Error	27.4m	33.7m	25.3m	0.0168 (rad)	0.01634 (rad)	0.029 (rad)	
2 (No Ground Control, but Weights on $X_0$ , $T_0$ , $Z_0$ & Omega)							
	246389.2	307482.1	957.3	0.11825	-0.05574	0.032031	0.5
Stand. Error	0.6m	0.6m	0.6m	0.0006 (rad)	0.0010 (rad)	0.003 (rad)	

The difference between  $w$  by the two methods is 0.00019 radians, which compares well with the value obtained by the second-order model, indicating that the relative orientation and scaling between photos in the Calib software automatically compensates for the second-order correction.

Table 5.6 also shows that the standard error of the exterior orientation elements of the second method is better than that of the first method. So the first method is better than the second because the weight on  $w$  for the second method is 10,000 (this is required to constrain  $w$  within  $\pm 0.0001$  radians). However, the maximum photo coordinate residual (25 microns) for the second method is better than the first method (27 microns), indicating the ground coordinates are better for the second than the first.

## **6. ANALYSIS OF FINAL TEST**

### **6.1. ISU and Highway 30 Project**

The final project to test the concept in the airborne GPS was done from June 1994 through February 1995. Previous studies have shown that reliable GPS data can be collected with antennas at the fuselage and wing locations of the aircraft. For the fast static data processing, we need at least seven satellites and  $L_1/L_2$  receivers. For reliable photogrammetry observations, we need targeted control and pass points. Thus, for the final project, the aircraft was fitted with four antennas; two on the wings, one on the fuselage, and one above the camera (see Fig. 2.7). Six state-of-the-art GPS Z12 receivers were used; four in the aircraft and two on the ground base stations.

Two test photographic sites were selected: one on the ISU campus and the other between Nevada and Colo on Highway 30.

### **6.2. Ground and Flight Control**

The ISU test site consisted of nine pre-targeted points (see Fig. 6.1). The coordinates of the targeted points were determined by GPS with an Ashtech  $L_{12}$  GPS receiver, using Iowa DOT as the reference point. The Geolab software was used to adjust the vectors.

The Highway 30 test site consisted of a number of pre-targeted points (see Fig. 6.2). The four control points (NW, NE, SW, SE) were established by Ashtech  $L_{12}$  GPS receivers using the Town Engineering Building and the Iowa DOT as reference points. The Geolab software was used to adjust the vectors (see Fig. 6.3). The control points along Highway 30 were established by the use of a total station traverse using the four corners (NW, NE, SW, SE) as control points. The points along Highway 30 were painted and the pass points in the field were targeted prior to flight.

The Base 1, Base 2, and Taxi, used for flight control at the Ames airport, reference points were established by Ashtech  $L_{12}$  GPS receivers using Town Engineering Building and the Iowa DOT as reference points. Geolab was again used to adjust the vectors (see Fig. 6.4).

### **6.3. Flight Mission**

On June 20, 1994, the Cessna aircraft fitted with four  $L_1/L_2$  antennas and a  $L_1$  antenna for navigation was used to test the airborne GPS concepts (see Fig. 2.7)

The aircraft was taxied over the Taxi point; the four GPS Z12 receivers were connected to the  $L_1/L_2$  antennas and arranged to collect the data on flight (see Fig. 6.5). Two Z12 GPS receivers were set on the nearby reference points Base 1 and Base 2 (see Fig. 6.6).

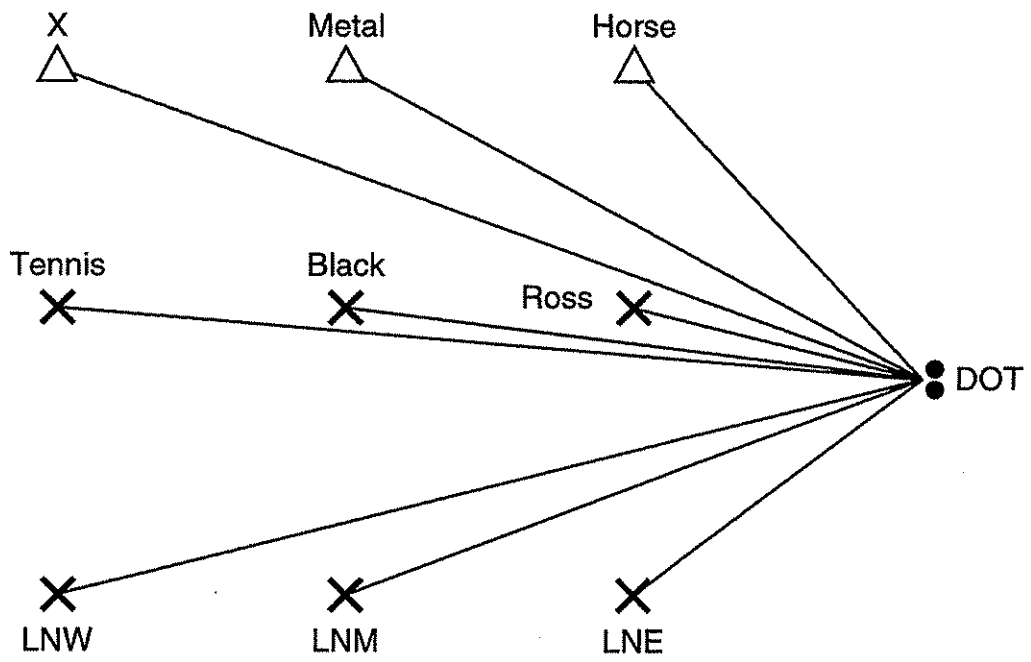


Figure 6.1. ISU campus control.

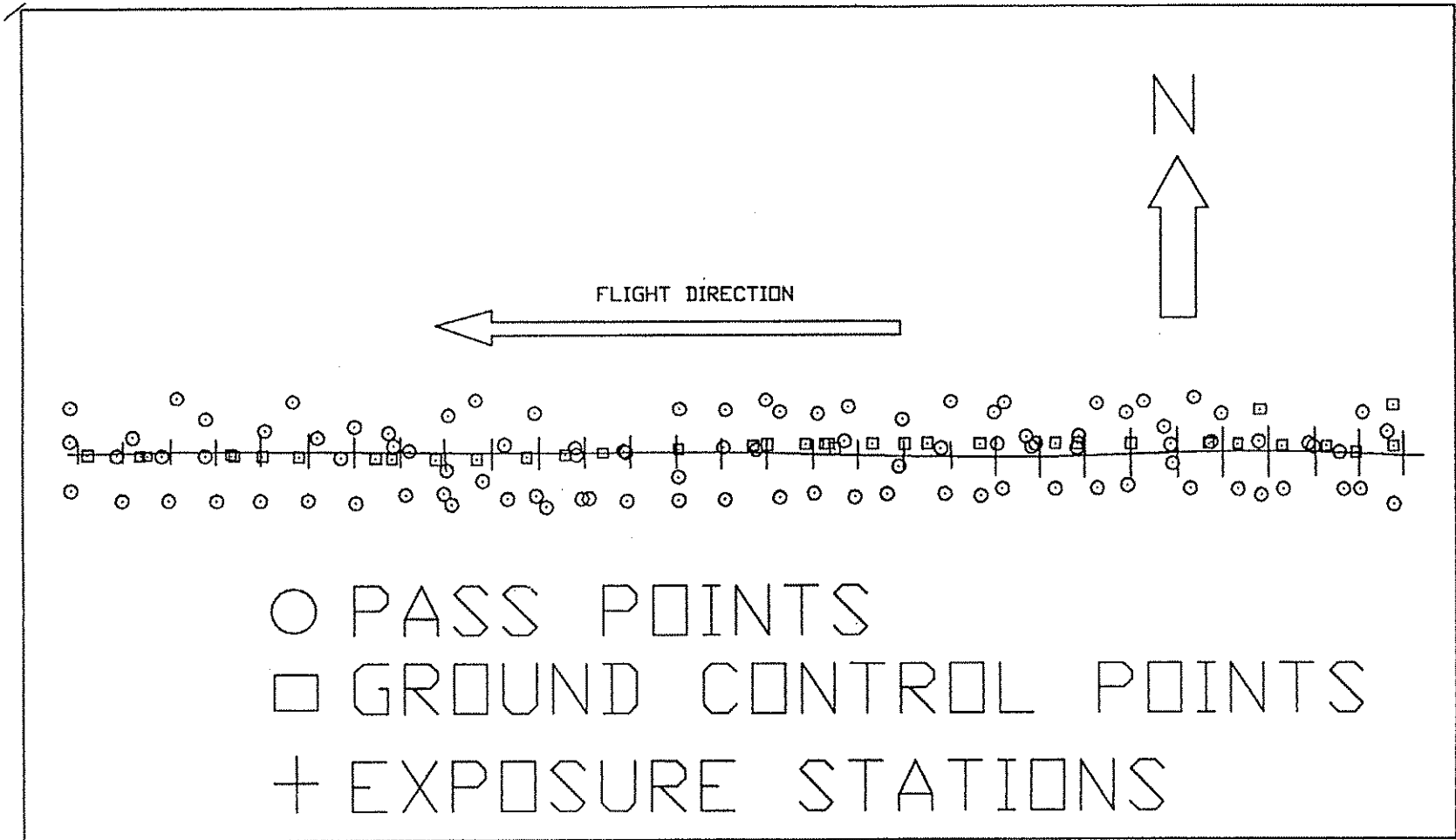


Figure 6.2. Highway 30 flight, 1994.

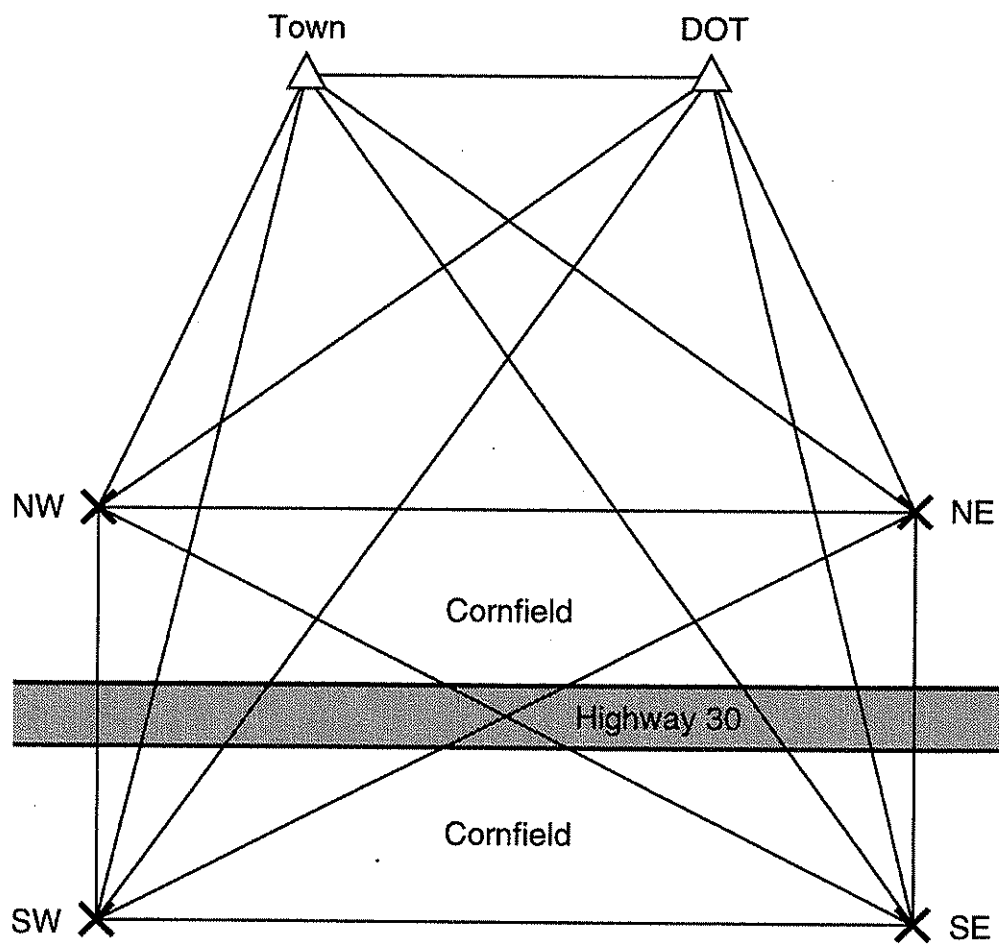


Figure 6.3. Highway 30 control.

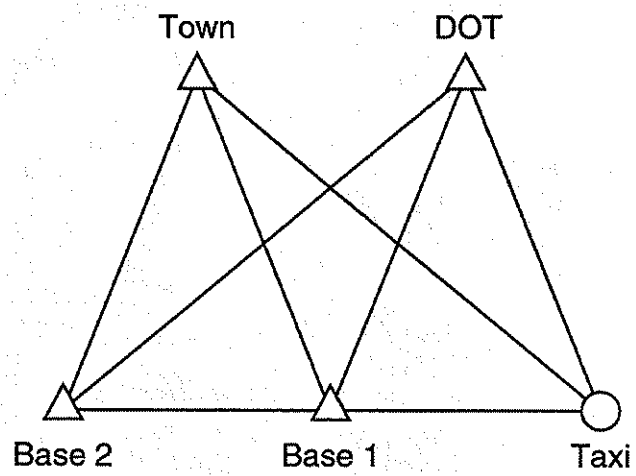


Figure 6.4. Airport control.

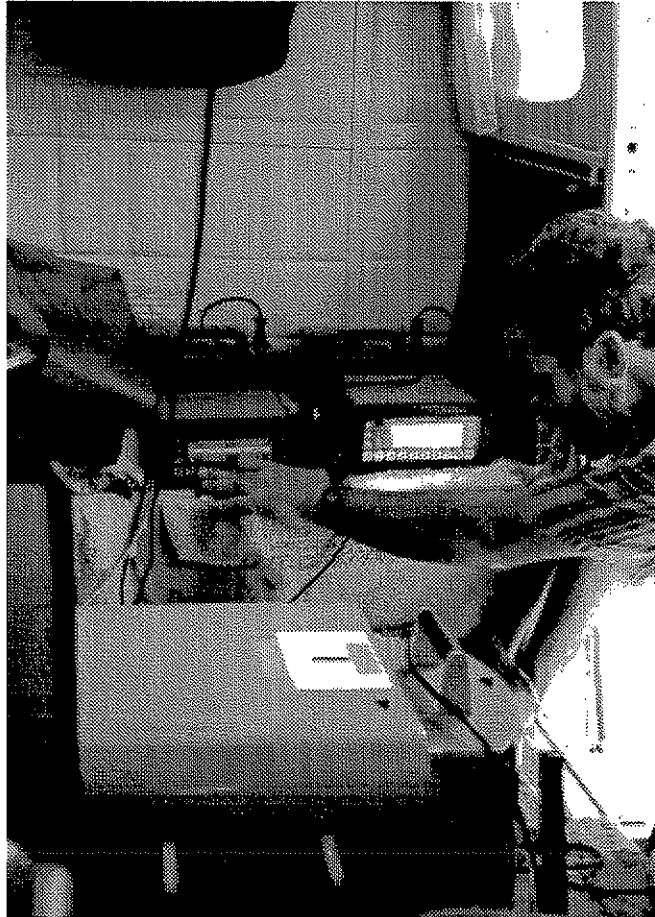


Figure 6.5. GPS receiver arrangement in the aircraft.



Figure 6.6. Base station GPS data collection

The flight plan consists of one flight in the east - west direction at a flying height of 3,000 feet over the ISU campus, and another over the ISU campus and continuing over the Highway 30 test site at a flying height of 1,500 feet (see Fig. 6.7). The campus site is 3 to 5 kilometers from the airport and the Highway 30 site is about 17 to 30 kilometers from the airport.

Each flight collected data for a few minutes at the Taxi point, then flew over the test site, took photographs at the pre-determined location using pinpoint navigation (see Figs. 6.2 and 6.8), then returned to the Taxi point, and collected additional data for a few minutes. During the entire mission, GPS data were collected every half second by the four receivers on board and the two receivers on the ground base station (see Fig. 6.9). The LMK 2000 camera was used on this flight mission, and the exposure times were also recorded on the GPS receiver.

#### 6.4. Processing of GPS Data

The GPS data were processed using Prism (a new version of GPPS) and PNAV software developed by Ashtech. The data from the receivers were downloaded to a personal computer network and the position of the aircraft antennas with respect to both base stations were determined. Also, the position of the left and right antennas with respect to the camera station was processed. The data were processed both in the forward and reverse direction, which allowed the software to eliminate any integer ambiguity.

The results were smooth and the positions of the antennas with respect to all three references agreed within acceptable limits. Figure 6.10 shows the location of the left wing, right wing, and camera antennas with respect to the Taxi point. The difference between the camera antenna coordinates determined by PNAV when the aircraft is over the Taxi point and the coordinates from the control survey is 0.06 meters in x and 0.13 meters in y, indicating that the PNAV position determination is accurate. The small difference shows the pilot's ability to taxi the aircraft exactly over the Taxi point. The height of the camera antenna above the camera's nodal point given by PNAV and the tape measurement is 1.541 meters, which compares with the previous calibrated value of 1.464 meters. The difference is due to the use of a cloth tape for measurement and the lack of knowledge about the exact location of the nodal point.

The PNAV software gives the antenna location in spherical coordinates ( $\phi, \lambda, h$ ) or in local three-dimensional coordinates (X,Y,Z) with respect to the reference points. PNAV also interpolates the position of the antenna at the exposure time of the camera. For practical applications, the spherical coordinates can be converted to the state plane coordinate system. The angle omega (assuming the y axis is parallel to the camera and to the left and right wing antennas), the angle phi (assuming the x axis is parallel to the camera and the front antenna), and the angle kappa (assuming the z axis is parallel to the vertical) can be calculated (see Fig. 6.11). Table 6.1

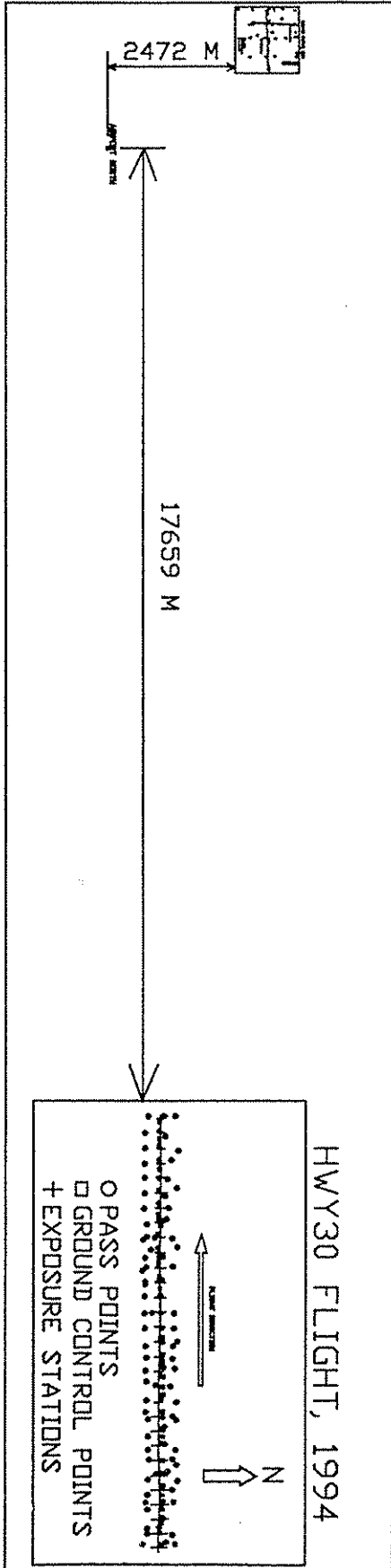


Figure 6.7. Project 1994.

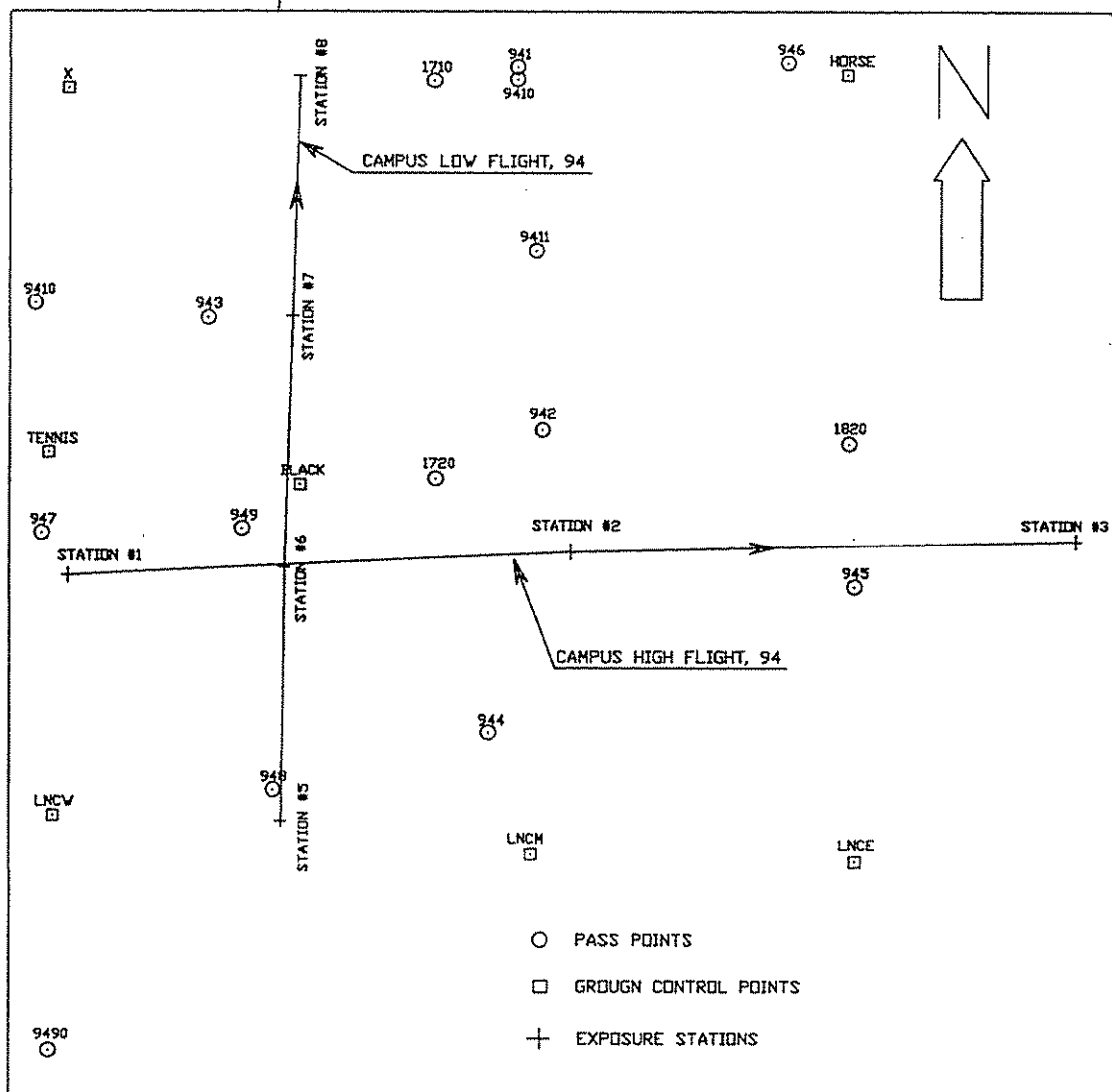
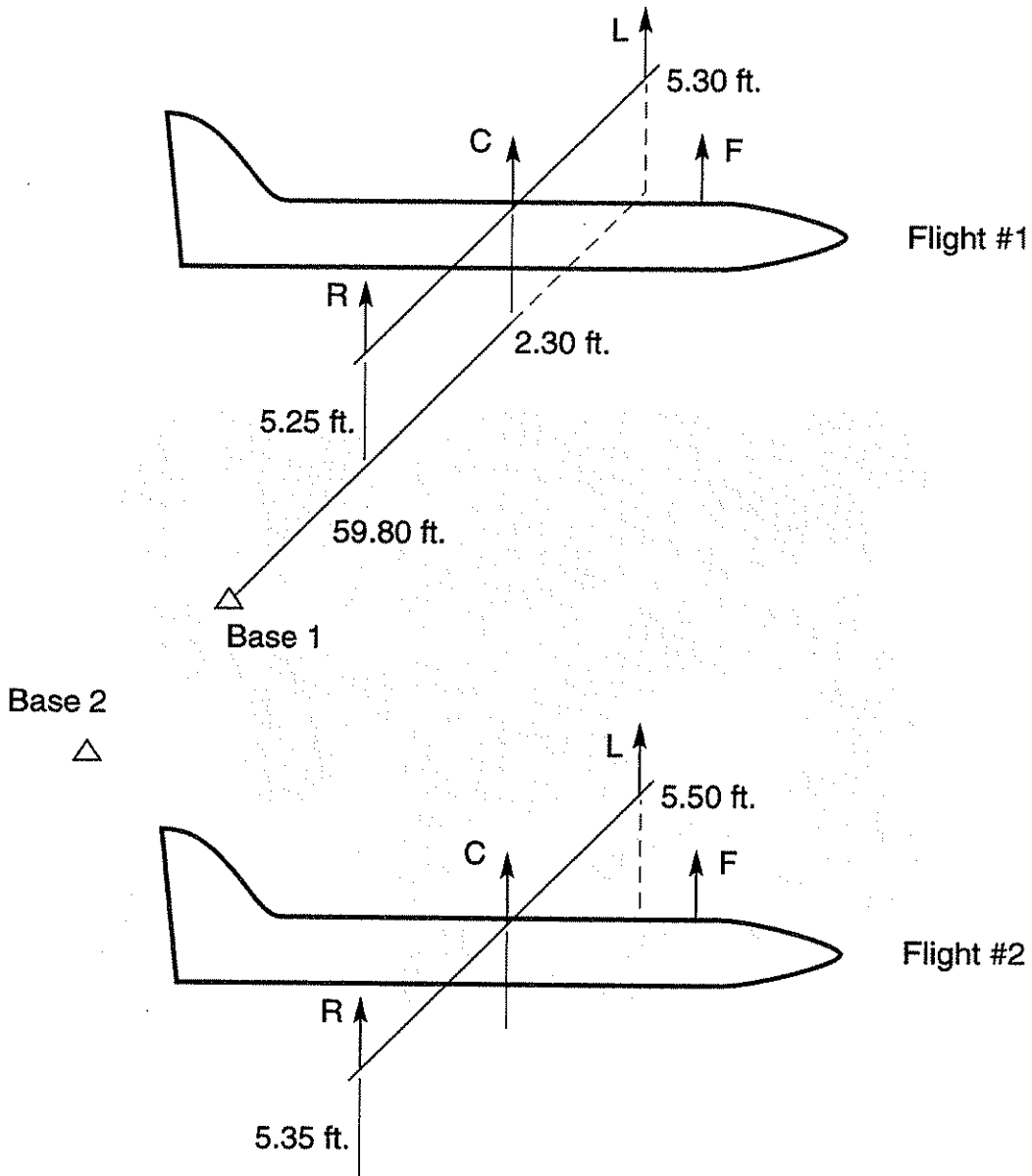


Figure 6.8. Campus flight 1994.



Figure 6.9. GPS data collection on photo mission.



$$\begin{aligned} \text{Height of antenna above lens} &= 283.5799 - (281.3376 + 0.701) \\ &= 1.541\text{m} \end{aligned}$$

	<u>X</u>	<u>Y</u>	<u>Scale</u>	<u>Convergence</u>
BS1 1,	1055376.0072,	1489846.9346,	1.0000130779, -, 0,	4, 58.9877, 1401
BS2 2,	1055444.7742,	1489831.4460,	1.0000129530, -, 0,	4, 59.4467, 1401
AIRP 3,	1055358.2282,	1489850.9376,	1.0000131103, -, 0,	4, 58.8690, 1401
PNAV } AIRP3 }	1055358.2885,	1489850.8052,		
	0.0603	0.1324		

Figure 6.10. Antenna locations at taxi point.

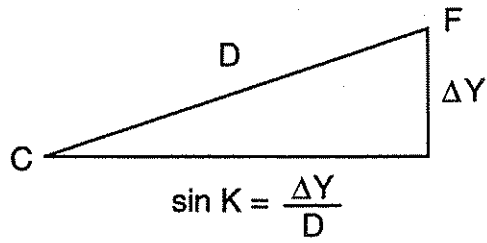
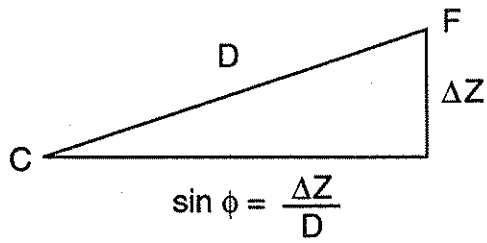
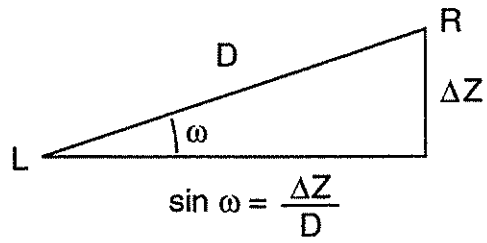


Figure 6.11. Computation of  $\phi_G$ ,  $\omega_G$ ,  $k_G$ .



shows the time, antenna locations, and angles at all times of flight prepared by using a spreadsheet. Table 6.2 shows the results for the camera exposure times.

For this study, it was sufficient to accept the data with Base 2 as a reference and the interpolated antenna positions given by the PNAV software.

### **6.5. Photo Coordinate Observation**

The photo coordinates of flight 1 and flight 2 were observed using a Wild STK1 stereo comparator. On the campus site, only controls were targeted and the natural points were used as pass points. Wherever possible, the same natural points were used for flights 1 and 2.

On the Highway 30 site, most of the painted targets along Highway 30 were clearly seen but some points on the side roads were obstructed by construction activities. Most of the targeted pass points on the south side were clearly seen but most of the targeted points on the north side were not, perhaps as a result of overgrowth of the corn and shade caused by the sun.

The coordinates were observed by two graduate students. The comparator coordinates were processed by Sat9 software to get the photo coordinates. These photo coordinates were then processed by RO software for agreement between adjoining photos. Finally, the coordinates were processed through Albany software for agreement between strip and ground coordinates. At each stage, if there was disagreement, the coordinates were re-observed and the inconsistencies eliminated. Again, in this study, errors due to refraction and lens distortion were assumed to be negligible.

### **6.6. Analysis of the Flight Data**

The output of the Albany software, namely, the approximate ground coordinates, the camera location and orientation, and the photo coordinates, were used as the input into the Calib software. The Calib software is a self-calibration software that runs on Project Vincent, a state-of-the-art computer network with Unix workstations.

Table 6.3 shows the comparison between results by Calib (photogrammetry) and PNAV (GPS). In this table, Photos 1–3 are from flight 1; Photos 4–7 are from flight 2 (campus site); and Photos 8 and 9 are from flight 2 (Highway 30 site).

Unfortunately, many of the targeted pass points north of Highway 30 and some of the targeted controls on the side roads were not visible on the photo. Due to this, the accuracy of the Highway 30 site strip was questionable. Thus, the results of only the first two photos on the Highway 30 site were used in the analysis.

Table 6.3 also shows that the difference in Z is large for the campus site. Upon investigation it was found that a focal length of 152.44 was used instead of 152.21, that the camera

Table 6.2. Data of flight 1 for exposure time.

TIME	Xc	CAMERA			LEFT		RIGHT			FORE		
		Yc	Zc	Xl	Yl	Zl	Xr	Yr	Zr	Xf	Yf	Zf
148201.670116	-2597.614	2937.324	951.740	-2598.014	2942.955	951.382	-2597.086	2931.801	950.848	-2596.623	2937.402	951.801
148207.775577	-2044.807	2964.387	951.969	-2045.027	2970.025	951.615	-2044.451	2958.846	951.083	-2043.810	2964.432	952.030
148213.882438	-1490.306	2977.848	951.362	-1490.500	2983.477	950.855	-1489.979	2972.282	950.638	-1489.308	2977.889	951.419
148754.715104	-39.466	-1380.126	9.324	-34.459	-1382.474	8.098	-44.608	-1377.851	8.630	-39.908	-1381.025	9.376

Table 6.3. Photo-GPS location.

	X	Y	Z	Dist. from Ref. Pt.	Flying Ht.	Direction	Geoid Undulation
1	-0.242	-0.367	4.102	3.5 km	3,000 ft f=152.442	W → E	28.87
2	0.385	-0.606	4.254				
3	0.709	-0.344	4.295				
4	0.265	0.502	4.0632	3.5 km	1,500 ft f=152.442	S → N	28.87
5	0.361	0.262	3.678				
6	0.317	0.042	3.418				
7	0.1962	-0.124	3.365	26 km	1,500 ft f=152.212	E → W	29.45
8	-1.050	-0.984	1.473				
9	-1.25	-0.862	1.025				

location by GPS was not corrected for antenna height, and that the elevations of control points, because they were determined using L<sub>12</sub> GPS receivers, were not accurate.

In addition, Table 6.3 shows that the difference in x and y is large for the campus site. Upon investigation it was found that the ground control for Highway 30 was on a surface state plane while the GPS was on a state plane. The side road controls at the end of the strip were covered by construction. Corn obstructed the targeted and pass points north of Highway 30.

Table 6.4 shows that the difference in orientation angles between the photogrammetry and GPS methods was consistent for the campus site in flight 1 and flight 2 but not consistent between the campus site and the Highway 30 site in flight 2 for the following two reasons:

- (1) The Highway 30 site is about 25 kilometers from Base 2, which is beyond the acceptable limit of 10 kilometers for reliable ambiguity resolution by the PNAV software. The campus site is only 5 kilometers from Base 2 and the ambiguity resolution is reliable.
- (2) Lack of good targeted pass points and control points at the end of the Highway 30 strip.

As discussed earlier, to do strip adjustment using airborne GPS without any ground control, the omega orientation angle needs to be determined by airborne GPS. Previous tests have shown that:

$$\omega_p = \omega_o + (a \cos K_G + b \sin K_G)\omega_G + c\phi_G$$

where

$\omega_p$  = omega by photogrammetry

$\omega_G$  = omega by GPS

$\omega_o$  = a constant parameter

Table 6.5 shows the results of the least-squares fit of the above equation using the campus site flight 1 and flight 2 data. The standard error of 0.0005 indicates that the accuracy of  $\omega_o$  is better than or equal to 0.0005 radians and is acceptable for highway application using 1,500 feet or 500 meters in flying height photos. The following reasons support the conclusion:

- (1) As discussed earlier, the accuracy of phase measurement in the Z12 receiver is 0.2 millimeters. Assuming a noise of 0.2 millimeters due to multipath etc., the relative error in the z direction between the left and right wing antennas can be assumed to be about 0.5 millimeters. Because the distance between the left and right wing antennas is about 10 meters, the error in  $\omega_o$  is = 0.00005 radians.

Table 6.4. GPS-Photo orientation.

	$\omega$	$\phi$	$\kappa$
1	0.0045	0.0151	0.0032
2	0.0053	0.0130	0.0024
3	0.0037	0.0117	0.0019
Std. mean	0.0045	0.0133	0.0025
Std. error	0.0006	0.0014	0.0005
4	0.0055	0.0168	0.0076
5	0.0071	0.0255	-0.0117
6	0.0054	0.0177	-0.0010
7	0.0036	0.0188	+0.0089
Std. mean	0.0055	0.0197	0.00094
Std. error	0.0012	0.0034	0.0082
8	0.0116	0.0027	-0.0061
9	0.0118	0.0029	-0.0057
Std. mean	0.0117	0.0028	-0.0059
Std. error	0.0001	0.0001	0.0003

Table 6.5. Results of combination of high and low flights.

INPUT DATA ARE: (OMEGAp, OMEGAg, KAPPAg, PHIG)

OMEGAp	OMEGAg	KAPPAg	PHIG
0.043108000	0.047640007	0.075824965	-0.061304218
0.042177000	0.047439621	0.044556999	-0.060995646
0.015774000	0.019469214	0.041470049	-0.057373606
0.036485000	0.042290545	0.045362608	-0.030498599
0.047588000	0.054703783	0.023387758	-0.023387548
0.011352000	0.016753616	0.052766161	-0.040786984
0.007231000	0.010923818	0.067033636	-0.033132291

FORMULA IS  $OMEGAp - OMEGAg = OMEGAo + OMEGAg (a * \cos(KAPPAg) + b * \sin(KAPPAg)) + d * PHIG$

-0.0048850666   -0.0641132373   0.4197135928   -0.0300743669

THESE ARE THE ERRORS, (COMPUTED - REAL)

-0.000040   0.000060   -0.000373   -0.000066   -0.000035  
 0.001041   -0.000587

THE STANDARD DEVIATION IS  
 0.000513

- (2) The elevation of the control points in the campus site are determined by the L<sub>12</sub> GPS receiver from the Iowa DOT. Thus, the relative error of the ground control is about 0.1 meters, and therefore, the error in  $W_p$  due to ground control for the lower flight is about = 0.0001 radians.
- (3) The error in elevation by photogrammetry due to error in the photo coordinate,  $\Delta r$ , is given by:

$$dH = (H/r) * dr$$

Thus, if  $r = 100$  millimeters,  $dr = 0.01$  millimeters, and  $H = 1000$  meters for flight 1, then  $dH = 0.1$  meters.

The error of 0.1 meters in  $dH$  will result in an additional error of 0.0001 radians in  $\omega_p$  due to photogrammetry and this together with the ground control error will result in a total error of 0.0002 radians in  $\omega_p$  (see Fig. 6.12).

- (4) An error of 0.0005 radians in  $\omega_G$  for an airborne GPS without any ground control will result in an elevation error of 0.25 meters for flight 2 (500-meter flying height). Thus the elevation error is good for drawing one meter contour at either flying height.

Table 6.5 shows the transformation parameters for transferring  $\omega_a$  to  $\omega_p$  obtained from campus site data. They are not suitable for the Highway 30 site perhaps for the following reasons:

1. The Highway 30 site is more than 10 kilometers from the reference base station, which is beyond the acceptable limit for integer resolution by PNAV.
2. The difference in the geoid undulation at Base station and the Highway 30 site is about 0.7 meters and that between the base station and campus site is 0.1 meters, suggesting that there may be a large difference in the deviation of the vertical between the campus and Highway 30 sites.
3. The direction of flight 1 is from west to east and the direction of flight 2 over campus is from south to north, while the flight over Highway 30 is from east to west. The different directions and time of flight may result in a different error in  $W_G$  due to different multipath errors in the left and right wing antennas. The differences between  $W_G$  and  $W_p$  for flight 1 and flight 2 over the campus site agree, suggesting that the multipath error is negligible and the asymmetrical motion of the left and right wing is also negligible. Also, the shape of the aircraft at the location of the antenna is a crest; therefore, any reflection will be away from the antenna, resulting in negligible multipath.

To test the feasibility of using the transformation parameters from the campus site to the Highway 30 site, a combined adjustment of flights 1 and 2 was done using the Calib software. By trial and error, a satisfactory solution was found by assigning different weights to interior orientation elements ( $x_o, y_o, f$ ) (see Table 6.6), to airborne GPS coordinates ( $X_c, Y_c, Z_c$ ) and to

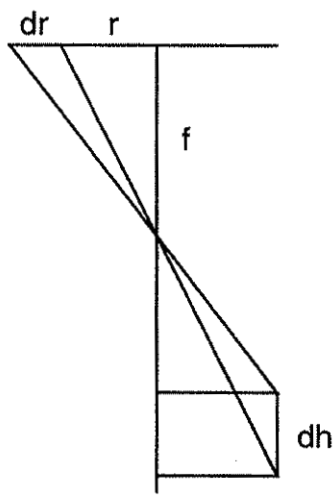
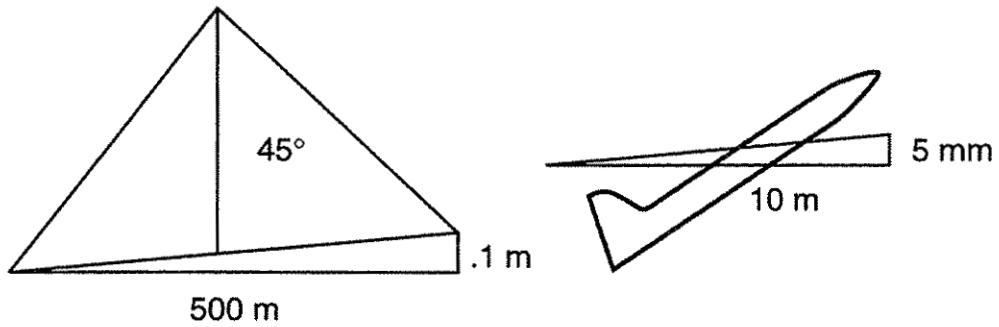


Figure 6.12. Sources of error in  $\omega_p$

Table 6.6.  $\omega_G$  to  $w_p$  using different weights.

Weight on photo coordinates = 5000

Standard error on ground contact = 0.01m

Standard error on Airborne GPS (low flight)

$X_G, Y_G = 0.01m$

$Z_G = 0.001m$

Standard error on Airborne GPS (high flight)

$X_G, Y_G, Z_G = 0.01m$

FORMULA IS  $\Omega_{Gp} = \Omega_{Go} + \Omega_{Gg} (a * \cos(KAPPAg) + b * \sin(KAPPAg)) + d * \phi$

-0.0107795884    0.8991249682    0.7631507940    -0.0508904326

THESE ARE THE  $\Omega_{Gp}$ :

-0.0128428	-0.0205923	-0.0156900	-0.0372186	-0.0150666	-0.0230069
-0.0091735	-0.0128985	0.0087594	-0.0011218	-0.0134105	-0.0244845
-0.0076987	-0.0044199	-0.0056232	-0.0213606	-0.0143648	-0.0108987
0.0026834	-0.0073671	-0.0023437	-0.0119827	-0.0178356	-0.0114358
-0.0118249	-0.0080444	-0.0273579	-0.0311399	-0.0261177	-0.0109928

ground control. The parameters from the campus site were used to obtain  $\omega_p$  from  $\omega_G$  in the Highway 30 site strip. When these values were used in the Highway 30 site strip adjustment, even without ground control, they gave satisfactory pass point coordinates, suggesting a self calibration for a site (e.g., Highway 30) can be used to convert  $\omega_G$  to  $\omega_p$ .

Table 6.4 shows the error of  $(K_p - K_G)$  is about 0.0005 radians and  $(\phi_p - \phi_G)$  is about 0.001 radians even though the distance between the camera antenna and the forward antenna is only 1 meter, suggesting that the relative error of GPS coordinates is better than 1 millimeter and that  $\phi_G$  and  $K_G$  can be used to rectify aerial photos and also produce orthophoto. The error in  $(K_p - K_G)$  is better than  $(\phi_p - \phi_G)$  because the determination of  $K_p$  by photogrammetry is more accurate than  $\phi_p$ .

### 6.7. Analysis of Refined Test Flight Data

Because of the possibility of small errors in the initial data, the following steps were taken to refine the ground control, the photogrammetric coordinates, and the GPS data.

1. Two ground control points at both the ISU Campus site and the Highway 30 site were connected to the Base 2 reference point using  $L_1$  and  $L_2$  GPS receivers. This procedure eliminated any possible constant, rotation, and scale errors between GPS and ground control.
2. A spirit leveling was done between ground control points in the campus site and between the three control points of the first model of Highway 30. This process eliminated any relative error greater than 5 centimeters in elevation between the ground control points.
3. The photo coordinates of all the points in the nine photos were re-observed by three observers. Each did observations twice and the mean of the six observations was adopted. For obscure reasons there was a constant error of 0.040 millimeters between the initial coordinates and the refined coordinates at a few of the observed points.
4. The GPS coordinates of the antennas were corrected for antenna heights and geoid undulation.

The refined data for the nine photos were then adjusted by Calib. The difference in camera coordinates for the campus site (Photos 1–7) (see Table 6.7), clearly show that the airborne GPS coordinates are better than 10 centimeters irrespective of the flight altitude and flights. The error in the z direction of 0.8 meters for the Highway 30 site is probably due to integer ambiguity resolution by the PNAV software because the Highway 30 site is more than 10 kilometers from the reference station Base 2.

Table 6.7. GPS-Photo locations using refined data.

	X	Y	Z
1	-0.081	0.277	0.008
2	0.305	0.205	-0.148
3	0.005	0.491	-0.167
Mean	0.076	0.324	-0.102
Std. Error	0.165	0.120	0.078
4	0.048	0.343	0.258
5	-0.004	0.1	0.081
6	-0.099	-0.204	0.046
7	0.059	-0.359	0.131
Mean	0.001	-0.03	0.124
Std. Error	0.062	0.27	0.080
8	-0.243	0.286	-0.916
9	0.467	0.249	-0.865
Mean	0.112	0.267	-0.891
Std. Error	0.335	0.018	0.025

Table 6.4 shows that the difference in orientation angles between GPS and photogrammetry is constant for flight 1 and flight 2 on the campus site. However, the orientation angles from GPS for the Highway 30 and for the campus site appear to be different. Again, this is because the Highway 30 site is more than 10 kilometers away from the reference station Base 2, suggesting the importance of having the reference station within 10 kilometers of the site or of knowing the elevation difference for two or more points in the y direction perpendicular to the flight to determine the transformation parameter when obtaining  $\omega_p$  from  $\omega_G$ .

Table 6.8 shows that the standard error of the fit between  $\omega_p$ , from refined data and  $\omega_G$  is 0.00008 radians. The accuracy of 0.0001 radians in  $\omega$  is sufficient for drawing 2-foot contours either from 1,500 or 3,000 feet flying height photos.

Table 6.9 shows the difference between  $\Delta\omega_1 = \omega_G - \omega_p$  of flight 1 and  $\Delta\omega_2 = \omega_G - \omega_p$  of flight 2. The table also shows the second difference,  $\Delta\omega_{12} = \Delta\omega_1 - \Delta\omega_2$ . The standard error of  $\Delta\omega_{12}$ , is 0.00003 radians, which agrees with the expected error of 0.00002 for a height difference of 0.2 millimeters at 10 meters apart.

Table 6.8.  $\omega_G$  to  $\omega_p$  using refined data.

INPUT DATA ARE: (OMEGAp, OMEGAg, KAPPag, PHIG, TIME)

OMEGAp	OMEGAg	KAPPag	PHIG	SECONDS
0.042392	0.047640	0.075825	-0.061304	0.670116
0.041186	0.047440	0.044557	-0.060996	6.775577
0.014783	0.019469	0.041470	-0.057374	12.882438
0.036995	0.042291	0.045363	-0.030499	1457.599484
0.048136	0.054704	0.023388	-0.023388	1460.871496
0.012002	0.016754	0.052766	-0.040787	1464.134522
0.007390	0.010924	0.067034	-0.033132	1467.263800

FORMULA:  $OMEGAp - OMEGAg = OMEGAo + OMEGAg (a * \cos(KAPPag) + b * \sin(KAPPag)) + d * \phi + E * Kp + F * T$

0.0000550947	-0.0763984723	0.5237227962	0.0729936964
0.0129816652	-0.0000011097		

THESE ARE THE ERRORS, (COMPUTED - REAL)

0.0000727	-0.0000867	0.0000140	-0.0001274	0.0000901	0.0000744
-0.0000370					

THE STANDARD ERROR IS  
0.0000859

Table 6.9. First and second difference in  $\omega_p - \omega_G$

Flight	Photo	Omega GPS-Photo (radians)	Average	Difference 1st & 2nd	Average
1	1	0.005242	0.005396		
	2	0.006254			
	3	0.004686			
2	4	0.005296	0.0050375	0.000048	0.000142
	5	0.006568		0.000314	
	6	0.004752		0.000066	
	7	0.003535			

## 7. APPLICATIONS OF AIRBORNE GPS

Airborne GPS has three main applications in photogrammetry: (1) rectifying aerial photos, (2) producing orthophotos from aerial photos, and (3) stereo plotting without ground control.

### 7.1. Rectifying of Aerial Photos

An aerial photo can be rectified using the equations,

$$x = f * \{a_{11}(X - X_0) + a_{12}(Y - Y_0) + a_{13}(Z - Z_0)\} / \{a_{31}(X - X_0) + a_{32}(Y - Y_0) + a_{33}(Z - Z_0)\}$$

$$y = f * \{a_{21}(X - X_0) + a_{22}(Y - Y_0) + a_{23}(Z - Z_0)\} / \{a_{31}(X - X_0) + a_{32}(Y - Y_0) + a_{33}(Z - Z_0)\}$$

where  $(X - X_0)$ ,  $(Y - Y_0)$  are the rectified photo coordinates at a scale of  $f/(Z - Z_0)$  and  $(x, y)$  are the photo coordinates (see Fig. 7.1). The matrix  $A$ , which makes the photo coordinate axis parallel to the rectified photo coordinates, is given by:

$$A = R_k R_\phi R_\omega = \begin{pmatrix} a_{11} & a_{12} & a_{13} \\ a_{21} & a_{22} & a_{23} \\ a_{31} & a_{32} & a_{33} \end{pmatrix}$$

Thus,

$$(X - X_0) = (Z - Z_0) * (a_{11}x + a_{21}y + a_{31}f) / (a_{13}x + a_{23}y + a_{33}f)$$

$$(Y - Y_0) = (Z - Z_0) * (a_{12}x + a_{22}y + a_{32}f) / (a_{13}x + a_{23}y + a_{33}f)$$

For example, given  $(x, y)$  we can calculate  $(X - X_0)$ ,  $(Y - Y_0)$  at  $Z$  using  $X_0, Y_0, Z_0, K, \phi, \omega$  from airborne GPS.

An aerial photo was scanned and all of its pixels  $(x, y)$  were then transformed to pixel  $(X - X_0)$ ,  $(Y - Y_0)$ . The transformed pixels were then imported to an image analysis software such as ERDAS software to display the rectified photo. ERDAS is an image analysis software which works on Project Vincent. This was tested using campus site photos and found to be satisfactory.

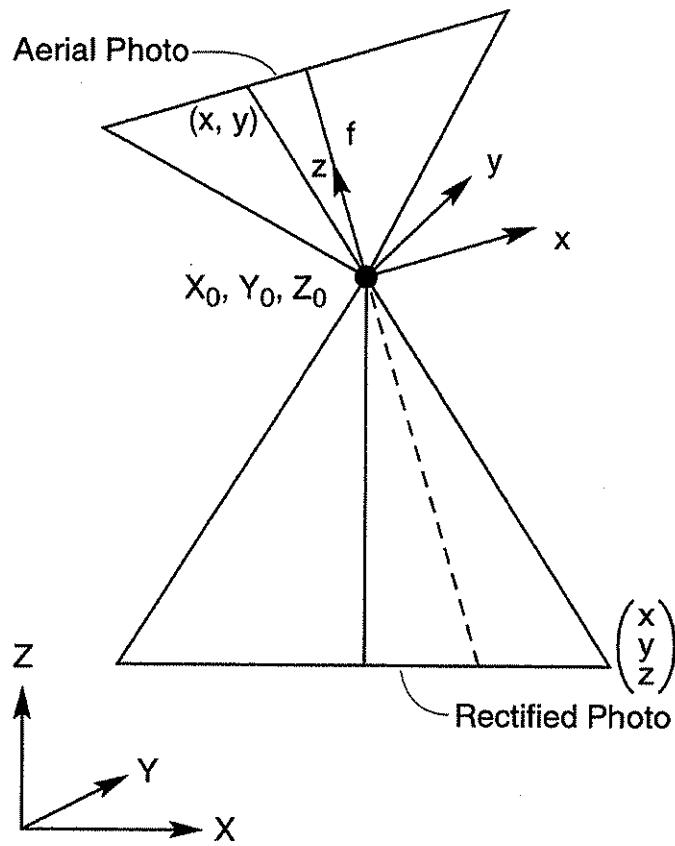


Figure 7.1. Rectification.

## 7.2. Producing Orthophotos

An orthophoto is a rectified point in which each pixel coordinate  $(X - X_0)$ ,  $(Y - Y_0)$  is computed for its own elevation  $Z_1$  using the equation

$$(X - X_0) = (Z_1 - Z_0) * (a_{11}x + a_{21}y + a_{31}f) / (a_{13}x + a_{23}y + a_{33}f)$$

$$(Y - Y_0) = (Z_1 - Z_0) * (a_{12}x + a_{22}y + a_{32}f) / (a_{13}x + a_{23}y + a_{33}f)$$

Thus, the ground elevation for every pixel in the photo must be known. If a contour map exists, then the pixels can be digitized and fed into software such as Arc Info, which will create the Digital Terrain Model for the area. Arc Info will also compute the elevation,  $Z_1$ , of the pixel for given  $x, y$ , which can then be used to compute the pixel coordinate of the orthophoto.

Alternatively, if  $(x_1, y_1)$  and  $(x_2, y_2)$  are the rectified photo coordinates of two adjoining aerial photos at scale  $f/(Z - Z_0)$  and  $f/(Z - Z'_0)$ , then both can be brought to the same scale by multiplying the second by a factor of  $(Z - Z_0)/(Z - Z'_0)$ . The elevation  $z_1$  of the pixel is given by:

$$Z_0 - Z_1 = B * (x_1 + x'_2) / (z_0 - z)$$

where

$$x'_2 = x_2 * (Z_0 - Z) / (Z'_0 - Z)$$

$Z'_0$  is the nodal point coordinate of the second photo (see Fig. 7.2). Thus, if  $(x_1, y_1)$  and  $(x_2, y_2)$  are known from adjoining photos, then  $z_1$  can be computed. From  $z_1$  the orthophoto coordinate can be computed from the pixel coordinate of each rectified photo. This method was tested using a pair of photos from the campus site and found to be satisfactory.

## 7.3. Stereo Plotting

In direct stereo plotting after the relative orientation, the following information is required:

- The base components for scaling
- The  $\phi$  and  $\omega$  angles for leveling
- The orientation angle,  $K$ , and translation  $(x_0, y_0, z_0)$  for plotting

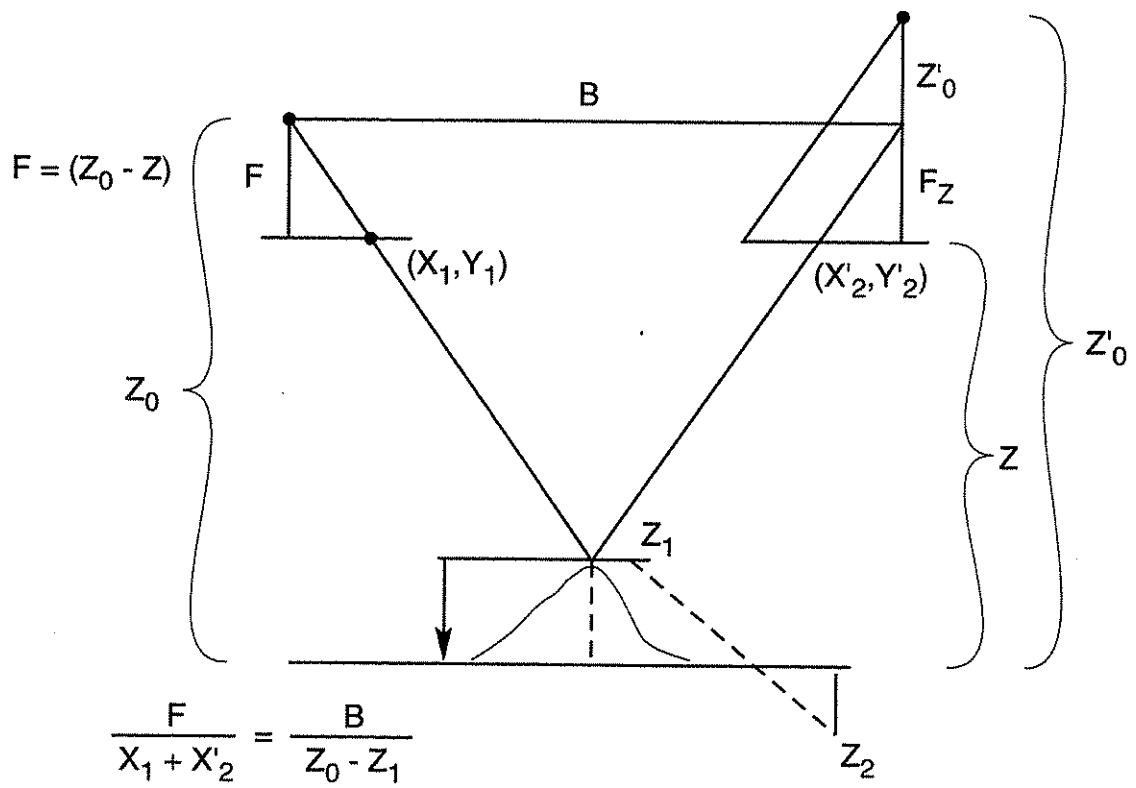


Figure 7.2. Orthophoto production.

#### 7.4. Base Components

The base components are computed as follows:

$$B_x = S (X'_o - X_o)$$

$$B_y = S (Y'_o - Y_o)$$

$$B_z = S (z'_o - z_o)$$

where  $(x_o, y_o, z_o)$  and  $(x'_o, y'_o, z'_o)$  are obtained from GPS and S is the plotting scale.

#### 7.5. $\phi$ and $\omega$ Angles for Leveling

The leveling angles are obtained from:

$$\omega = \cos K \omega' \pm \sin K \phi' = \omega'$$

$$\phi = \cos K \phi' \pm \sin K \omega' = \phi'$$

where  $\tan K = (Y_o - Y'_o) / (X_o - X'_o)$  and  $\omega', \phi'$  are from GPS.

#### 7.6. Orientation Angle and Translation

The orientation angle is given by:

$$\tan K = (Y_o - Y'_o) / (X_o - X'_o)$$

and the translation is

$$(X_o, Y_o(Z_o + Z_{om} - Z_m))$$

where  $x_o, y_o, z_o$ , and  $x'_o, y'_o, z'_o$  are from airborne GPS.  $Z_{om}$  is the nodal coordinate of the left projector nodal point and  $Z_m$  is the model coordinate of a point.

Thus, for small  $\phi$  and  $\omega$  angles, the nodal coordinates can be transformed to ground coordinates using matrices.

$$\begin{pmatrix} X \\ Y \\ Z \end{pmatrix} = \begin{pmatrix} \cos k & -\sin k & \phi \\ \sin k & \cos & \omega \\ -\phi & \omega & 1 \end{pmatrix} \begin{pmatrix} x_m \\ y_m \\ z_m \end{pmatrix} + \begin{pmatrix} X_o \\ Y_o \\ Z_o \end{pmatrix}$$

Again, this was tested using the campus site photos and the Zeiss Z8 stereo plotter and found to be satisfactory.

When the concept of airborne GPS is accepted and developed fully, further research will be needed for rectification, orthophoto production, and stereo plotting from airborne GPS.

## 8. CONCLUSIONS AND RECOMMENDATIONS

Airborne GPS is feasible. The coordinates of the camera antenna can be determined with an accuracy better than  $\pm 10$  centimeters if the base reference station is within 10 kilometers of the photographic site, which is acceptable for mapping at all scales.

The PNAV software resolves the integer ambiguity satisfactorily for fast static computation if the rover receiver is within 10 kilometers of the base station.

Camera, wings, and foresight positions are suitable for antenna location; however, the tail is not. The motion of the left and wing antennas are symmetrical and can be used for computing the angle of rotation.

The accuracy of the Z12 GPS receiver is 0.2 millimeters, and the noise due to multipath at the camera, foresight, and wing locations is negligible. The accuracy of the  $\omega$  obtained from left and right wing antennas at a separation of 10 meters is better than  $\pm 0.0001$  radians, which is acceptable for 2-foot contours using 3,000 feet or lower flying heights.

For a block with more than one strip, no ground control is required. The base station has to be within 10 kilometers of the block, and local geoid undulation has to be applied to the elevations.

For a strip, self calibration is required for transferring  $\omega_G$  to  $\omega_p$  and is valid for projects within 10 kilometers. If the project is at a distance greater than 10 kilometers, however, the elevation differences between the two control points separated in the direction perpendicular to the line of flight are required.

Further research is required to obtain  $\omega_p$  from  $\omega_G$  with an accuracy of  $\pm 0.00002$  radians, an accuracy that GPS is capable of providing. Also, further research is required to use airborne GPS data for rectification, orthophoto production, and direct stereo plotting.

## 9. ACKNOWLEDGMENT

The authors wish to thank the Iowa Highway Research Board for supporting this research project. They appreciate the confidence shown by Mr. George Sisson and Mr. Mel Nutt of the Iowa Department of Transportation (DOT). Thanks are due to Mr. Vernon Marks of the Iowa DOT for his assistance in getting this project completed on time. Thanks also are due to members of the Photogrammetric Section of the Iowa DOT, especially Marlee Walton, Alice Walsh, Roland Popelka, Dennis O'Brien, John Rainey, Jeff Danielson, Mel Holmberg, and others for their unselfish support and assistance during this research period.

Our thanks also go to Rick Hoffman and others from Surdex Inc. for obtaining the aerial photographs for the St. Louis and Ames Project. Mr. Bill Curtrell of Ashtech Inc. obtained airborne GPS data for the projects. Mr. Gary Brown of Aerial Services Inc. supplied the information for evaluating the GPS pinpoint navigation. Dr. Jerry Vogel of the Department of Aerospace Engineering and his students assisted with the analyzing of the aircraft wing motions. We thank them all for their support.

Finally, we also wish to thank Dr. Lowell Greimann, Chairman, and the staff of the Department of Civil and Construction Engineering; Dr. Lord and staff of the Engineering Research Institute; and Iowa State University for their assistance in getting this project completed on time.

## 10. BIBLIOGRAPHY

1. ACSM-NGS. Coordinate Transformation Workshop (unpublished xeroxed paper), ACSM, Falls Church, Virginia, 1987.
2. Ashjaee, J. New Results on the Accuracy of the C/A Code GPS Receiver: *Proceedings of the First International Symposium on Precise Positioning with the Global Positioning System*, U.S. Department of Commerce, Rockville, Maryland, Vol. 1, 207–214. 1985.
3. Ashtech Inc. *PRISM II Advanced Software Modules*, Sunnyvale, California, September 1994.
4. Ashtech Inc. *Ashtech XII Receiver Operations Manual*, Sunnyvale, California, 1990.
5. Ashtech Inc. *Ashtech XII Model L Operating and Processing Manual*, Sunnyvale, California, 1989.
6. Ashtech Inc. *Documentation for Ashtech GPPS Software*, Sunnyvale, California, 1989.
7. Baker, P. J. Global Positioning System (GPS) Policy: *Proceedings of the Fourth International Geodetic Symposium on Satellite Positioning*, Sponsored by the Defense Mapping Agency and the National Geodetic Survey at Austin, Texas, Volume 1, 51–64, 1986.
8. Bitwise Ideas Inc. *Geolab Documentation*, Ottawa, Ontario, Canada, 1988.
9. Bitwise Ideas Inc. *The GPS Environment for Geolab Manual*, Ottawa, Ontario, Canada, 1987.
10. Bodnar, A. N. Jr. *User's Guide for the Establishment of Tidal Bench Marks and Leveling Requirements for Tide Stations*, National Geodetic Survey Charting and Geodetic Services National Ocean Service, NOAA, Rockville, Maryland, 1975.
11. Bomford, G. *Geodesy*, 4th ed., Clarendon Press, Oxford, 736–739, 1980.
12. Bouchard, R. H. *Optimized Observation Periods Required to Achieve Geodetic Accuracies Using the Global Positioning System*, M. S. thesis, Naval Postgraduate School, Monterey, California, 1988.
13. Brown, R. G., and Hwang, P. Y. C. GPS Geodesy: A Kalman Filter Solution to the Wavelength Ambiguity Problem, *Proceedings of the 39th Annual Meeting of the Institute of Navigation*, 87–92, June 20–23, 1983.

14. Brown, R. G., and Hwang, P. Y. C. A Kalman Filter Approach to GPS Geodesy, In *Global Positioning System*, Volume II, Institute of Navigation, Washington, D.C., 155–166, 1984.
15. Brown, R. G., and Hwang, P. Y. C. GPS Geodesy: Real-Time Processing Possibilities with Karman Filter Approach, Institute of Navigation, Washington, D.C., January 1987.
16. Brown, R. G., Jeyapalan, K., and Rector, Jack. *Use of Global Positioning System for Precise Relative Positioning and Land Surveying*, Final Report, Iowa High Technology Council, July 1985.
17. Counselman, C. C., and Shapiro, I. I. Miniature Interferometric Terminals for Earth Surveying, *Bulletin Geodesic* 53 (2), 1979.
18. Davis, R. E., Foote, F. S., Anderson, J. M., and Mikhail, E. M. *Surveying: Theory and Practice*, 6th ed., McGraw-Hill, New York, 160–168, 1986.
19. Defense Mapping Agency, Department of Defense, *World Geodetic System*, DMA Technical Report 8350.2, Washington, D.C., 3–10, 3–11, 1987.
20. Defense Mapping Agency, Department of Defense, *Geodesy for the Layman*, DMA Technical Report 80–003, Washington, D.C., 24, 29, 64, 1983.
21. Denker, H., and Wenzel, G. Local Geoid Determination and Comparison with GPS Result, *Bulletin Geodesique* 61 (4), 349–366, 1987.
22. Erck, E. S. Orthometric Height Difference Recovery Tests from GPS Observations and Gravimetry, M.S. thesis, Iowa State University, 1989.
23. Ewing, C. E., and Mitchell, M. M. *Introduction to Geodesy*, New York: Elsevier, 1979.
24. Fell, P. J. The Use of Standard Values and Refraction Bias Parameters in Orbit Determination, *The Canadian Surveyor* 29 (3), 301–305, 1975.
25. Fell, P. J. Geodetic Positioning Using a Global Positioning System of Satellites, Report No. 289, Dept. of Geodetic Science, Ohio State University, 1980.
26. Fury, R. J. Prediction of the Deflections of the Vertical by Gravimetric Methods, NOAA Technical Report NOS NGS 28, 1984.
27. Fury, R. J. National Geodetic Survey, U.S. Dept. of Commerce, Rockville, Maryland, Personal communication, 1988.
28. Gigierano, J. D. Geological Survey Bureau, Iowa City, Iowa, Personal communication, 1988.

29. Heiskanen, W. A., and Moritz, H. *Physical Geodesy*, Graaz, Austria: Institute of Physical Geodesy, Technical University, Reprint, 1984.
30. Howell, T. F. Surveying and Mapping in Texas - A Case Study Using Automation for Transportation Application, *Surveying and Land Information Systems*, 50 (2), 1990.
31. Jeyapalan, K. Photogrammetry, In *Encyclopedia of the Earth System Science*, Volume 3, Academic Press, Inc., 1992.
32. Jeyapalan, K. Feasibility Study of the Triangulation of Tanzania, California State University, Fresno, 1979.
33. Jeyapalan, K., Ma, Wei-ming, and Tucker, Stevens P. Use of GPS for Precise Prediction of Local Geoid Undulation, ASCM-ASPRS Annual Convention, 78-83, Denver, Colorado, 1990.
34. Jeyapalan, K., Stein, M. A., Awuch-Baffour, R., Wang, Jijong, Luzen, B., and Wang, Yan. *Use of GPS for Photogrammetry*, Iowa State University, Ames, 1992.
35. Jeyapalan, K., Bandiman, S., Byrne, M. A., Erick, E. S., and Stein, M. A. Maximized Utility of the Global Positioning System, Iowa State University, Ames 1991.
36. Jeyapalan, K. Data Snooping Using Observations and Parameters with Constraints, *International Archives of Photogrammetry*, Vol. XXXV, 1984.
37. Jeyapalan, K. Evaluation of a Prototype Global Positioning System (GPS) Satellite Receiver, ACSM-ASPRS Annual Convention, Volume 2, 1986.
38. Jeyapalan, K., and Mohamed, M. The Accuracy Obtainable Using Global Positioning Satellite Systems, ACSM-ASP Annual Convention, Washington, D.C., 1984.
39. Jeyapalan, K. Calibration of Comparators by the Method of Collocation, Unpublished report, Topograph Division, U.S. Geological Survey, Reston, Virginia, 2-7, 1977.
40. Kaula, W. M. The Need for Vertical Control, *Surveying and Mapping* 47 (1), 57-64, 1987.
41. Kearsley, A. H. W. Tests on the Recovery of Precise Geoid Height Differences from Gravimetry, *Journal of Geophysical Research* 93 (B6), 6559-6570, June 1988.
42. King, R. W., Masters, E. G., Rizos, C., and Collins, J. *Surveying with GPS*, School of Surveying. The University of New South Wales, Kensington, Australia, 128, 1985.
43. Lapine, L. A. NOAA Tests Kinematic GPS, *ACSM Bulletin* 12-14, August 1990.
44. Ma, Wei-ming. *Local Geoid Determination Using the Global Positioning System*, M.S. thesis, Naval Postgraduate School, Monterey, California, 1988.

45. Mikhail, E. M. *Observations and Least Squares*, IEP-Dun-Donnelley, New York, 418–426, 1976.
46. Milliken, R. J., and Zoller, C. J. Principle of Operation of NAVSTAR and System Characteristics, *Global Positioning System*, Institute of Navigation, Washington, D.C., Volume 1, 3–14, 1980.
47. Moritz, H. Geodetic Reference System 1980, *Bulletin Geodesique* 54 (3), 395–405, 1980.
48. NASA. *Directory of Station Locations*, 4th ed., Goddard Space Flight Center, Greenbelt, Maryland, 1–11, 1978.
49. National Geodetic Survey. *Geodetic Glossary*, Rockville, Maryland: U.S. Government Printing Office, 1986.
50. Rapp, R. H., and Cruz, J. Y. Spherical Harmonic Expansions of the Earth's Gravitational Potential to Degree 360 Using 30' Mean Anomalies, Rep no. 376. Department of Geodetic Science and Surveying. The Ohio State University, Columbus, December 1986.
51. Rapp, R. H. Department of Geodetic Science and Surveying, The Ohio State University, Columbus, Personal communication, 1988.
52. Reilly, J. Surveying with GPS (unpublished xeroxed paper), Presented at ASCE/ICEA Surveying Conference, Ames, Iowa, ASCE/ICEA, 1988.
53. Remondi, B. W. Global Positioning System Carrier Phase: Description and Use, *Bulletin Geodesique* 59 (4), 361–377, 1985.
54. Remondi, B. W. *Using the Global Positioning System (GPS) Phase Observable for Relative Geodesy: Modeling, Processing and Results*, Ph.D. dissertation, The University of Texas at Austin, 1984.
55. Rockwell International. *Instruction Manual Collins Navcore I GPS C/A Receiver*, Cedar Rapids, Iowa, August 1986.
56. Strange, W. E., Vincent, S. F., Berry, R. H., and Marsh, J. G. Detailed Gravimetric Geoid for the United States, *The Use of Artificial Satellites for Geodesy*, Geophysical monograph 15. Eds. S. W. Henriksen, A. Mancicni, B. H. Chovitz. Washington: American Geophysical Union, 169–176, 1972.
57. Tetley, L., and Calcutt, D. *Electronic Aids to Navigation*, London, Edward Arnold Ltd., 225–232, 1986.
58. Torge, W. *Geodesy*, Berlin: DeGruyter, 1980.
59. Trimble Navigation. *Trimble Model 40000SX GPS Surveyor-Preliminary-Installation and Operation Manual*, Sunnyvale, California, 96, 1987.

60. Van Dierendonck, A. J., Russell, S. S., Kopitzke, E. R., and Birnbaum, M. The GPS Navigation Message, In *Global Positioning System*, Institute of Navigation, Washington, D.C., 1980.
61. Wells, David G. *Guide to GPS Positioning*, Fredericton, New Brunswick, Canada: University of New Brunswick Graphic Services, 1987.

## **APPENDIX. PROCESSING OF GPS DATA FOR 1994 PROJECT**

### **1. INTRODUCTION**

The 1994 project includes two flights. The processing procedures for the two parts are the same. This appendix discusses the procedures of downloading and processing of the data with PNAV software from Ashtech on a PC and Xess on Project Vincent. Then the processing results are given.

### **2. PROCEDURES**

#### **2.1. Downloading Data from the GPS Receivers**

Six GPS receivers are used in this project. Two of them are at the ground base stations base 1 (airport south) and base 2 (airport north). The other four receivers are placed on the left wing, right wing, center, and head of the airplane, which are called left, right, camera, and fore respectively in the data processing.

Using a program called HOST in PNAV, all of the data files in the six GPS receivers are downloaded into the hard driver on the PC. In the receivers, different data file names have been given according to the different stations in the flights. You just select Yes or No for each station in the program HOST to decide if it is downloaded. Since there are two flights, we made two directories to store the data of one flight in one directory. The data files from the receivers are B, E, and S files. Photo file is from the receiver on camera.

#### **2.2. Data Processing Using PNAV**

To get the positions of left, right, camera, and fore, we use PNAV for the data processing. PNAV performs several task. The input files for data processing in PNAV are B-file (Binary Measurement File) and E-file (Ephemeris File). The S-file (Site Data File) is not used in this release of version. The photo file is used in the procedure of "PHOTOGRAMMETRY" to produce the output for the exposure time.

(a) Run PNAV and select submenu "COMPARE NAV SOLUTIONS" in the main menu "POST MISSIONS." Taking one of the two base stations as base station and the other as rover station, we get the location of the rover station, which is used to compare with the given coordinate of the rover station and find out if the given coordinates of the base stations are correct. The rover motion dynamics for this procedure is "Static."

(b) In data processing, we take base 1, base 2, camera, and left as the base station. Since there are many rover stations for one base, that is, a batch job, we select "BATCH PROCESSING" in the main menu of PNAV. The execution mode is "FORWARD AND

BACKWARD.” The processing mode is “NAVIGATION” and the rover station dynamics is “STATIC.” Each time we select base 1, base 2, camera, and left as the base station and the others as rover stations (except the ground base stations base 1 or base 2). Note that the ground base stations base 1 and base 2 can only be used as base station in the data processing. In this step PNAV creates C-file (rover position in WGS-84 Coordinates) and J-file (relative position in either XYZ or ENU Coordinates) as output files.

(c) After running “BATCH PROCESSING” in the main menu of PNAV, select “POST MISSION” in the main menu. Then run “PHOTOGRAMMETRY” which uses the photo data file to create the position of these receivers at the time of exposures.

(d) The final work done by PNAV is to create P files that are the plot files. Select “CREATE PLOT FILE” in the submenu of “POST MISSION” and input the name of the photo data file.

(e) Select “VIEW PLOT FILE” in the main menu to see the processing results.

### **2.3. Data Processing Using Xess on Project Vincent**

In part two we got the position of left, right, camera, and fore for each flight. In this part for the whole flight we calculate the  $\omega$ ,  $\phi$ , and  $\kappa$  of the aircraft according to these coordinates in the J-file given by PNAV. For those of the exposure time, we get the angles of  $\omega$ ,  $\phi$ , and  $\kappa$  both from the ENU coordinates in J-file and the XYZ coordinates, which are converted from the WGS-84 latitude and longitude coordinates in C-file.

Xess is a spreadsheet software similar to Lotus 1-2-3. We use it to complete the computation for those angles.

(a) For each flight, import the J-file of left, right, camera, and fore that are the results based on base 2 into Xess on Project Vincent. The x, y, and z of each station occupy the adjacent three columns. Then calculate the differences of height, distances, and scale factors between those stations. Finally get the angles  $\omega$ ,  $\phi$ , and  $k$ .

(b) To obtain the state plane coordinates from C-file, we use a program “UTM&STPL” to convert the latitude and longitude in C-file. Then repeat the procedure in (a).

## **3. DATA PROCESSING AND RESULTS**

### **3.1. Data and Results from PNAV**

The results data from PNAV are the C-file, J-file, and P-file (Plot file). Viewing the P-file by the “VIEW PLOT FILE” in PNAV, we know that the PDOP are less than two and there are five to seven satellites in the data collecting. In the step “COMPARE NAV SOLUTIONS” we find a error of about 18 meters in the northern direction between base 1 and base 2. The coordinate of

base 2 is regarded as correct one. So we take the results that are based on base 2. The recording interval for the 1994 project is 0.5 second. So the volume of the data is very big and it takes a long time to process all the data by PNAV.

### 3.2. Data and Results from Xess

There are six sets of data and results from Xess: three for flight 1 and the other three for flight 2.

#### (a) Data and results from Flight 1

Flight 1 is the high flight on the ISU campus. Only four shots are taken in flight 1. One of them is for the test. So there are relatively less data in flight 1.

Table 1 gives the data of flight 1 for the entire data recording time, exposure time, and data of the SPC converted from WGS-84 in C-file for the exposure time, respectively. Table 2 gives the result from these data.

#### (b) Data and Results from Flight 2

Flight 2 is the low flight on the ISU campus and on Highway 30. A total of 57 shots occur during flight 2. One is taken on the ground. Four are on the campus. Fifty-one shots are on Highway 30.

## 4. CONCLUSIONS

From these results, we can reach the following conclusions:

- (1) The results from PNAV are good. In the exposure time interval, there are seven satellites. The PDOPs are also very small.
- (2) The results from Xess shows that for both flights the distances, three angles, and the scale factors are good. The variances of  $\phi$  and  $\omega$  for both flights are about  $2^\circ$ .
- (3) The results from the ENU coordinates in J-file and the SPC converted from C-file coincide very well, meaning that the results from different methods are consistent.

Table A-1. Data of flight 1 for entire time.

TIME	DATA for FLIGHT 1											
	CAMERA			LEFT			RIGHT			FORE		
	Xc	Yc	Zc	Xl	Yl	Zl	Xr	Yr	Zr	Xf	Yf	Zf
148196.00	-3110.462	2905.171	947.792	-3111.182	2910.756	947.289	-3109.592	2899.671	947.040	-3109.474	2905.311	947.855
148196.50	-3065.145	2907.787	948.438	-3065.833	2913.378	947.963	-3064.308	2902.294	947.654	-3064.156	2907.920	948.501
148197.00	-3019.867	2910.520	949.092	-3020.491	2916.116	948.597	-3019.097	2905.002	948.343	-3018.878	2910.641	949.155
148197.50	-2974.615	2913.300	949.737	-2975.204	2918.904	949.256	-2973.880	2907.778	948.961	-2973.626	2913.414	949.805
148198.00	-2929.384	2916.118	950.317	-2929.961	2921.726	949.876	-2928.666	2910.598	949.506	-2928.395	2916.228	950.380
148198.50	-2884.173	2918.981	950.796	-2884.733	2924.594	950.366	-2883.475	2913.461	949.962	-2883.182	2919.088	950.857
148199.00	-2838.978	2921.928	951.074	-2839.485	2927.541	950.602	-2838.334	2916.397	950.284	-2837.988	2922.028	951.129
148199.50	-2793.787	2924.854	951.182	-2794.294	2930.471	950.764	-2793.142	2919.329	950.350	-2792.796	2924.951	951.244
148200.00	-2748.592	2927.741	951.302	-2749.141	2933.356	950.911	-2747.907	2922.224	950.436	-2747.602	2927.844	951.360
148200.50	-2703.399	2930.632	951.470	-2703.956	2936.247	951.069	-2702.710	2925.115	950.609	-2702.409	2930.738	951.524
148201.00	-2658.203	2933.527	951.620	-2658.695	2939.150	951.240	-2657.583	2928.012	950.747	-2657.211	2933.621	951.677
148201.50	-2612.999	2936.385	951.726	-2613.412	2942.014	951.365	-2612.459	2930.862	950.839	-2612.009	2936.465	951.788
148202.00	-2567.779	2939.146	951.767	-2568.156	2944.780	951.415	-2567.276	2933.621	950.865	-2566.788	2939.218	951.827
148202.50	-2522.548	2941.808	951.681	-2522.925	2947.441	951.312	-2522.044	2936.280	950.802	-2521.556	2941.881	951.742
148203.00	-2477.304	2944.388	951.545	-2477.704	2950.013	951.140	-2476.775	2938.856	950.702	-2476.312	2944.466	951.603
148203.50	-2432.051	2946.923	951.366	-2432.442	2952.548	950.937	-2431.531	2941.386	950.549	-2431.060	2947.000	951.426
148204.00	-2386.792	2949.407	951.181	-2387.153	2955.036	950.779	-2386.298	2943.870	950.343	-2385.800	2949.479	951.242
148204.50	-2341.528	2951.813	951.030	-2341.852	2957.447	950.650	-2341.067	2946.278	950.170	-2340.534	2951.879	951.092
148205.00	-2296.258	2954.119	950.951	-2296.556	2959.754	950.578	-2295.821	2948.582	950.084	-2295.261	2954.180	951.009
148205.50	-2250.985	2956.342	950.927	-2251.225	2961.978	950.530	-2250.604	2950.798	950.082	-2249.987	2956.394	950.984
148206.00	-2205.704	2958.417	951.018	-2205.905	2964.055	950.657	-2205.363	2952.875	950.137	-2204.705	2958.459	951.081
148206.50	-2160.407	2960.313	951.247	-2160.599	2966.957	950.931	-2160.082	2954.776	950.327	-2159.409	2960.352	951.311
148207.00	-2115.103	2962.036	951.517	-2115.305	2969.678	951.215	-2114.764	2956.500	950.590	-2114.105	2962.076	951.584
148207.50	-2069.788	2963.605	951.817	-2069.991	2972.246	951.479	-2069.449	2958.065	950.911	-2068.791	2963.647	951.880
148208.00	-2024.464	2965.024	952.092	-2024.697	2974.660	951.725	-2024.093	2959.482	951.223	-2023.466	2965.072	952.152
148208.50	-1979.131	2966.351	952.316	-1979.397	2976.984	951.907	-1978.729	2960.805	951.480	-1978.134	2966.406	952.373
148209.00	-1933.791	2967.621	952.467	-1934.061	2979.254	952.065	-1933.388	2962.077	951.628	-1932.794	2967.676	952.521
148209.50	-1888.438	2968.848	952.577	-1888.687	2981.482	952.170	-1888.053	2963.299	951.742	-1887.440	2968.899	952.635
148210.00	-1843.069	2970.014	952.679	-1843.299	2983.649	952.275	-1842.702	2964.467	951.837	-1842.070	2970.063	952.730
148210.50	-1797.661	2971.147	952.728	-1797.899	2985.781	952.306	-1797.333	2965.594	951.902	-1796.683	2971.191	952.779
148211.00	-1752.283	2972.256	952.658	-1752.455	2987.889	952.237	-1751.981	2966.699	951.838	-1751.285	2972.291	952.711
148211.50	-1706.871	2973.294	952.535	-1707.039	2989.929	952.129	-1706.570	2967.742	951.703	-1705.874	2973.331	952.591
148212.00	-1661.445	2974.282	952.386	-1661.623	2991.915	951.959	-1661.134	2968.727	951.571	-1660.447	2974.319	952.441
148212.50	-1616.007	2975.237	952.190	-1616.199	2993.869	951.728	-1615.681	2969.676	951.412	-1615.009	2975.278	952.243
148213.00	-1570.559	2976.170	951.940	-1570.770	2995.800	951.449	-1570.213	2970.607	951.194	-1569.560	2976.215	951.997
148213.50	-1525.093	2977.109	951.605	-1525.307	2997.738	951.114	-1524.746	2971.546	950.867	-1524.095	2977.154	951.663
148214.00	-1479.613	2978.075	951.287	-1479.800	2999.704	950.776	-1479.291	2972.508	950.567	-1478.615	2978.115	951.344
148750.00	-23.417	-1331.563	9.093	-18.097	-1333.287	8.415	-28.866	-1330.047	8.430	-23.721	-1332.518	9.160
148750.50	-25.144	-1337.256	9.123	-19.826	-1338.990	8.446	-30.587	-1335.726	8.459	-25.449	-1338.208	9.183
148751.00	-26.837	-1342.828	9.149	-21.527	-1344.579	8.467	-32.276	-1341.281	8.493	-27.148	-1343.781	9.208
148751.50	-28.523	-1348.276	9.174	-23.215	-1350.048	8.516	-33.951	-1346.709	8.497	-28.833	-1349.227	9.233
148752.00	-30.187	-1353.594	9.196	-24.886	-1355.386	8.535	-35.607	-1352.009	8.521	-30.502	-1354.545	9.257
148752.50	-31.822	-1358.784	9.227	-26.536	-1360.629	8.564	-37.228	-1357.153	8.567	-32.149	-1359.733	9.292
148753.00	-33.442	-1363.846	9.256	-28.195	-1365.780	8.598	-38.823	-1362.119	8.587	-33.784	-1364.788	9.315
148753.50	-35.084	-1368.774	9.272	-29.885	-1370.838	8.598	-40.418	-1366.911	8.623	-35.447	-1369.709	9.328
148754.00	-36.797	-1373.561	9.304	-31.674	-1375.801	8.635	-42.069	-1371.514	8.641	-37.191	-1374.480	9.358
148754.50	-38.626	-1378.200	9.325	-33.575	-1380.355	7.667	-43.819	-1375.974	8.656	-39.054	-1379.106	9.375
148755.00	-40.578	-1382.678	9.322	-35.630	-1385.281	8.669	-45.654	-1380.336	8.595	-41.039	-1383.567	9.377
148755.50	-42.661	-1387.007	9.351	-37.802	-1389.784	8.694	-47.643	-1384.489	8.619	-43.151	-1387.878	9.400
148756.00	-44.835	-1391.160	9.368	-40.075	-1394.099	8.694	-49.734	-1388.472	8.648	-45.354	-1392.016	9.420
148756.50	-47.098	-1395.136	9.382	-42.435	-1398.228	8.705	-51.903	-1392.292	8.667	-47.645	-1395.977	9.436
148757.00	-49.427	-1398.928	9.390	-44.876	-1402.179	8.731	-54.126	-1395.918	8.654	-50.004	-1399.748	9.446
148757.50	-51.810	-1402.531	9.406	-47.411	-1405.987	8.754	-56.365	-1399.317	8.663	-52.422	-1403.324	9.459
148758.00	-54.242	-1405.888	9.427	-50.049	-1409.588	8.778	-58.601	-1402.421	8.688	-54.902	-1406.645	9.472
148758.50	-56.726	-1408.953	9.429	-52.788	-1412.923	8.768	-60.833	-1405.210	8.700	-57.434	-1409.665	9.475
148759.00	-59.289	-1411.708	9.424	-55.669	-1415.976	8.794	-63.086	-1407.658	8.658	-60.051	-1412.365	9.464

